The internal variability of the regional climate model RegCM3 over southern Africa

by

Mary-Jane Morongwa Kgatuke

A dissertation submitted in partial fulfilment of the requirements for the degree

MASTER OF SCIENCE (METEOROLOGY)

in the

FACULTY OF NATURAL AND AGRICULTURAL SCIENCES

UNIVERSITY OF PRETORIA

Pretoria

August 2006

In him we were also chosen, having been predestined according to the plan of him who works out everything in conformity with the purpose of his will, in order that we, who were first to hope in Christ, might be for the praise of his glory.

Ephesians 1:11, 12

DISSERTATION SUMMARY

The internal variability of the regional climate model, RegCM3 over southern Africa

Mary-Jane Morongwa Kgatuke

Supervisor: Professor W. A. Landman
Faculty: Faculty of Natural and Agricultural Sciences
Department: Geography, GeoInformatics and Meteorology
University: University of Pretoria
Degree: Master of Science (Meteorology)

Global Climate Models (GCMs) and Regional Climate Models (RCMs) represent the atmospheric processes that are nonlinear by nature and are therefore sensitive to small perturbations. The RCMs are provided time dependent Lateral Boundary Conditions (LBCs) either from the GCM or the reanalyses and hence the RCMs are not expected to deviate much from the forcing fields as expected for a free non-linear system. If a GCM is used in a nested system, the nested solutions will be subject to the internal variability of both the GCM and the RCM. The study aims to investigate the variability caused by the internal variability of the GCM and the RCM. The study then looks into the contribution of the RCM's internal variability to the total variability of the different nested system solutions. In this study four solutions obtained through perturbing the wind fields at initialisation for the ECHAM4.5 are used to force an RCM, the RegCM3, over South Africa. The solutions that are obtained are functions of the internal variability of the ECHAM4.5 as well as of the RegCM3. To determine the amount of the variability that is introduced by the RCM's internal variability, four other RegCM3 simulations are made through initialising the RegCM3 on different days but using a single realisation from the GCM. The rainfall variability associated with the combined internal variability of both the models is high to an extent that ensemble members produce anomalies that have opposite signs in the same season. However, the sign of the ensemble average anomaly generally corresponds

with the observed anomaly. The variability associated with the internal variability of the RCM is negligible when seasonal totals are analysed while with the daily rainfall totals the variability is larger. The variability in areas where small amounts of rainfall occur is smaller than that of the high rainfall regions. The number of events that fall into the three rainfall categories (i.e. below-normal, normal and above-normal) for the RegCM3 ensemble members are close to one another however the timing of the events is different. The results suggest that in operational forecasting making ensemble members associated with the internal variability of an RCM is not necessary because the information obtained from the ensemble members is almost similar.

PREFACE

The Global Climate Models (GCMs) have been found to have skill in predicting seasonal total rainfall and average temperature over large forecast areas using a low resolution of about 300 km. The low resolution makes it impossible for the models to represent the land surface characteristics that lead to large small scale variations in the climate variables adequately. The Regional Climate Models (RCMs) are used to produce detailed high resolution simulations with lesser computer resources than those required for a GCM with the same resolution.

The atmosphere is chaotic and therefore the equations that represent the atmospheric processes in the models are nonlinear. As a result the models, especially the GCMs are sensitive to the initial conditions. Two simulations started with slightly different initial conditions will diverge from one another substantially after a few days of simulation. In regional climate modelling, the RCMs are nested within the reanalyses or GCM solutions and therefore the RCM solutions are restricted at the boundaries. Although the RCMs are restricted at the boundaries, they are also nonlinear and are therefore expected to exhibit a certain level of the internal variability.

The main aim of the study is to investigate the internal variability of an RCM. In a nested system where a GCM is used the final solutions of the system will be subject to the internal variability of the GCM and of the RCM. The variability caused by the internal variability of both the models will be analysed. The contribution of the RCM's internal variability to the total variability of the nested system solutions will then be investigated.

Chapter 1 of the dissertation gives the background of the study. The climate of South Africa is described and how it varies according to different seasons and it is noted that it is important that seasonal forecasts are produced. The predictability problem is then discussed with concentration on the characteristic of the atmosphere. Different methods that have been used to associate the atmospheric circulations with the boundary conditions of sea-surface temperatures (SSTs) are discussed. Some of these are numerical

(GCMs) and statistical models. Due to the problem of the coarse resolution of the GCMs, the downscaling procedure is discussed. The inter-annual variability as simulated by the RCMs has been studied over many parts of the world but the studies are limited over South Africa. The status of seasonal forecasting at the South African Weather Service is discussed and it is noted that RCMs are not yet operational in the organisation. When operational forecasts are made researchers have to get the best possible simulations using the available models. The problem of the internal variability of the models is then discussed because understanding the problem will help in obtaining the best possible simulations from the RCMs for operational forecasting purposes.

Chapter 2 describes all the data, the models and the methods used in the study. Chapter 3 discusses the differences in the nested system solutions due to the internal variability of the GCM and the RCM. Chapter 4 discusses comparisons between the results that are discussed in the Chapter 3 with observations. Chapter 5 discusses the inter-annual variability in the simulations that is associated with the internal variability of the RCM. Chapter 6 discusses the intra-seasonal variability in the simulations that is associated with the internal variability of the RCM. Chapter 7 is summary and conclusion.

ACKNOWLEDGEMENTS

The author would like to express her utmost appreciation to the following people for their valued contribution that made this work possible.

1. Prof. Willem Landman for supervising this study and for his support.
2. Dr. Fillipo Giorgi, from the International Centre for Theoretical Physics (ICTP), for his advice in structuring the experiment. Dr Bi and Dr Jeremy Pal, also from ICTP for helping with the implementation of the RegCM3 at the South African Weather Service (SAWS).
3. Water Research Commission (WRC) for funding the project under which the study falls.
4. The International Research Institute for Climate and Society (IRI) for providing data and scripts to implement the ECHAM4.5-RegCM3 system, the three people in particular who contributed are Dr Joshua Qian, Dr David DeWitt and Dr Anji Seth who is now at the University of Connecticut.
5. Mr. Asmeron Beraki for writing the post processing programmes that extract the homogeneous rainfall data.
6. Mr Mzukisi Ka-Gwata for helping with the use of the Geographic Information System (GIS) system, ArcMap and also for providing observed daily rainfall data.
7. My colleagues, Ms Annelise du Piesanie and Mr Maluta Mbedzi, for helping with the generation of the simulations.
8. Ms Anna Bartman for making the homogeneous regions.
9. Dr Warren Tennant for helping with the problems related to the compiler on the machines, and any programming problems. The ICT section is also acknowledged for helping with machines.
10. The South African Weather Service for its computer and data resources.
11. My husband, Mapogo Kgatuke and my mother, Mantwa Bopape for their support.

CONTENTS

LIST OF FIGURES

CHAPTER 1

CHAPTER 2

CHAPTER 3

CHAPTER 4

CHAPTER 6

LIST OF TABLES

CHAPTER 2

CHAPTER 6

CHAPTER 1: INTRODUCTION

1.1. The Rainfall patterns over South Africa

1.1.1. The general rainfall pattern in South Africa

The precipitation of South Africa generally increases from west to the east, except along the southern coast (Figure 1.1; Taljaard, 1986). Most of the regions experience their rain during austral summer; however, over the southern coast the rainfall occurs throughout the year. The Western Cape normally has its highest rainfall during the winter months (Figure1.1; Taljaard, 1986). The east coastal belt receives slightly more rainfall in winter than the adjacent interior (Taljaard, 1986). Most of the rainfall received in the eastern part of the country is of convective origin (Harrison, 1984a; Tyson and Preston-Whyte, 2000) while the rainfall received in the Western Cape is due mainly to cold fronts (Tyson and Preston-Whyte, 2000).

1.1.2. Major controls of rainfall in South Africa

1.1.2.1. Ocean temperatures and Topography

The east-west total rainfall gradient over South Africa is due to amongst others, the temperatures in the oceans adjacent to the country (Van Heerden and Taljaard, 1998; Tyson and Preston-Whyte, 2000). The Agulhas Current drives warm water to the east coast while the water to the west coast is cold as a result of the cold Benguela Ocean Current (Van Heerden and Taljaard, 1998). Another major controller of rainfall is the topography (Van Heerden and Taljaard, 1998). The interior of South Africa is characterised by an elevated plateau with altitudes of more than 1,000m above sea level (Engelbrecht et al, 2002, Van Heerden and Taljaard, 1998; Joubert et al, 1999). The coastal margins along the east and south-east coast of South Africa are narrow and are followed by steep topographic gradients into the interior of the country (Joubert et al, 1999).

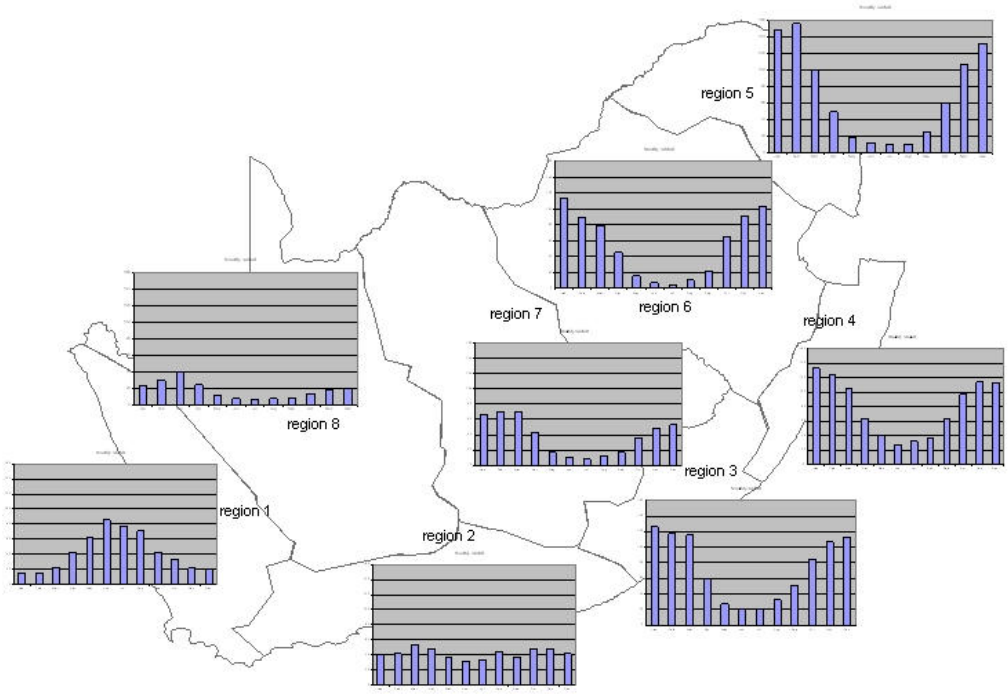

Figure 1.1: *Average total monthly rainfall in mm from January until December calculated using 44 years of station data from 1960 to 2004.*

1.1.2.2. Mean atmospheric circulation

The rainfall of South Africa is also controlled to a large extent by the mean circulation of the atmosphere (Taljaard, 1995a; Taljaard, 1994; Van Heerden and Taljaard, 1998). South Africa is located in the subtropics and therefore it is affected by circulation systems prevailing in the tropics, the subtropics and the temperate or middle latitudes (Tyson and Preston-Whyte, 2000).

1.1.2.2.1. Subtropical control

The subtropical control is effected by the anticyclones: the Indian Ocean High (IOH), the continental high and the Atlantic Ocean High (AOH). The anticyclones are a part of a discontinuous high pressure belt that circles the southern hemisphere at about 30° S (Taljaard, 1995b;c; Joubert et al, 1999; Tyson and Preston-Whyte, 2000). The near-surface circulation at 850hPa is characterised by a heat low over the interior in summer (Taljaard, 1995c;

Joubert et al, 1999) while in winter a high pressure cell dominates (Tyson and Preston-Whyte, 2000).

The AOH and IOH vary significantly in position throughout the year (Taljaard and Steyn, 1991; Van Heerden and Taljaard, 1998). The monthly zonal shifts in position of the AOH are twice that of the latitudinal variation. The longitudinal variations of the AOH do not materially affect the weather of the subcontinent (Tyson and Preston-Whyte, 2000). The AOH may, however, ridge eastward and to the south of the continent, on a scale of days and therefore affect the weather. The IOH varies on a half-yearly basis in its meridional movement while the longitudinal displacement is annually. The IOH variations influence the weather and climate of the northern and eastern parts of South Africa.

1.1.2.2.2. Tropical control

The easterly flow that may be accompanied by the occurrence of easterly waves and lows is a characteristic of the tropical atmosphere which affects the climate of South Africa. The mean circulation of the atmosphere is evident in the tropical easterly flows that converge in the region called the Inter-tropical Convergence Zone (ITCZ) (Van Heerden and Taljaard, 1998). Throughout the year the ITCZ is located in the northern hemisphere in the eastern Pacific and Atlantic regions. Over Africa, the Indian Ocean and western Pacific regions the ITCZ migrates from the southern to the northern hemisphere between January and July (Tyson and Preston-Whyte, 2000). The cloud bands that are associated with most of the rainfall in late summer are a result of the ITCZ.

1.1.2.2.3. Temperate control

Temperate or middle latitude control is effected over South Africa through travelling perturbations in the westerlies (Harrison, 1984b). The frequent occurrence of fronts is a characteristic of middle latitudes throughout the year. Whenever two air masses with different temperature characteristics come into contact, a zone of discontinuity and temperature gradient will exist between

them. The zone of discontinuity is called a front. Cold fronts usually occur south of the country due to discontinuities between polar and subtropical air. The cold fronts form part of the mid-latitude cyclones and they are a major cause of the winter rainfall over the south-western and south coast because of their northward migration in the winter season (Tyson and Preston-Whyte, 2000).

1.1.3. Rainfall oscillations

The rainfall of South Africa varies around the mean values. There exists an oscillation with a periodicity of about 18 years over the summer rainfall region of South Africa (Tyson and Preston-Whyte, 2000). Three to five of the 18 years in a full cycle usually have rainfall anomalies with an opposite sign to that required by the phase of the oscillation. The opposite sign is usually due to phenomena such as the El Niño - Southern Oscillation (Ropelewski and Halpert, 1987) that affect the circulation systems (Taljaard, 1986).

1.1.4. Mean circulation perturbations

The perturbation from the mean circulation of the atmosphere influences the climate and weather of South Africa. The perturbations from the mean circulation are the synoptic and smaller scale disturbances that constitute individual weather systems. The seasonal perturbations may be as a result of forcing factors such as the sea-surface temperatures (SSTs) that determine the seasonal rainfall and temperature anomalies (Tyson and Preston-Whyte, 2000). The seasons vary considerably from year to year because they are affected by the day to day statistics within the season (Tyson and Preston Whyte, 2000).

1.1.5. Circulation patterns

The studies conducted over southern Africa have shown that the mean circulation patterns are different during wet and dry years (Taljaard, 1989; Miron and Lindesay, 1983 a;b; Harrison, 1984; Rautenbach, 1998; Van Heerden and Taljaard, 1998) and forecast models have been proposed (Jury

et al, 1998; Landman and Mason, 1999a). Climatological pressure anomaly fields give an idea of the frequency of occurrence of specific perturbations in the atmosphere. They show opposite characteristics between wet and dry conditions on time scales ranging from months to seasons and years (Miron and Tyson, 1984). The surface pressure anomaly fields during dry years are negative south, and positive east and west of the African continent (Miron and Tyson, 1984; Taljaard and Steyn, 1991). The negative surface pressure anomalies to the south are associated with weak ridging anticyclones, while positive anomalies over the east and west of the African continent are associated with shallow surface troughs.

When the convective activity across equatorial Africa, north-eastern Madagascar and the south-west Indian Ocean is above-normal, southern Africa is characterised by below-normal convective activity. During wet conditions over South Africa the air mostly ascends over the subcontinent and sinks east of Madagascar. During dry conditions over the subcontinent the mean vertical circulation reverses (Taljaard, 1986). Surface air flow patterns over South Africa have a more northerly or easterly component during the wet years and a more westerly component during dry years (D'Abreton and Lindesay, 1992).

1.1.6. Moisture fluxes

The vapour fluxes change between October and January and these are important for the rainfall of South Africa (Makarau and Jury, 1997). The zonal fluxes are more important in October while the meridional fluxes are important in January (D'Abreton and Lindesay, 1992). Wet October (January) months are characterised by enhanced zonal (meridional) flow and reduced importance of these flows in the dry months (D'Abreton and Lindesay, 1992). The moisture that contributes to rainfall over the summer rainfall region of South Africa is largely imported from other areas. During dry synoptic spells there is usually inflow from the mid-latitude ocean regions to the south. Increased moisture flux from the tropical or subtropical south-west Indian Ocean tends to occur during wet synoptic spells (Cook et al, 2004).

1.1.7. Percent of rainfall caused by tropical systems

The statistics of central South African rainfall for a number of rain-bearing synoptic systems was analysed for the period 1967 to 1997 (Harrison, 1994a). Tropical systems accounted for about 60% of the rainfall events over central South Africa. In January this contribution exceeded 80%. Cloud bands linking the tropical and temperate circulations were the major contributors. The December rainfall is caused mainly by the circulation over tropical Africa. Temperate systems made an important contribution to the late season rainfall maximum over the central South Africa (Harrison, 1994a).

1.1.8. The importance of seasonal predictions

More than 80% of the annual rainfall over most parts of South Africa is received between October and March (Tyson and Preston-Whyte, 2000; Taljaard, 1986). It was found that the summer rainfall in the period 1980-1999 was closely associated with the Gross Domestic Product (GDP) (Jury, 2002). The management of environmental and financial resources in the country would be greatly improved by the availability of seasonal rainfall forecasts at least one season in advance, if the forecasts are accurate enough (Jury, 2001). The summer season defined as December-February (DJF) is important meteorologically because during this part of the season tropical circulations dominate over South Africa (Harrison, 1984a; Landman and Goddard, 2002). The reason why this season is important is that seasonal predictability is derived from the characteristic of the tropical atmosphere (Shukla, 1998).

1.2. The atmospheric characteristic and seasonal predictability

1.2.1. Chaos in the atmosphere and models

The earth's atmosphere is a chaotic system (Shukla, 1998) and hence the models representing the atmospheric processes are comprised of nonlinear

equations (Giorgi and Bi, 2000). Simulations started with initial conditions that are slightly different from one another will diverge substantially after a few days of simulation (Giorgi and Bi, 2000; Chervin et al, 1974). The divergence of the simulations is an issue of concern because of the lack of observations and errors in observations that are available for the initial conditions (Shukla, 1998). The forecast becomes useless after a finite amount of time because of the uncertainty in the initial conditions which will grow exponential as expected for a nonlinear system (Giorgi and Bi, 2000).

1.2.2. Limit of weather forecasts

Weather forecasts are usually fairly accurate for 1 to 2 days ahead (Shukla, 1998). However, the accuracy of weather forecasts decreases as the lead time increases. A forecast for a few days in the future often needs to be revised as that day approaches. The forecast at these time ranges is said to be an initial value problem. Beyond a week or two there is little or no accuracy in the forecasts. The correspondence between modelled precipitation distributions and observational evidence was found to be best within the first 3 days after the initial conditions were introduced in a study conducted over Brazil (Druyan et al, 2002). Simulated precipitation rates became unrealistic after about 5 days and into the second week.

1.2.3. Tropical atmosphere and sea-surface temperatures

The tropical atmosphere is not as chaotic as the extra-tropical one (Shukla, 1998). The tropical flow patterns and rainfall are strongly determined by the SSTs since they show little sensitivity to changes in the initial conditions of the atmosphere (Shukla, 1998; Anderson et al, 1999). When large changes in the atmospheric ICs were introduced in previous studies, the resulting large scale wind patterns and rainfall in certain tropical regions did not diverge as would be the case for a chaotic system. Instead, they converged to nearly identical values determined by SST anomalies. It is impossible to make accurate forecasts of the day-to-day sequence of weather events beyond 1 or 2 weeks. The predictability of the large scale seasonal tropical circulation is however

made possible by the characteristic of the tropical atmosphere (Shukla, 1998; Robertson et al, 2004; AMS, 2000).

1.2.4. Extra-tropical atmosphere

The predictability of seasonal mean circulation in certain extra-tropical regions is enhanced by the high predictability of the tropical rainfall for a given SST (Shukla, 1998). Prediction of regional climate anomalies for lead times beyond the limit of deterministic predictability (Fennessy and Shukla, 1999) even outside the tropics would be possible given accurate predictions of surface boundaries. The natural internal atmospheric variability of the extra-tropical atmosphere limits the impact of tropical SST forcing. However, strong evidence that the statistics of the extra-tropical climate still depend on the tropical SSTs, especially when these SSTs are strongly anomalous, has been demonstrated (Anderson et al, 1999). The most understood tropical SST – atmospheric relation is a phenomenon called the El Niño Southern Oscillation (ENSO) (Philander, 1990).

1.2.5. The El Niño - Southern Oscillation

The ENSO phenomenon is a free oscillation of the ocean-atmosphere system (AMS, 2001; Ropelewski and Halpert, 1987). The southern oscillation describes the large east-west shifts of mass in the tropical atmosphere. El Niño occurs when the SSTs over the eastern tropical Pacific Ocean are anomalously high. During an El Niño event the trade winds are weak and the pressure is low over the eastern and high over the western tropical Pacific (Philander, 1990). La Niña is the opposite phase of El Niño when SSTs in the central and eastern tropical Pacific are unusually low and when the trade winds are very intense. The ENSO phenomenon is important to the inter-annual climate variability worldwide including southern Africa (Jury et al, 1998; Philander, 1990).

1.2.5.1. ENSO influence on South African rainfall

The southern oscillation affects the rainfall of South Africa through affecting the location of the major cloud bands that lead to most of the summer rainfall (Tyson and Preston-Whyte, 2000). During the El Niño low phase of the oscillation the cloud band convergence zone moves offshore of South Africa and hence the country receives generally below-normal rainfall (Ropelewski and Halpert, 1989; Tyson and Preston-Whyte, 2000). During the high phase cloud bands locate over southern Africa and rainfall is higher. The ENSO phenomenon explains about 30% of the southern African rainfall variability (Tyson and Preston-Whyte, 2000). The association between ENSO and South African rainfall is strongest in a north-west to south-east line across the South African central summer rainfall region (Kruger, 1998; Landman and Mason, 1999a).

1.2.6. Atlantic and Indian Ocean SSTs

1.2.6.1. The role of the oceans adjacent to South Africa

The rainfall over South Africa is not only influenced by the SSTs in the equatorial Pacific Ocean. SSTs in the oceans adjacent to South Africa, the Indian and the Atlantic also play a role (Reason and Lutjeharms, 1998; Landman and Mason, 1999(b); Allan et al, 1994). On synoptic time scales, the atmosphere may be influenced by the surface fluxes and moisture that result from the variability of the SSTs in the adjacent oceans. The evolution of rain producing systems over southern Africa may be affected by the fluxes. The background atmospheric circulation in which synoptic rain-producing systems evolve, and changes in the preferred locations of large scale convection may be caused by the regional SST variability on longer time scales (Reason and Lutjeharms, 1998).

1.2.6.2. The Indian Ocean SSTs, ENSO and rainfall over South Africa

There is a high correlation between the SST variability in the Indian Ocean with that of the tropical Pacific, with the tropical Pacific leading by

approximately 3 months. The atmospheric changes associated with the ENSO events have been found to influence the Indian Ocean (Goddard et al, 2001). Since the late 1970s the ENSO signal in the Indian Ocean has weakened (Landman and Mason, 1999 (b)). The weakened signal has introduced important changes between the Indian Ocean SSTs and DJF rainfall variability over South Africa. Warm (cold) events in the tropical western Indian Ocean have become associated with wet (dry) conditions over the north-eastern half of South Africa since the late 1970s. This positive association is inconsistent with the influence of ENSO warm events on southern African rainfall (Landman and Mason, 1999(b)).

1.2.6.3. The Indian Ocean SSTs and rainfall over South Africa

The association between SSTs surrounding South Africa and South African rainfall are located distant from land in the tropical Indian Ocean east of 50° E, but with the strongest rainfall/SST association in the western equatorial Indian Ocean (Mason, 1995; Landman and Mason; 1999(b)). The correlation between the changes in the SSTs in the western tropical Indian Ocean to the north of Madagascar and rainfall over South Africa is negative (Tyson and Preston-Whyte, 2000). Wetter conditions over eastern and central South Africa tend to be linked to warmer SSTs in the south-west Indian Ocean (Reason and Mulenga, 1999).

An atmospheric general circulation model was used to investigate the sensitivity of the regional circulation and rainfall over southern Africa to the dipole SST anomalies in the subtropical south Indian Ocean (Reason, 2001). Increased rainfall over South Africa occurred when the model was forced with positive SST anomalies in the west and negative SST anomalies in the east. The increased rainfall was as a result of the enhanced convergence of moister than average air over the region. When SST poles were reversed in sign, decreased precipitation occurred over south-eastern Africa. The decreased precipitation was a result of drier than average air and increased low-level divergence (Reason, 2001)

There is a weak positive correlation between the SST changes in the Agulhas system and late summer rainfall. Warmer (cooler) than average SSTs in the Agulhas system are associated with wetter (drier) than average rainfall over parts of the summer rainfall region of South Africa (Landman and Mason, 1999(b); Tyson and Preston-Whyte, 2000). The potential influence of the Agulhas Current on the regional atmosphere was studied using two ensembles of an atmospheric general circulation model simulated over a one year period (Reason, 2000). In the first ensemble, the monthly climatology of the SST forcing was used. In the second ensemble, the signature of the Agulhas current was smoothed out so that the waters of the region only show a latitudinal variation in SST. In the smoothed SST ensemble, a near-surface cold anticylonic anomaly was generated over the greater Agulhas Current region. Cyclonic systems were weaker in this ensemble compared to climatology with significant reductions in rainfall over South Africa (Reason, 2000).

1.2.6.4. The Atlantic Ocean SSTs and rainfall over South Africa

The strongest association between South African rainfall and the Atlantic Ocean SSTs is in the central South Atlantic Ocean (Mason, 1995). The South African rainfall correlates negatively with the SST anomalies in the eastern South Atlantic Ocean off Namibia (Tyson and Preston-Whyte, 2000). SST gradient intensity in both the far south-western and the south-eastern Atlantic Ocean varies closely in phase with the annual rainfall totals of the summer rainfall region (Mason, 1995). A number of models to represent the response of the atmosphere to the SST forcing have been developed and are discussed next.

1.3. Seasonal modelling

1.3.1. Introduction to modelling

The future behaviour of the climate system can be determined through knowledge of its present state, and past behaviour from the first principles of the processes governing the climate system (Lau, 1992). The procedure described above is known as ocean or atmospheric modelling. The first principles are represented through the basic non-derived equations (primitive equations) describing the state of the atmosphere (Tyson and Preston-Whyte, 2004). The equations are believed to represent the physical, chemical and biological processes governing the climate systems (Lau, 1992). Global models to represent the processes governing the climate system are more generally called general circulation models (AMS, 2001). The general circulation models used for climate studies are called global climate models (GCMs) (Leung et al, 2002).

1.3.2. Seasonal forecasting

The atmospheric response to SST forcing is being predicted using a variety of methods. These methods include numerical and statistical models (Anderson et al, 1999). Measurable predictive skill has been demonstrated by statistical and dynamical models on seasonal timescales. The statistical and dynamical models are routinely used to predict SST anomalies. Links between the predicted SST anomalies and seasonal temperature and precipitation anomalies over the globe are then made. Seasonal forecasts are less specific than weather forecasts because the dynamics of the climate system are chaotic. The evolution of the individual weather events cannot be explicitly forecast on long-term time scales with any confidence. The predictands in existing operational seasonal are as a result aggregated (seasonal average temperature and seasonal total precipitation) (Fenessy and Shukla, 2000).

The internal variability of the atmospheric system introduces uncertainty into seasonal statistics. Seasonal climate predictions are probabilistic because of

the weather noise and the lack of understanding of all of the components of the climate system (AMS, 2001). The predictions are commonly expressed in terms of three-category probabilities: below-normal, normal and above-normal with quantiles computed from a climatological period (Robertson et al, 2004). Some potential useful information has been demonstrated from past seasonal forecasts when compared with corresponding observed outcomes (Wilks, 2001). Much of the aggregated forecasts' predictive ability is a result of the effects of ENSO on other parts of the climate system (Goddard et al, 2001). However, the operational forecasts have demonstrated predictive skill during non-ENSO periods as well (Shukla, 1998; Landman and Mason, 1999a).

1.3.3. Statistical seasonal modelling

In statistical modelling, techniques that relate the atmospheric conditions to a set of independent variables such as SSTs are used. The statistical models are generally less expensive to develop and to run than the numerical models, but are dependent upon the quality and quantity of historical observations (Anderson et al, 1999).

The skill of a statistical model to make monthly SST anomaly forecasts using the evolution of the SSTs as predictors was investigated (Landman and Mason, 2001). The model forecasts for an 18-year independent period (1982/1983-1999/2000), outscored forecasts of persisted anomalies beyond 6 months' lead time over the eastern Pacific Ocean. The model predictions also outscored persistence in the tropical Indian Ocean during the March-May spring season, but the skill was poor during the autumn months from September to November. The tropical Atlantic Ocean forecast skill was found to be generally poor (Landman and Mason, 2001).

Multivariate regression models were used over southern Africa to estimate summer rainfall and climate impact one season in advance. The preliminary statistical formulations included many variables influenced by the ENSO such as tropical SST in the Indian and Atlantic Ocean. Atmospheric circulation responses to ENSO that were noted include the alternation of tropical zonal

winds over Africa and changes in convective activity within oceanic monsoon troughs (Jury et al, 1998).

A statistical model that provides operational rainfall forecasts of austral summer rainfall over South Africa was developed (Landman and Mason, 1999a). The model used global-scale SSTs as the only predictors. The most important contribution of the predictive skill came from the equatorial Pacific Ocean, with weaker predictability from the equatorial Indian Ocean and Atlantic Ocean. Low to modest skill was found with the model (Landman and Mason, 1999a). The model was highly successful during ENSO years, and had a success hit rate of 40% for the non-ENSO years.

1.3.4. Dynamical seasonal modelling

GCMs are used at several centres as part of a two-tiered system for making seasonal climate forecasts up to several seasons in advance. The SSTs are predicted first, and these are then used as surface boundary conditions for ensembles of predictions with GCMs (Robertson et al, 2004). GCMs simulate precipitation and temperature and other atmospheric variables, with a resolution of about 300 km across the globe. It is necessary that multiple realisations are made for each model to make the predictions more robust and to quantify the uncertainty.

The multiple realisations can be produced by perturbing the initial conditions used in each model and repeating the model integration with each perturbed initial state (Fenessy and Shukla, 2000). Lagged average forecasting (LAF) can also be used to produce ensemble members (Hoffman et al, 1982). Each LAF ensemble member is started from the initial conditions observed at a time lagging the start of the forecast period by a different amount. The differences among the ensemble members give forecasts some measure of the likelihood that a particular seasonal climate state will be above, in, or below the normal interval (AMS, 2001).

A multi institutional joint study project named Dynamical Seasonal Prediction (DSP) was conducted to investigate the predictability of seasonal mean

climate anomalies using GCMs forced with the observed SSTs (Shukla et al, 2000). This kind of study where multiple models are compared is helpful in understanding which aspects of results are robust and which depend on the model used. All models showed higher forecast skill over the Pacific-North America for ENSO years compared to the non-ENSO years. Different models showed quite different levels of inter-annual variability even though identical global SST boundary conditions were utilised (Shukla et al, 2000).

An assessment of 13 year simulations of three atmospheric GCMs forced with observed SSTs were presented and compared with the NCEP reanalysis (Tennant, 2003). AGCM inter-annual variability as forced by SSTs was realistic. It reproduced the ENSO signal above noise levels that were determined from simulations using climatological SSTs (Tennant, 2003).

There is a need to combine model simulations because there is a huge amount of information, sometimes contradicting, regarding the seasonal climate of the region that is available to the user from the different models (Klopper and Landman, 2003). Different GCMs may perform better in different geographical locations and a combination of models has been shown to outperform a single model globally (Klopper and Landman, 2003; Robertson et al, 2004). Several methods exist for combining together the ensemble simulations from multiple GCMs. A Bayesian optimal weighting scheme was used to combine six atmospheric GCM seasonal hindcast ensembles (Robertson et al, 2004). The skill of the combination scheme was almost always increased when the number of models in the combination was increased from three to six, regardless of which models were included in the three-model combination (Robertson et al, 2004).

On a seasonal time scale, the importance of the effects of initial conditions is weakened considerably but these initial conditions do have a detectable influence (Goddard et al, 2001). Anderson and Ploshay (2000) conducted a study in which they investigated the influence of the initial conditions on seasonal forecasts. They found that the effects of introducing IC information for the land surface and atmosphere might actually reduce the skill of seasonal simulations in some instances. They interpreted this as being the

results of initial-error growth due to the shock of inserting observed ICs which are inconsistent with the model climatology and therefore extending the spin up period. One therefore needs to carefully evaluate the efficiency of using ICs when making seasonal predictions with atmospheric GCMs (Anderson and Ploshay, 2000).

1.3.5. Dynamical vs. statistical models

An assessment of the capabilities of one statistical model and two numerical models to simulate the extra-tropical atmosphere was investigated (Anderson et al, 1999). On average, the statistical model was found to produce considerably better simulations than either numerical model, even when numerical model simulations were bias corrected. The simulation skill was found to be generally low, but there were some individual seasons for which all three models produced simulations with good skill (Anderson et al, 1999).

The skill of a statistical model and a GCM's summer rainfall forecast for southern Africa were compared over a 10-year retro-active period from 1987/1988 to 1996/1997 (Landman et al, 2000). The multi-tiered scheme (numerical) was able to produce skill levels that were better than chance and outscored the baseline skill level of a linear statistical model. GCM simulations using persisted August SST anomalies instead of forecast SSTs produced skill levels similar to those of the baseline for longer lead-times (Landman et al, 2000).

Klopper and Landman (2003) proposed a system to produce a combined forecast from output from different models (statistical and dynamical) to predict seasonal rainfall for southern Africa in DJF. Three models used in the study were a linear statistical model (Landman and Mason, 1999a), a non-linear statistical model (Mason, 1998) and output from the Model Output Statistics (MOS) recalibrated atmospheric GCM (Landman and Goddard, 2003). The conditional probabilities were assumed to be equally probable and therefore the proposed method took a simple unweighted average. The combined forecasts performed generally better than any of the individual

forecasts. The proposed procedure was able to capture rainfall scenarios sufficiently during ENSO events.

1.4. Global Climate Models limitations and downscaling procedures

1.4.1. Global Climate Model's limitations

GCMs are generally run at a resolution of roughly 300 km (Robertson et al, 2004). The GCMs are restricted to this grid point spacing by computing power - running a GCM at a mesoscale resolution of about 60 km in the horizontal will require increased computer resources (Ji and Verneker, 1996). There are GCMs that are currently run at a much higher resolution but due to the amount of computer power needed, most centres continue to make low resolution GCM simulations.

1.4.1.1. Small scale features

Small scale features can affect the mean model climatology significantly; however the GCMs cannot parameterise these features adequately due to the course resolution of the models (McGregor et al, 1993). GCM simulations of rainfall, in particular, are unreliable and there is a need to provide accurate simulations of present and future climate (Joubert et al, 1999). The temperature extremes normally cover large areas (Kunkel et al, 2002) and the large scale structure and variability of the atmosphere are well characterised by the GCMs (Wilby and Wigley, 2000) while precipitation events are often highly localised in time and space (Kunkel et al, 2002).

1.4.1.1.1. Precipitation

Temperature and circulation patterns are larger scale and hence their predictive skill is usually higher than that of precipitation for the same location and time (Gong et al, 2003). Precipitation has smaller-scale complex features

that result in its noisier and less predictable character. The discrete individual convective cells producing precipitation are the major reasons for the noisy small-scale character of the precipitation events. Even non-convective precipitation usually contains pockets of locally heavy rainfall. Even when totalled over a 3-month period, substantial irregularities in the spatial pattern of rainfall are likely (Gong et al, 2003; Kunkel et al, 2002).

1.4.1.2. The topographic representation

One of the reasons why the coarse resolution of the GCMs leads to unrealistic small scale feature simulations is the poor representation of the topography in the models (McGregor et al, 1993). The topography influences the representation of the climate variables such as rainfall and temperature. The influence topography has on temperature is clearly visible over the escarpment situated over the southern and eastern part of South Africa, where the highest altitudes are characterised by the lowest temperatures (Figure 1.2 and 1.3). The large scale spatial differences in rainfall totals over relatively short distances over South Africa are also due to the escarpment (Tyson and Preston-Whyte, 2000; Engelbrecht et al, 2002; Joubert et al, 1999).

1.4.2. Downscaling/recalibrating

An alternative to produce high resolution simulations using less computing power is downscaling, which is possible through statistical (Wilby and Wigley, 2000) and dynamical methods (McGregor et al, 1993; Giorgi, 1990). The word recalibrating is normally used when making forecasts or simulations for spatial scales larger than the resolution of the model. For downscaling, forecasts or simulations are made using statistical or dynamical methods or a combination

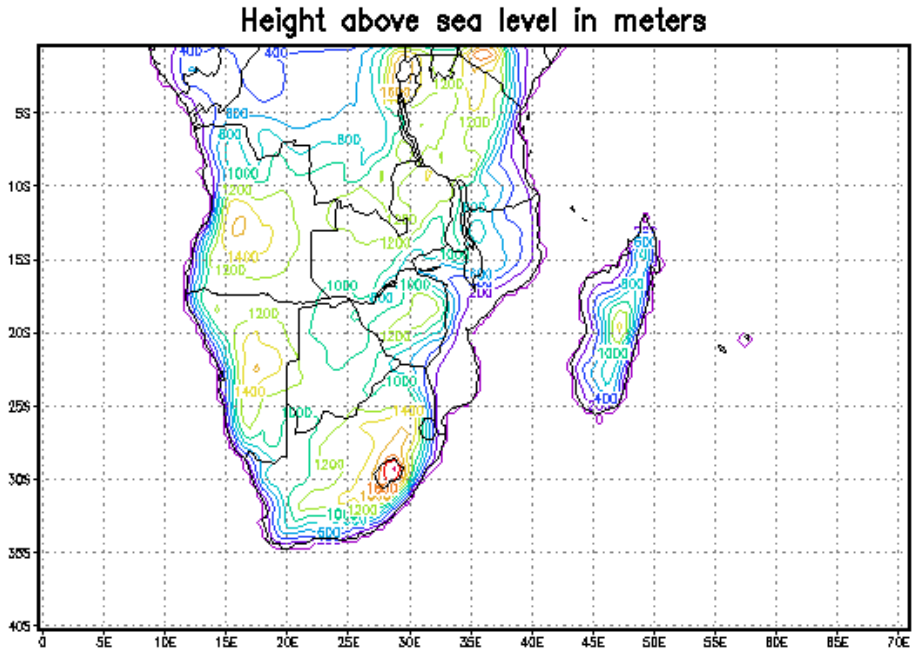

Figure 1.2: *The topography of southern Africa in meters above sea level and the domain of the RegCM3.*

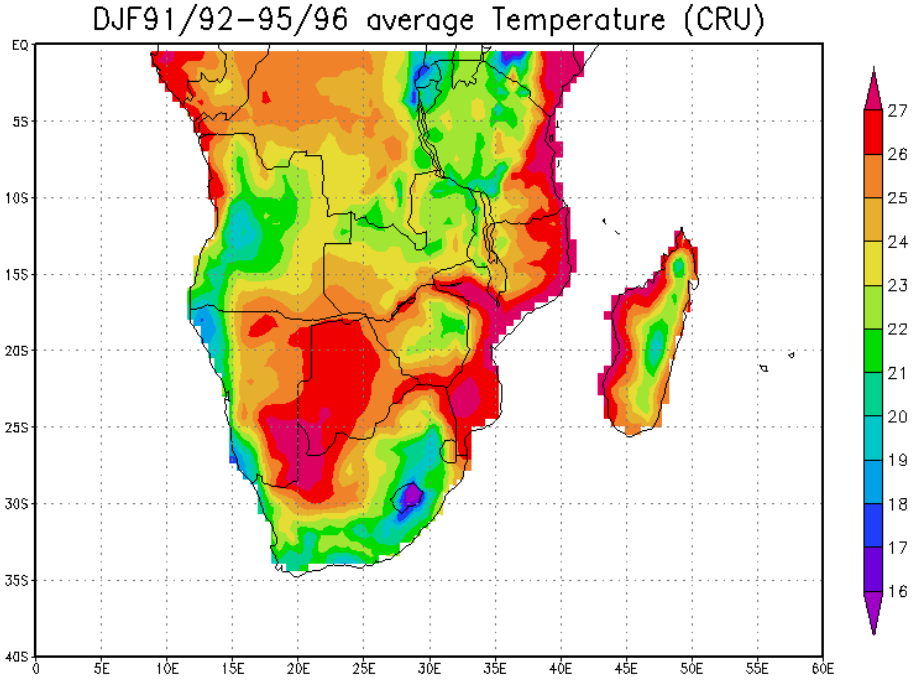

Figure 1.3: *The average Climate Research Unit observed temperature for the summer season defined as December, January and February (DJF) from 1991/1992 to 2000/2001 in ℃.*

of the two, for grid-points at a resolution finer than that of the GCM or for stations. These downscaling procedures are especially relevant for developing countries where computer resources are limited. The simulated large-scale circulation by GCMs generally compares well with the observed circulation. It is therefore expected that downscaling GCM large scale output to specific rainfall regions of interest will produce improved rainfall forecasts (Landman and Goddard, 2005).

1.4.2.1. Statistical downscaling

Statistical downscaling is based on three assumptions (Wilby and Wigley, 2000). The first one is that suitable relationships exist between large scale predictor circulation and smaller scale predictand variables. The second assumption is that these empirical relationships are valid under future climate conditions. The last assumption is that the predictor variables and their changes are well characterised by GCMs. If these assumptions are met, mathematical equations can be constructed to predict local precipitation from simulated large scale circulation. The two methods used in statistical downscaling are Perfect Prognosis (PP) and Model Output Statistics (MOS) (Wilks, 1995). In PP the same system of equations obtained through relating the observed (simulated) large scale features and the observed (simulated) small scale features is applied in a forecast setting. PP assumes that the relationships between the variables do not change in the forecast setting (Wilby and Wigley, 2000). In MOS a system of equations are obtained through analysing the relationship between the simulated large scale fields and the observed small scale fields.

The statistical downscaling procedures have been applied over many regions including southern Africa. A MOS recalibration technique was applied over southern Africa to recalibrate large scale circulation features produced by the ECHAM3.6 GCM to observed regional rainfall for the December-January-February (DJF) season (Landman and Goddard, 2002). The 850 hPa geopotential heights were used as the predictor. The recalibrated forecasts were found to outscore the GCM-simulated rainfall anomalies (Landman and Goddard, 2003). The PP procedure has also been applied in South Africa to

recalibrate COLA T30 simulations to streamflow for DJF 1987/1988 to 1994/1995 seasons (Landman et al, 2001). Successful forecasts of streamflow categories (below-normal, normal and above-normal) were obtained for some years.

A MOS procedure was used to downscale bias-corrected GCM (COLA T30) sea-level pressure and 500 hPa height fields to the regional rainfall of seven homogeneous regions in South Africa for 30-day periods within the DJF season. The best skill was found for the central interior, followed by the western interior, the eastern coast, the north-eastern interior and the Lowveld. Forecasts of extreme events (droughts and floods) were predicted skilfully over the larger area of the summer rainfall region, even during years that were not associated with El Niño and La Niña events. (Landman and Tennant, 2000).

The PP and MOS techniques were utilised to recalibrate the CSIRO 9 GCM large scale fields statistically to three equi-probable rainfall categories for DJF over southern Africa. MOS produced the higher skill for the independent test period (Bartman et al, 2003). A method of combining the attributes of MOS and PP called MOS-PP into a single forecast system has been proposed, and tested over southern Africa (Landman and Goddard, 2005). The proposed system uses atmospheric GCM simulation data to construct MOS equations and subsequently uses forecast fields of the same atmospheric GCM at various lead times in the simulation MOS-equations. High skill was found over most of the regions when the driest and the wettest years were forecast using the system.

1.4.2.2. Dynamical downscaling

Dynamical downscaling utilizes high resolution regional climate models (RCMs) to derive regional climate information, on a selected domain that covers an area of interest (Leung et al, 2003; Giorgi, 1990; McGregor et al, 1993). An RCM is nested within a GCM or global analyses of observations which provides the required large-scale conditions (the initial conditions (ICs)

and the time dependant lateral boundary conditions (LBCs)) (Fennessy and Shukla, 2000). The RCMs produce high resolution simulation of surface variables which are most affected by vegetation, land use and topographic features that can vary substantially over spatial scales of a few kilometres (Kim et al, 2000). Regional climate simulations are more than an interpolation of the lower resolution data from GCMs or the reanalyses. Regional climate modelling exploits the four dimensional dynamics of the model, which account for the interaction of mesoscale circulations with a high-resolution representation of the local topography (Druyan et al, 2002). The RCMs, therefore, also offer a chance of understanding the regional climate better because they use physically and dynamically consistent ways (Kim et al, 2000).

1.4.2.2.1 RCMs vs. LAMs used for short term

Limited Area Models (LAMs) are nested models, and hence RCMs are also called LAMs. The primary difference between RCMs and LAMs used for short-term weather forecasting is that RCM simulations are initialised only once. They are then extended for long simulation times (months to years) with the large-scale meteorological fields provided at the lateral boundaries at consecutive time periods (Giorgi and Bi, 2000). Initialisation is less important for an RCM's climatology while for LAMs used for weather forecasting initialisation is crucial (Giorgi and Mearns, 1999). A dynamical equilibrium among the LBC forcing, the model-generated forcing from the interior of the domain, and the internal model physics and dynamics determine an RCM's climatology (Giorgi and Bi, 2000). Some sensitivity studies have been conducted to investigate the sensitivity of the regional model's simulations on factors such as the domain choice (Seth and Giorgi, 1998; Seth and Rojas, 2003; Landman et al, 2005), model reinitialisations (Pan et al, 1998; Qian et al, 2003) and the model resolution (Giorgi and Marinucci, 1995).

1.4.2.2.2. Domain

The RCM simulations are affected by the domain size and location of the lateral boundaries (Seth and Giorgi, 1997). Sensitivity to model domain (size

and location) depends on whether large scale forcings originate from within or outside of the regional domain (Leung et al, 2003). The model domain should be large enough to encompass all regions that include forcings and circulations which directly affect climate over the area of interest as much as possible (Giorgi and Mearns, 1999; Seth and Giorgi, 1997). If the domain size is small and the region of interest is closer to the lateral boundaries, the influence of the LBCs on the model solution will be large. In a study by Seth and Giorgi (1997) it was found that when the reanalyses were used as forcing fields that a smaller domain produced the best simulations. It was established in a study where an RCM, DARLAM, was used that simulations were improved away from the boundaries of the domain, and were generally best in mid-latitude regions (Walsh and McGregor, 1995).

The effects of the model domain size and the positions of its lateral boundaries on the simulation of tropical cyclone-like vortices and their tracks on a seasonal time scale in the Indian ocean were investigated (Landman et al, 2005). The simulation of the life-cycle of tropical cyclone-like vortices were affected by the positioning of the eastern and northern boundary of the RCM's domain. The size of the domain was found to have a bearing on the ability of the regional model to simulate vortices in the Mozambique Channel. Madagascar also influences the storm tracks and therefore it is advisable that for the sensitivity studies over southern Africa Madagascar is included in the RCM's domain (Landman et al, 2005).

1.4.2.2.3. Model reinitialisation

Every time a model is reinitialised, spin up problems are introduced (Pan et al, 1998). The advantages of model reinitialisation are that long simulations can be run in parallel and also that accumulated model errors can be reduced. The effects of reinitialisation frequency were analysed by Pan et al (1998) and Qian et al (2003). In the integrations that continued without reinitialisation, locations of specific meteorological features drifted downstream, implying the need for periodic reinitialisation of the model (Qian et al, 2003; Pan et al, 1998). When model reinitialisation interval is relatively long, simulated domain-averaged variables, including rainfall, were not very sensitive to

model reinitialisation because they are controlled to a large extent by boundary conditions.

1.4.2.2.4. Resolution and topography

The RCM's sensitivity to horizontal resolution and topographic forcing has been investigated (Giorgi and Marinucci, 1995). The model was run for January and July month-long simulations over Europe with a resolution that ranged from 200 to 50 km and with various topography configurations. The precipitation amounts were found to be more sensitive to the resolution than to topographic forcing. The topographic effect was found to be on the spatial distribution of precipitation only in areas of complex topographic features (Giorgi and Marinucci, 1995).

1.4.2.2.5. Large scale features in GCMs and RCMs

The utility of RCMs is not to improve the GCM's large scale circulation simulations (Leung and Ghan, 1998). The downscaling procedures assume that GCMs are able to simulate the characteristics of the large scale circulations (Leung et al, 2003). It then follows that the successful application of nested modelling approach requires that the GCM provides a sufficiently accurate broad-scale simulation (Giorgi and Mearns, 1999). RCM simulations should be expected to deviate from GCM simulations at the lower atmosphere, on spatial scales influenced by surface boundary conditions. In practise the large scale simulated by the RCMs might differ from those simulated by GCMs mainly because of differences in the physical parameterisations used by the models (Leung and Ghan, 1998; McGregor, 1993).

In reality the GCM large scale circulation have errors. In a nested system the errors in the large scale circulations produced by the driving model are transmitted to the nested model. Nested models can sometimes improve the large scale patterns of surface fields compared to the driving GCMs (Giorgi and Mearns, 1999). However, in general if a GCM misplaces the location of major storm tracks or other large scale circulation features, this misplacement

will be reflected in the nested model. When output from a GCM simulation is used to drive a regional model, an evaluation of the model performance in simulating large scale circulation patterns over the region of interest needs to be carried out. If different GCM simulations are available, the best performing one should be selected for model nesting in order to minimise the effects of errors in the large-scale fields provided to the RCM at the lateral boundaries (Giorgi and Mearns, 1999).

1.4.2.2.6. GCM forced vs. reanalyses forced

Rojas and Seth (2003) and Seth and Rojas (2003) used a regional climate model driven by reanalyses and ensemble integrations of a GCM to simulate two extreme rainfall seasons over south America. The nested model rainfall forced with GCM output was found to be degraded compared to those from the reanalyses-driven RegCM integrations. Druyan et al (2002) nested an RCM within a GCM and the NCEP reanalyses and used the predicted SSTs and observed SSTs to force the model at the surface boundary. The results from the experiment showed that using actual climate data to drive the RCMs does not guarantee realistic modelled precipitation distributions.

1.4.2.2.7. Details vs. accuracy

Dynamical downscaling provides enhanced details of climate simulations due to the high resolution of the RCMs. However, detail does not imply accuracy. It is therefore important to evaluate statistical structures of climate signals at various spatial scales to determine if predictability is improved with regional over global modelling (Leung et al, 2002). Since one of the objectives of nested climate runs is to model mesoscale features affecting a region, it also needs to be verified that the RCM realistically simulates those features. The rainfall events are highly localised in time and space (Kunkel et al, 2002) and hence are regarded as small scale. A considerable amount of work has been done on regional climate modelling and as a result a number of RCMs have been developed.

1.4.2.2.8. Long-term RCM simulations

A number of studies have been conducted where simulations were made over a number of years to determine if the RCMs capture the general atmospheric patterns (Giorgi, 1990; Fennesy and Shukla, 1999; Ji and Verneker, 1996; Kim et al, 2000; Druyan et al, 2000; Leung and Ghan, 1998; Gallee et al, 2004). Some simulations were made just for two months, one in winter and one in summer, which are thought of as representing the middle of the season concerned (Giorgi et al, 1993a;b; Renwick et al, 1999; Walsh and McGregor, 1995). These studies determine if an RCM's solution is sensitive to the general mean atmospheric circulation patterns that determine the intra-annual seasonal changes. The studies have shown that the nested models are generally as good as or better than the GCMs. In some cases the RCMs even reduced the errors in the large scale simulations.

Similar kinds of regional modelling studies have been conducted over South Africa by Engelbrecht et al (2000) and Joubert et al (1999) using the Division of Atmospheric Research Limited Area Model (DARLAM). DARLAM was nested within the CSIRO 9 Mark 2 GCM for January (Joubert et al, 1999) and July (Engelbrecht et al, 2000) for a period of 10-years. The simulations have demonstrated that DARLAM is generally able to simulate the details of regional climate better than the GCM, although rainfall was often overestimated in regions of steep topography (Joubert et al, 1999; Engelbrecht et al 2000). The problem is related to the fact that regional climate models tend to simulate too many rain days, as well as rainfall intensity (rain per day) which is lower than observed (Joubert et al, 1999).

1.4.2.2.9. Inter-annual RCM simulations

In order to be useful for practical climate applications, a nested model must be able to predict features of the observed inter-annual variability (Fenessy and Shukla, 2000). The inter-annual variability of the RCMs has been investigated by looking at the dry and wet years (Walsh and McGregor, 1997; Druyan et al, 2002; Seth and Rojas, 2003; Rojas and Seth, 2003). The RCMs used in these

studies were able to capture the differences in the mean rainfall for the different years over the different areas of interest.

1.5. Intra-seasonal

1.5.1. The need for intra-seasonal studies

The changes in the statistics of the daily events within a season lead to changes in the statistics of a season (Wilks, 2001). The character of the rainfall within the season often exerts a greater influence than does the seasonal total, as a result, seasonal forecasts are only marginally useful. Seasons with similar rainfall totals can have quite diverse characteristics of rainfall (Tennant and Hewitson, 2002). The prediction of wet and dry seasons is useful, but agricultural production and water resource management require a more detailed knowledge of the rainfall and temperature characteristics on the day to week event scale (Matarira and Jury, 1991). Agriculture drives the country's economy and therefore it is important to understand and predict the temporal and spatial distribution of rainfall in the austral summer season (Harrison, 1984a).

The chaotic characteristic of the atmosphere makes prediction of about two weeks to two months challenging (AMS, 2001). The noise-levels are reduced when simulations are averaged out (Chervin, 1974). Hence the forecasts in the range from several weeks to less than a season tend to be less skilful than seasonal climate forecasts. There is however, evidence that under some conditions strong regional boundary forcing useful skill may be realised on shorter climate timescales (AMS, 2001).

The distribution of the number of rain days per year can be expected to resemble that of the total rainfall. However, it is not a case of direct proportionality because of the different characteristics of precipitation events, their types and time distribution (Taljaard, 1986). The distribution of the wet and dry spells within the season was found to be related to seasonal total

rainfall over South Africa (Cook et al, 2004). Wetter seasons tend to have longer or more intense wet spells rather than a greater number of wet spells (Cook et al, 2004). Seasons with a high total rainfall generally have a higher number of heavy rain days and not necessarily an increase in light rain days (Tennant and Hewitson, 2002). It was found that the length of the period between rain days has a low correlation to seasonal totals, and therefore that seasons with a high total rainfall may still contain prolonged dry periods (Tennant and Hewitson, 2002).

The intra-seasonal climate variability over southern Africa has been studied based on observational analyses of selected wet and dry spells (Taljaard, 1986; Miron and Lindesay, 1983). The historical distribution of summer rainfall over southern Africa is typically composed of five wet spells, occurring at approximately monthly intervals from late November to late March. During the dry summers of 1987 and 1992 there were only two wet spells in December and January. The relatively wet years of 1989 and 1990 exhibit continuously wet periods in January and February (Taljaard, 1986).

In addition to getting a reasonable prediction of seasonal mean precipitation, it is important that a model correctly predicts the intra-seasonal variability, particularly for precipitation (Fennessy and Shukla, 2000). Over many parts of the world, ENSO forcing of the seasonal total rainfall is accomplished through affecting the frequency and intensity of rainfall in different regions. A study was conducted where attempts were made to predict the intra-seasonal characteristics over the US using ENSO as the predictor (Gershunov et al, 2000; Gershunov, 1998). Given a perfect forecast of ENSO, the frequency of intra-seasonal extremes is specified as the average frequency of occurrence during similar-phased ENSO seasons on record. The skill was found to depend on varying ENSO sensitivity in different geographic regions. The quantile ranges and consistency or variability from one ENSO event to another ENSO sensitivity varied according to the intensity of the tropical forcing. Good predictability is likely for variables and in regions displaying a strong and consistent ENSO signal (Gershunov, 1998).

An assessment of 13 year simulations of three atmospheric GCMs forced with observed SSTs were presented and compared with the NCEP reanalysis. Daily circulation statistics were well represented by the Hadley Centre Atmospheric Climate Model (HADAM3) but the COLA and CSIRO9 models produced flow patterns biased toward atmospheric archetype modes (Tennant, 2003).

The atmospheric GCM and nested model simulations of the daily precipitation variability was examined over different regions of the United States and the regional model was found to have a more realistic intra-seasonal variability compared to the atmospheric GCM alone (Fennessy and Shukla, 2000). Time series of daily mean rainfall were averaged over two 2.5° x 2.5° grid meshes in the Niamey region in West Africa from the MAR regional model (Gallee et al, 2004). Maxima reaching up to 40 mm/day are found in the same areas in the simulations as in the observations.

Kunkel et al (2002) presented a paper that described an analysis of a 10-year simulation from a regional climate model, comparing model estimates with observations of heavy precipitation and seasonal anomalies. Model thresholds for heavy precipitation events were generally greater than the observed thresholds in the mountainous regions of the western United States and less than observed along the west coast. The timing of specific events between model solutions and observations did not correspond generally, reflecting differences between model and observations in the speed and path of many of the synoptic-scale events triggering the precipitation (Kunkel et al, 2002).

1.6. The status of long-range forecasting at the South African Weather Service

Considerable progress has been made since the early 1990s to develop models that are able to predict the seasonal climate behaviour over southern African. Seasonal forecasts have been issued since the early 1990s by

groups both locally and internationally. Most algorithms for predicting southern African inter-seasonal climate variability have made use of linear statistics, relating seasonal rainfall to global SSTs, outgoing long-wave radiation and various atmospheric pressure and wind indices (Jury et al, 1998; Landman and Mason, 2001). In addition to statistical methods, the COLA T30 GCM has been used successfully operationally to predict seasonal rainfall over the summer rainfall region of southern Africa at the South African Weather Service (SAWS) (Landman and Tennant, 2000).

A combination of models has shown to outperform a single model globally (Klopper and Landman, 2003) and as a result SAWS combines a number of models to produce its forecasts. The procedure to come up with seasonal forecasts at the SAWS is as follows: The output from statistical models and GCMs run at the SAWS, and GCMs run at the University of Cape Town (UCT), the European Centre for Medium-Range Weather Forecasts (ECMWF) and the United Kingdom Met Office (UK Met-Office) are used as input to derive the forecasts. The International Research Institute for Climate and Society (IRI) maps derived from the models run at the IRI and as well other meteorological centres are also used. A group of seasonal forecast specialists from the SAWS, UCT and the Agricultural Research Council (ARC) produce the forecasts based on the model output and expert interpretation on the current climatic conditions (SAWS, 2006).

An example of the seasonal forecast issued by the SAWS and the corresponding observations are given in Figure 1.4 and Figure 1.5 for November-January 2005/2006. During the season the greatest part of the country received normal to above-normal rainfall with the exception of the south-western part of the country. In the forecast issued for the summer rainfall regions, a higher probability was assigned to the normal category and the next likely category was above-normal. The highest probability of 40% of the below-normal category was given to the southern and western coast and the adjacent interior.

It has been found that the GCMs are unable to simulate precipitation with a high level of skill due to their low resolution ((McGregor, 1993; Giorgi, 1990).

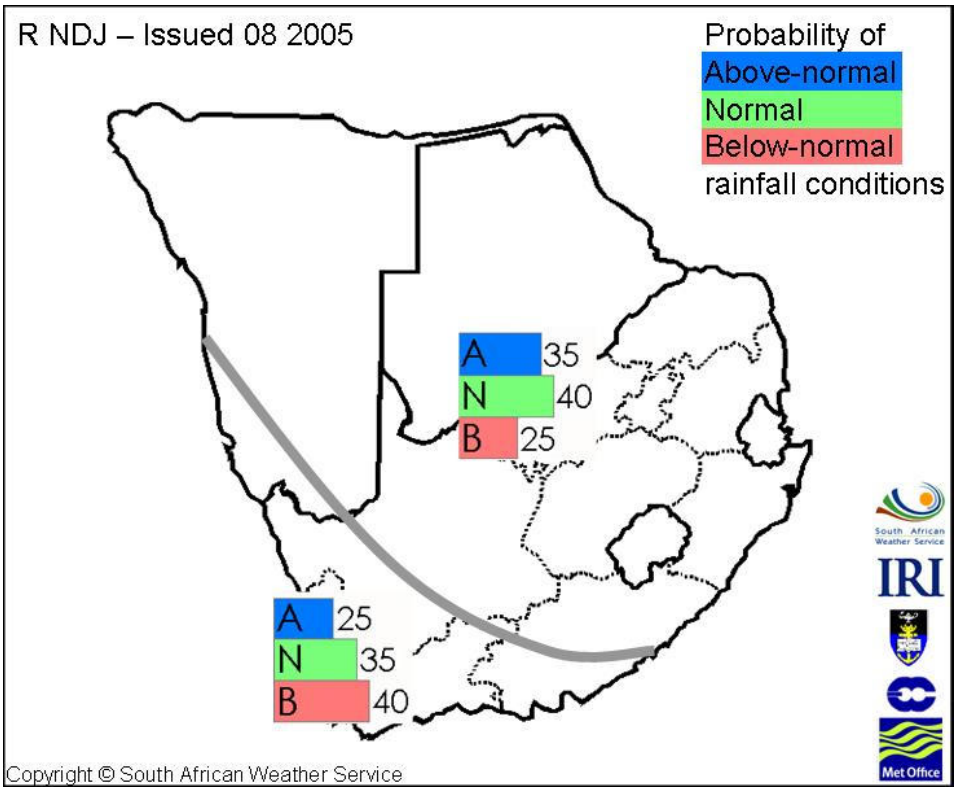

***Figure 1.4**: The probabilistic seasonal rainfall forecast for November-January 2005/2006 as issued by the South African Weather Service in August 2005.*

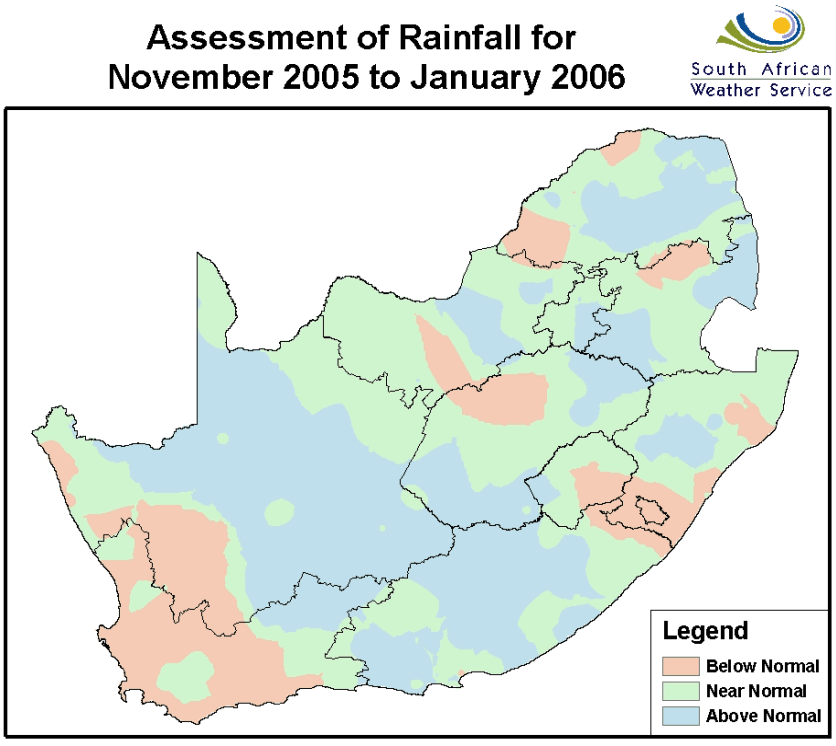

***Figure 1.5**: The observed seasonal rainfall in three categories in the three categories over South Africa for the season November-January 2005/2006.*

The downscaling procedure was developed to correct the biases in the GCM simulations (statistical downscaling) and also to produce simulations with high resolution (RCMs). At the SAWS a statistical downscaling procedure called MOS-PP (Landman and Goddard, 2005) is also used operationally in addition to all the models mentioned above. The RCMs are not used operationally yet and it is the plan of SAWS to produce an operational regional climate modelling system by the end of the 2006. In addition to the high resolution model simulations that will be obtained from the RCMs, intra-seasonal forecasts will be made using the RCM, if the RCM is found to produce the intra-seasonal characteristic skilfully. The best possible way to produce the simulations using the available models has to be determined before the models are used operationally.

1.7. The Internal variability of the GCM and the RCM

1.7.1. A GCM's internal variability

The internal variability of the models is central to the question of the predictability of the atmosphere. In operational forecasting, multiple realisations are made using the GCM due to non-linearities in the GCM (Giorgi and Bi, 2000). GCM solutions started with initial conditions that are slightly different from one another will diverge substantially after a few days of simulations. The solutions will diverge from one another as a result of the internal variability of the GCM. The differences among the ensemble members give the forecasts some measure of the likelihood that a particular seasonal climate state will be below, in, or above the normal interval (AMS, 2001). The seasonal forecasts produced in this way have proved to be skilful.

1.7.2. An RCM's internal variability

In regional climate modelling an RCM is nested within a GCM which provides the ICs and the time dependent LBCs. The lateral boundary forcing limits the degrees of freedom of RCMs, and as a result an RCM's climatology will not

diverge from the forcing fields strongly (Giorgi and Bi, 2000). The RCM's physics and dynamics are just as non-linear as the GCM's are, and so although they are restricted by the boundary forcing, they are expected to exhibit a certain level of the internal variability. If an RCM is nested within a GCM the solutions that are obtained are a function of the internal variability of GCM as well as of the RCM. It is therefore necessary to investigate the amount of variability introduced to the nested system solutions by the RCM's internal variability. The question is central to seasonal forecasting using an RCM because it has to be established as to whether or not it is necessary to produce multiple realisations to quantify the uncertainty associated with non-linearities in an RCM as it is done for the GCM.

Giorgi and Bi (2000) analysed sensitivity experiments in which random perturbations were applied to the ICs and LBCs of a set of seasonal RCM simulations over eastern Asia. In the experiment they found that the sensitivity to the perturbations grew for the first 5-15 days of the simulation and then reached a dynamical equilibrium. The perturbations did not affect the domain-wide average climatology significantly , but it substantially influenced the day-to-day model solution. The influence was significant especially for precipitation, and aspects of the model climate such as the frequency of occurrence of heavy precipitation events.

Estimates of external (SST forced signal) and internal (dynamics generated noise) variability were made for both the global model and the nested model predictions (Fennessy and Shukla, 2000). The signal, noise, and signal-to-noise ratios of the near-surface temperature and precipitation fields were generally quite similar between the nested model and the global model predictions. In the winter season the nested model had larger signal-to-noise ratios in both temperature and precipitation than did the GCM alone (Fennessy and Shukla, 2000).

1.8. Summary

In general, the precipitation of South Africa increases from west to east, except along the southern coast. Maximum altitudes in excess of 3500 m occur along the South African escarpment. The latter escarpment results in large scale spatial differences in rainfall totals over relatively short distances over South Africa. South Africa is situated in the subtropics and therefore it is affected by the circulations systems in the tropics, the subtropics and the middle latitudes. The atmospheric systems that are operating in the region result in the rainfall that is highly seasonal. More than 80% of the annual rainfall over the most part of the country is received in summer. Tropical circulations dominate during late summer. In a study conducted over the period 1980-1999 it was found that the GDP is closely associated with the summer rainfall and therefore forecasts issued one season in advance could greatly assist the management of environmental and financial resources in the country.

The atmosphere is chaotic and hence predictability is limited. Simulations started with slightly different initial conditions will diverge after a finite amount of time. This is an issue of concern because of the lack and errors in the observations that are available for the initial conditions. However, it was found that the tropical atmosphere does not adhere to the definition of chaos. The tropical seasonal circulation and rainfall are strongly affected by the boundary conditions of the SSTs. It should therefore be possible to predict the tropical large scale seasonal circulation and rainfall for as long as the SSTs can be predicted. The high predictability of tropical rainfall for a given SST can therefore enhance the predictability of seasonal mean circulation in certain extra-tropical regions.

Numerical models, especially GCMs, have been used to predict the response of the atmosphere to the forcing fields. Due to the non-linearities in the atmosphere the seasonal forecasts are aggregated (average temperature and total rainfall) and they are expressed probabilistically (below-normal, normal and above-normal). Comparison of past seasonal forecasts with the

corresponding observed seasonal outcomes has demonstrated real potential useful information content.

GCMs are generally run at a resolution of about 300 km and therefore are unable to simulate small scale features effectively and are generally skilful in producing the large scale structure of the atmosphere. However, the predictive skill for precipitation is limited because precipitation events are highly localised in time and space. Downscaling was introduced as a feasible method to produce high resolution simulations with less computer resources than those required if a GCM were to run with the same resolution. This procedure is possible through statistical and dynamical methods. In the latter method RCMs are nested within the GCM that provides the ICs and the time dependent LBCs. RCMs have been found to produce more skill as compared to the GCMs, especially when variables that are affected by the characteristic of the land surface are considered.

The skill of both the GCMs and RCMs to capture the inter-annual rainfall variability has been investigated over many parts of the world. The models were found to capture the inter-annual variability. The regional climate modelling work with special emphasis over South Africa is limited. That is also illustrated by the fact that at the SAWS where seasonal forecasts have been issued since 1994, RCMs are not used as yet to generate the raw model output. The SAWS aims to have an operational multi-regional climate modelling system. The best possible ways to implement the RCMs have to be determined before the models are used operationally.

The GCMs represent the atmospheric processes that by nature have a non-linear characteristic. To quantify the uncertainty associated with the internal variability of the GCM, multiple realisations for each GCM have to be produced in operational forecasting and also in experiments. In regional climate modelling an RCM is nested within a GCM which provides the ICs and the time dependent LBCs. The lateral boundary forcing limits the degrees of freedom of RCMs, and therefore an RCM's climatology will not diverge from the forcing fields strongly. The RCM's physics and dynamics are non-linear just as the GCM's are and so although they are restricted by the boundary

forcing, they are expected to exhibit a certain level of the internal variability. The solutions of a nested system of an RCM and a GCM are subject to the internal variability of both the GCM and the RCM.

1.9. Aim of the study

The core aim of the research in this dissertation is to investigate the internal variability of an RCM. In operational forecasting an RCM is nested within a GCM which also has an internal variability. The nested system solutions are therefore influenced by the internal variability of both the GCM and of the RCM.

Objective 1

To investigate the internal variability of the GCM and the RCM

GCM simulations started with initial conditions that are different from one another will diverge substantially after a few days of simulation. The divergence of the solutions is due to the internal variability of the GCMs. In this study GCM simulations are made using different initial conditions. The realisations obtained from each initial condition are used to force an RCM. An RCM also represents the atmospheric processes and therefore its internal variability influences the simulations. The divergence of the nested system solutions is therefore due to a combination of the internal variability of the GCM and the RCM. The question that is asked is to what extent will the nested system solutions obtained from the procedure explained above diverge from one another?

Objective 2

To investigate the internal variability of the RCM

In regional climate modelling an RCM is nested within a GCM which provides the ICs and the time dependent LBCs. The RCM's physics and dynamics are as non-linear as the GCM's are and so, although they are restricted by the

boundary forcing, they are expected to exhibit a certain level of the internal variability. In this part of the study, the question is, to what extent does the internal variability of the RCM influence the variability of the solutions obtained from a nested system. In other words, to what extent will the RCM solutions diverge from one another when started with different ICs with the LBCs kept the same?

CHAPTER 2: DATA, METHODS AND NUMERICAL MODELS

2.1. Introduction

More than 80% of the annual rainfall over most parts of South Africa is received between October and March (Taljaard, 1986). The GDP has been found to have a close association with the summer rainfall over South Africa (Jury, 2002). Forecasts of summer rainfall more than one season in advance could greatly assist the management of environmental and financial resources in the country. Seasonal forecasts have been issued by SAWS since 1994 and they have proved to be skilful. Seasonal predictability is derived from the fact that slowly evolving boundary conditions such as the SSTs leave some memory in the atmosphere and therefore render the atmosphere partly predictable (Shukla, 1998). This is especially true in the tropical atmosphere. The tropical circulations dominate over South Africa in late summer (Harrison, 1994a). Given that most of the rainfall is received in summer and that the tropical atmosphere dominates in late summer, the study concentrates only on the summer season defined as December to February (DJF).

The models that are used operationally at SAWS to produce forecasts are GCMs, statistical models and statistical downscaling models (SAWS, 2006). The RCMs are not used as yet in the production of seasonal forecasts and it is the plan of SAWS to have the RCMs used operationally by the end of 2006. Before a model is used to produce operational rainfall forecasts researchers have to determine ways in which they will obtain the best possible simulations from the models. The question of the internal variability of the model is very important in modelling because it lies at the centre of the predictability of the atmosphere using the dynamical models. The atmosphere is chaotic (Shukla, 1998) and as a result the models representing the climate system are nonlinear (Giorgi and Bi, 2000).

In order to make the predictions more robust and to quantify the uncertainty, it is necessary to make multiple realisations for a particular SST forecast. The multiple realisations can be produced by perturbing the initial conditions used

in each model and repeating the model integration with each perturbed initial state. LAF can also be used to make ensemble members (Hoffman et al, 1982). The departures from the ensemble mean are a measure of the model's internal variability. The aim of this study is to investigate the internal variability of the GCM and the RCM and then to determine to what extent does the internal variability of the RCM influence the variability of the nested system simulations.

In this study the internal variability of an RCM is studied using the GCM simulations as lateral boundary conditions, and observed SSTs at the surface boundary. Using observed global SSTs as lower boundary conditions helps determine the upper limit of SST forced predictability (Shukla et al, 2000). In operational forecasting an RCM is forced with the GCM simulations which are also subject to the GCM's internal variability (Giorgi and Bi, 2000). The nested solutions are therefore subject to the internal variability of both GCMs and the RCMs.

2.2. The GCM's and the RCM's internal variability

The GCM simulations are sensitive to the non-linearities in the model equations (Giorgi and Bi, 2000). As a result, solutions started with different initial conditions will diverge substantially after a few days of simulation. Seasonal predictability is based on the fact that the atmosphere responds to slowly evolving forcings such as the SSTs (Shukla, 1998). The use of ensembles provides some idea of the probability distribution of outcomes, as well as the mean outcome which may reasonably be regarded as a best guess for the forecast. It is expected that the signal resulting from SST forcing in a GCM over periods longer than a few weeks must be distinguished from the noise level if the signal is to be considered physically significant (Shukla et al, 2000). In other words, assuming that ENSO was the only factor influencing the seasonal rainfall over South Africa, during an El Niño season one will expect the greatest number of ensemble members to lean towards the below-normal rainfall category over South Africa. Some ensemble members will be

Table 2.1: *The design of the experiment to investigate of the internal variability of the ECHAM4.5 GCM and the RegCM3.*

Season	***No. of ensemble members***	***Start date of integration***	***End date of Integration***
DJF 1991/1992	4	01/11/1991	27/02/1992
DJF 1992/1993	4	01/11/1992	27/02/1993
DJF 1993/1994	4	01/11/1993	27/02/1994
DJF 1994/1995	4	01/11/1994	27/02/1995
DJF 1995/1996	4	01/11/1995	27/02/1996
DJF 1996/1997	4	01/11/1996	27/02/1997
DJF 1997/1998	4	01/11/1997	27/02/1998
DJF 1998/1999	4	01/11/1998	27/02/1999
DJF 1999/2000	4	01/11/1999	27/02/2000
DJF 2000/2001	4	01/11/2000	27/02/2001

expected to diverge from the expected forecast due to the internal variability of the models.

A GCM ensemble of 24 runs is produced, where the ensemble members are exposed to the same observed SST boundary conditions, but are initialised

with differing atmospheric initial conditions (pers. comm. DeWitt, 2006). Analysing the differences in the model solution when different initial conditions are used gives an idea of the model's internal variability. The GCM used in the study is the ECHAM4.5 and this model is used because it was found to outperform four other GCMs over southern Africa in a previous study (Landman and Goddard, 2003). The GCM integrations used in the study are made at the International Research Institute for Climate and Society (IRI).

Four out of the 24 ensemble members generated above are used to force a regional climate model called the RegCM3. The wind fields in the ensemble members that are used were perturbed at the beginning of the integration to make the initial conditions different (pers. comm. DeWitt, 2006). The analysis of the generated data gives the internal variability of the ECHAM4.5 and the RegCM3. The simulations are made over a 10-year period and for DJF. Table 2.1 summarises the design of the experiment to investigate the internal variability of the ECHAM4.5-RegCM3 nested system. The reason why model integrations are started on 1st of November as opposed to the 1st of December are explained below in the section on the spin up period.

2.3. The Global Climate Model

The ECHAM4.5 GCM was developed at the Max-Planck Institute for Meteorology, Hamburg, Germany (Roeckner et al, 1996). The ECHAM climate model was developed from the European Centre for Medium-range Weather-Forecasting (ECMWF) model with changes for climate simulations by a comprehensive parameterisation package developed at Hamburg. The model was configured at a triangular spectral truncation 42 (T42), and as a result the resolution is about 2.8º lat X lon with 19 vertical layers. The cumulus convection scheme developed by Tiedtke (1989) was employed in the production of the ECHAM4.5 simulations. The ECHAM4.5 GCM is used operationally at the IRI.

2.4. The Regional Climate Model

The RCM used in this study is the RegCM3 developed by the Abdus Salam International Centre for Theoretical Physics (ICTP) in Italy and released in 2003. The first generation National Centre for Atmospheric Research (NCAR) RegCM was built upon the NCAR-Pennsylvania State University Mesoscale version MM4 in the late 1980s. The dynamical component of the model originated from that of the MM4, which is a compressible, finite difference model with hydrostatic balance and vertical σ-coordinates. For application of the MM4 to climate studies, a number of physics parameterization were replaced, mostly in the areas of radiative transfer and land surface physics, which led to the first generation RegCM. A first major upgrade of the model physics and numerical schemes was documented by (Giorgi et al, 1993a, Giorgi et al, 1993b), and resulted in the second generation RegCM (RegCM2). The physics of the RegCM2 was based on that of the NCAR Community Climate Model 2 (CCM2), and the mesoscale model MM5 (Grell et al, 1994a).

There have been several improvements and additions to the newest version of the RegCM3. In the last few years, some new physics schemes have become available for use in the RegCM, mostly based on physics schemes of the latest version of the Community Climate Model, CCM3 (Kiehl et al, 1996). First the CCM2 radiative transfer package has been replaced by that of the CCM3. Changes in the model physics include a new large-scale cloud and precipitation scheme which accounts for the sub-grid scale variability of clouds (Pal et al, 2000) and new parameterisations for ocean surface fluxes (Zeng et al, 1998). The model has 18 sigma levels in the vertical and the cumulus parameterisation scheme used in this study is Grell with the Fritsh and Chappell closure (Grell, 1993).

ICs and LBCs fields are derived by standard interpolation procedures from the ECHAM 4.5 data grid to the RegCM3 grid. The USGS Global Land Cover Characterization and Global 30 Arc-Second Elevation datasets are used to create the terrain files. The monthly optimum interpolation sea-surface

temperature (OISST) analysis will be used as surface boundary conditions. A description of the OI can be found in Reynolds and Smith (1994). In this study the RegCM3 model is run with a horizontal resolution of 60 km.

2.5. The spin-up period

The period of interest in the study is DJF. However, the models were allowed to run for a period of about a month prior to the period of interest for spin-up purposes (Anthes et al, 1989). The atmosphere spins up rather quickly, meaning the regional model dynamics equilibrate with the boundary forcing. The land and in particular the soil moisture, can take much longer to spin up. Depending on how the soil moisture is initialised, it can take weeks to months to equilibrate. The RCM climatology is determined by a dynamical equilibrium among the LBC forcing, the model-generated forcing from the interior of the domain, and the internal model physics and dynamics (Giorgi and Bi, 2000). Studies by Qian et al (2004) and Pan et al (2000) have shown that reinitialisation improves the simulations because the simulations do not drift downstream. In this study we use a spin up period of one month to also allow a long enough lead time that can be used in operational forecasting.

2.6. The Domain

The selection of the domain is an issue that requires careful consideration. Seth and Giorgi (2000) suggested that in sensitivity studies the domains should be put well outside the area of interest so as to give the RCM solution allowance to respond to the internal physics and dynamics of the RCM. In some studies it was suggested that the important sources that influence the climate systems of the area of interest should be included in the domain (Fennessy and Shukla, 2000; Leung et al, 2002; Giorgi and Mearns, 1999). Southern Africa is influenced by ENSO which is very far removed from the region. For skilful simulations, ENSO related information should be provided to the RCM at the lateral boundaries (Fennessy and Shukla, 2000). Most of

the moisture that provides the rainfall in South Africa is advected from the Atlantic Ocean, the Indian Ocean and the Tropics (Cook et al, 2004; D'Aberton and Lindesay, 1982). The domain with interest over South Africa should include Madagascar because it affects the moisture flux from the Indian Ocean into South Africa and it also influences the migration of the cyclone-like vortices (Landman et al, 2005). With the consideration of the above mentioned facts the model domain was chosen from about the Equator to 40° S and from Greenwich to 70°E (Figure 1.2).

2.7. Observed data used for verification

The observed data from the 970 South African Weather Service rainfall stations is used to verify the simulated rainfall in South Africa. The spatial distribution of the stations is shown in Figure 3.7. The CAMS_OPI data is also used to verify the model rainfall simulations, especially over the oceans(Janowiak and Xie, 1999).. The "CAMS_OPI" (Climate Anomaly Monitoring System ("CAMS") and OLR Precipitation Index ("OPI") is a precipitation estimation technique which produces real-time monthly analyses of global precipitation. To do this, observations from raingauges ("CAMS" data) are merged with precipitation estimates from a satellite algorithm ("OPI"). The analyses are on a 2.5 x 2.5 ° latitude/longitude grid, are updated each month, and extend back to 1979.

For temperature and pressure verification the NCEP reanalyses are used. The NCEP reanalyses are generated using the Medium-Range Forecast (MRF) model (Kalnay et al, 1996). This dataset consists of a reanalysis of the global observation network of the meteorological variables and a forecast system at a triangular spectral truncation of T62 to perform data assimilation. Data are reported on a 2.5° and 2.5° grid every 6 hours (0000, 0600, 1200 and 1800 UTC), on 17 pressure levels from 1000 to 10hPa.

2.8. Signal and noise formulae

To determine the variability of the nested system ensemble members over the 10-year period the following variances are calculated. The total variance is the sum of the signal plus noise variances (Shukla et al, 2000). The variance of the ensemble average seasonal means among all the years is referred to as the SST forced variance or signal. The variance within each ensemble average for all the years is referred to as the internal dynamics variance, or noise. For a seasonal mean climate variable x_{ij} e.g. (temperature, rainfall, etc.) for N years (i=1, 2,…, N), and n ensemble members (j=1,2,…,n) ensemble mean and the climatological mean are defined respectively as

$$\overline{x}_i = \frac{1}{n}\sum_{j=1}^{n} x_{ij} \quad \text{and} \tag{3}$$

$$\overline{\overline{x}} = \frac{1}{nN}\sum_{i=1}^{N}\sum_{j=1}^{n} x_{ij} \; . \tag{4}$$

The internal dynamics variance (noise) is given by

$$\sigma^2_{noise} = \frac{1}{N(n-1)}\sum_{i=1}^{N}\sum_{j=1}^{n}\left(x_{ij} - \overline{x}_i\right)^2 \tag{5}$$

The SST forced variance is given by

$$\sigma^2_{signal} = \sigma^2_{EM} - \frac{1}{n}\sigma^2_{noise} \tag{6}$$

where the variance of the ensemble mean is

$$\sigma^2_{EM} = \frac{1}{N-1}\sum\left(\overline{x}_i - \overline{\overline{x}}\right)^2 \tag{7}$$

The total variance is given by

$$\sigma^2_{total} = \sigma^2_{noise} + \sigma^2_{signal} \tag{8}$$

All the above equations on the variance are found in Shukla et al (2000).

The simulations will be verified against the observations. To determine if the areas of the maximum variance in the simulations correspond with the areas of maximum variance in the observations the formula of the variance as written below (9) will be applied to the NCEP reanalysis and the CAMS_OPI

data (Janowiak and Xie, 1999). The formula for the total variance for the observed field x over N years (Steyn et al, 2004) is given by

$$\sigma^2 = \frac{1}{N-1}\sum_{i=1}^{N}(x_i - \bar{x})^2 \qquad (9).$$

2.9. The internal variability of the RegCM3

In regional climate modelling RCMs are nested within the GCM. What that means is that the GCM provides time dependent LBCs to the RCM. The procedure results in limited degrees of freedom of an RCM and hence the RCM solutions are not expected to deviate much from the forcing fields. The RCM solutions are also sensitive to the non-linearities in the RCM and as a result, although they are restricted at the boundaries, the solutions are expected to be affected by the internal variability of the RCM.

To investigate the internal variability of the RegCM3, the RegCM3 is nested within one realisation of the ECHAM4.5 (ensemble member 13). Four solutions of the RegCM3 are then generated through initialising the RegCM3 on different days. The difference between the RCM solutions is therefore caused only by the different initial conditions. The LBCs and surface conditions are constant for each year. The difference among the RCM solutions gives the internal variability of the RegCM3. To make sure that the results obtained using a single realisation from the ECHAM are consistent for all the other realisations one additional GCM realisation (ensemble member 18) is used and the procedure is repeated (see Table 2.2).

The main objective to be addressed in this study is to what extent is the internal variability of the RCM responsible for the variability of the nested system's solutions. For this study only two seasons that were highly anomalous are studied, 1991/1992 (Figure 2.1) and 1995/1996 (Figure 2.2).

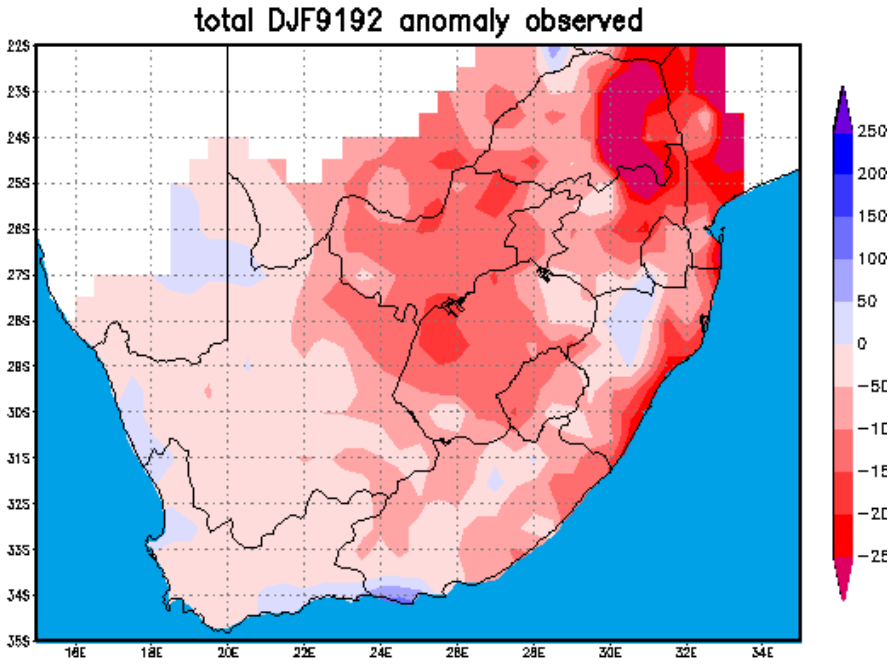

Figure 2.1: *The total DJF 1991/1992 rainfall anomaly in mm calculated based on the ten years average from 1991/1992 to 2000/2001 as observed from rainfall stations in South Africa.*

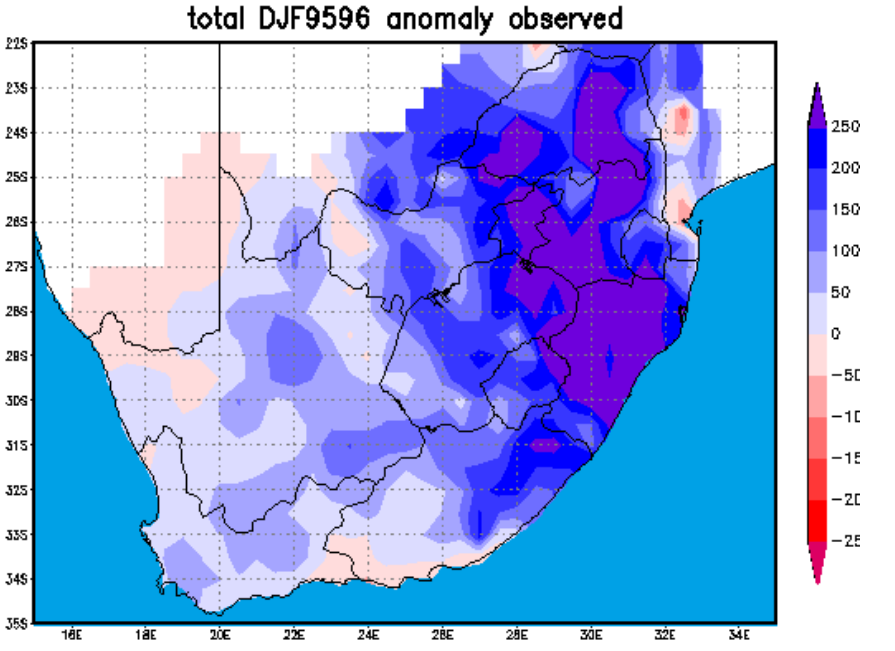

Figure 2.2: *The total DJF 1995/1996 rainfall anomaly in mm calculated based on the ten years average from 1991/1992 to 200/2001 as observed from rainfall stations in South Africa.*

Table 2.2: *The design of the experiment to investigate the internal variability of the RegCM3.*

Season	Ensemble member	Start date	End date	Rainfall
DJF1991/1992	13 and 18	01/11/1991	27/02/1992	Dry
		02/11/1991	27/02/1992	
		03/11/1991	27/02/1992	
		04/11/1991	27/02/1992	
DJF1995/1996	13 and 18	01/11/1995	27/02/1996	Wet
		02/11/1995	27/02/1996	
		03/11/1995	27/02/1996	
		04/11/1995	27/02/1996	

The experimental design is summarised in Table 2.2. The two seasons are associated with ENSO: 1991/1992 was an El Niño season, while 1995/1996 was a La Niña season. The rainfall anomalies in the two seasons were highly anomalous and as a result the seasons received some attention from meteorologists in the region (Landman et al, 2001; Rautenbach, 1998; Crimp and Mason, 1998).

2.10. MAD and BIAS

To measure the deviation between each ensemble member and the ensemble average the statistical measures, the mean absolute difference (MAD) and the average difference (BIAS) are used. The way the two measures are used here is based on Giorgi and Bi (2000). Giorgi and Bi (2000) compared the model results from the perturbed runs with those from the original unperturbed run, but in this study comparison of the model solution for each ensemble member for the different days and years is made relative to the ensemble average.

The MAD for any areal averaged variable x e.g (rainfall) over a particular region is given by

$$MAD_{x^{ens\_j}} = \left| x_i^{ens\_j} - x_i^{ens\_ave} \right| \quad (10)$$

where the superscripts refer to the run. ens_j is the ensemble member j simulation and the ens_ave is the ensemble average, while i refers to the different seasons, or in the case of intra-seasonal variability i refers to the different days. The MAD is a measure of the deviation in the different homogeneous regions (shown later). The corresponding BIAS is defined by

$$BIAS_{x^{ens\_j}} = \left(x_i^{ens\_j} - x_i^{ens\_ave} \right). \quad (11)$$

The BIAS is also a measure of the deviation but it measures the deviation in given directions.

2.11. ME and MAE

To analyse how the model is performing relative to the observations the mean error (ME) and the mean absolute error (MAE) are analysed. The equation of ME is as follows:

$$ME = \frac{1}{N} \sum_{i=1}^{N} (y_i - o_i) \quad (12)$$

where i is the different years and N is the total number of years or days for the intra-seasonal variability study.

The mean error is the difference between the average forecast and the average observation, and therefore expresses the bias of the forecasts (Wilks, 1995). Forecasts that are on average over-forecast will exhibit ME>0, and forecasts that are on average under-forecast will exhibit ME<0. The bias gives no information about the magnitude of individual forecast errors, and is therefore not an accuracy measure.

The mean absolute error is calculated and it is in the form

$$MAE = \frac{1}{N} \sum_{i=1}^{N} | y_i - o_i | \quad (13)$$

The MAE is the average absolute difference between the forecast and observation pairs (Wilks, 1995). Taking the absolute error necessarily

produces positive terms so that the MAE increases from zero for perfect forecasts through larger positive values as the errors increase.

2.12. Equi-probable categories

In the analysis of the intra-seasonal variability the 33.33 and the 66.67 percentiles will be used as cut-off values to determine three rainfall categories (below-normal, normal and above-normal). The n^{th} percentile can be determined as

$$n_P = \frac{P*(N+1)}{100}\text{th} \qquad (14)$$

value in the data array (Steyn et al, 1994), where P is the percentile, N is the total number of values associated with each ensemble member and all the days in DJF. The rainfall amount that corresponds with the n_p position of the data array is the n_p percentile. If n_p has decimal places after the comma, the number after the comma is multiplied by the difference of the number that follows the number before the comma and the number before the comma and then added to the number before the comma. For example if n_p is 25.67 then the 25^{th} value is added to 0.67 multiply by (the 26^{th} value minus the 25^{th} value). The same procedure is used for the observations where N is the total number of days in the two seasons under investigation.

2.13. Synopsis

The models, the GCM and the RCM that are used in the study have been described. The method through which the experiment to investigate the internal variability of the ECHAM4.5-RegCM3 system and of the RegCM3 has been described. The following Chapters describe the findings that are made from the data that is generated as described in this Chapter. The measures that are used to analyse the datasets in the next Chapters have also been described in this Chapter.

CHAPTER 3: THE INTERNAL VARIABILITY OF THE ECHAM4.5-RegCM3 SYSTEM

3.1. Introduction

The nested system solutions are sensitive to the internal variability of both the GCM and the RCM. An ensemble of ECHAM4.5 simulations are generated using lagged one-day starting dates of the integration as well as perturbing the wind fields. For the purpose of this study, four of the ensemble members that are obtained through perturbing the wind fields are used to force the RegCM3. The solutions obtained from the nested system are analysed to determine the internal variability of the ECHAM4.5-RegCM3 nested system. The total variance, the SST forced variance which is regarded as the signal, and the internal dynamics variance (noise), are analysed in the next section. In this chapter the variability of the ensemble members obtained from the nested system are analysed and comparison with the observations follows in the next chapter.

3.2. Different aspects of model variances

The variable of interest in this dissertation is precipitation, however, there are challenges with its simulation as mentioned in Chapter 1 because of its small scale spatial scale. It may be possible that the precipitation simulations are sensitive to the SST forcing, but the problems associated with parameterisation problems may overshadow the SST forcing. It is therefore necessary to analyse the large scale features' simulated variance to determine if the findings that are reflected in the rainfall simulations are consistent with the large scale simulations. The temperature and surface pressure variances are also analysed for the above mentioned reasons.

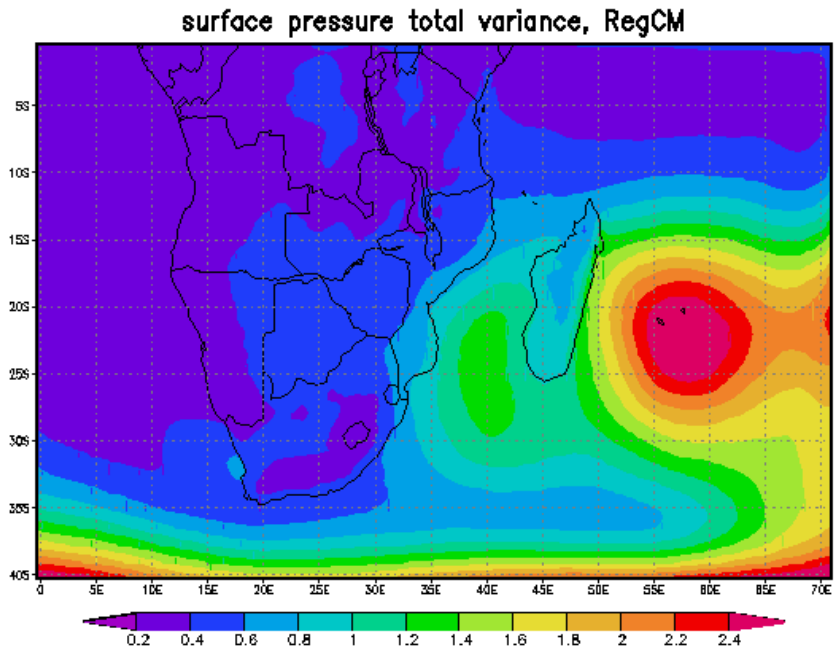

Figure 3.1: *The total surface pressure variance for 10 DJF seasons with 4 ensemble members.*

The SST forced variance (equation 6), the internal dynamics variance (equation 5) and the total variance (equation 8) are calculated as in Shukla et al, 2000 (the equations are summarised in Chapter 2). The variance of the ensemble average seasonal means among all the years is referred to as the SST forced variance or signal. The variance within each ensemble averaged for all the years is referred to as the internal dynamics variance or noise. The total variance is the sum of the signal plus noise variances. The different measures are calculated using 10-years of data as simulated by the RegCM3 nested within four ensemble members of the ECHAM4.5.

3.2.1. Surface Pressure

The highest simulated surface pressure variability occurs in the Indian Ocean and also south of the continent (Figure 3.1). The variance south of the country is due to cold fronts that are generally restricted to the ocean in summer (Tyson and Preston-Whyte, 2000). Cold fronts are responsible for the winter rainfall over the south-western and southern coast in winter because they migrate northward. In summer they are generally restricted to the south but

some of the cold fronts occasionally influence the south coast. The AOH sometimes ridges eastward and to the south of the continent causing favourable rainfall conditions. The transition from cold fronts that are part of the mid-latitude cyclones and have low pressure centres, to the ridging high pressure cells explains the high pressure variance in the area in DJF.

East of Madagascar there is an area that has a very high variance (Figure 3.1). The identified area is affected by tropical cyclones in summer. The sea-level pressures at the centre of the tropical cyclones may drop to 900 hPa and below (Tyson and Preston-Whyte, 2000). Over the Indian Ocean, there is generally an IOH and as the name describes, has a centre of high pressure. The transition from IOH to tropical cyclones explains the high surface pressure variability in the area.

The maximum surface pressure variance is associated with the internal dynamics variability of the nested system (Figure 3.2 and Figure 3.3). The results show that the variance associated with the internal variability model is greater than the SST forced one even when temperature (not shown) and rainfall are considered (Figure 3.5 and Figure 3.6). The results suggest that the variability between the ensemble members for a particular season (i.e. same year) exceeds the variability of the ensemble average over the ten year period. The MAD (equation 10) and the BIAS (equation 11) in Chapter 2 are analysed for the 10-years to confirm if the ensemble members' variability in a single year exceeds the ensemble average variance over a 10-year period. The areas of maximum variance correspond to areas of maximum MAD. The BIAS which is also calculated based on the ensemble average and each ensemble member for each year shows that there is a high variability amongst ensemble members in the same year. The high variability in the same season is illustrated by the BIAS of -2 and 2 hPa for two ensemble members over the same area (i.e. the Indian Ocean) (not shown).

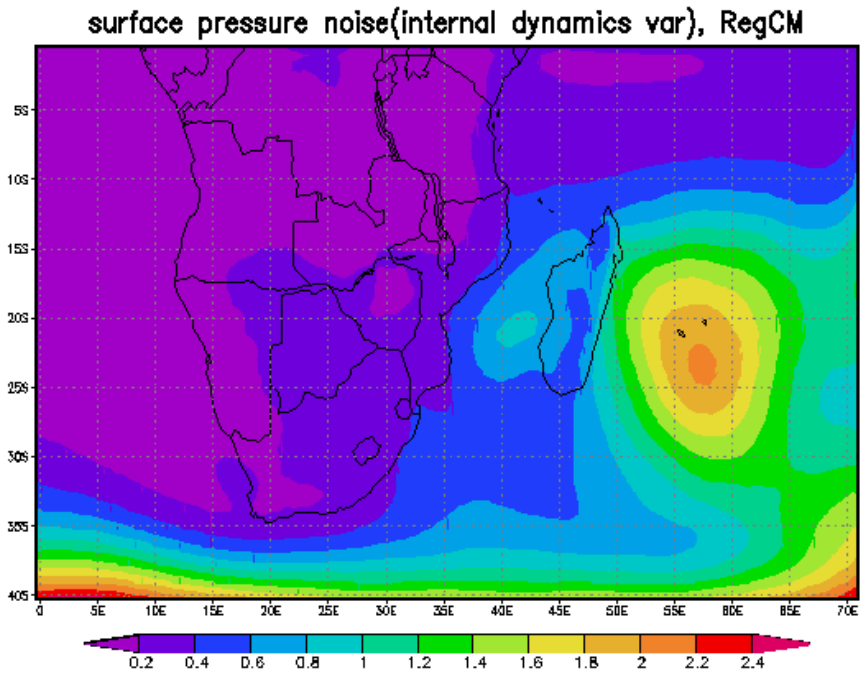

Figure 3.2: *The internal dynamics surface pressure variance for 10 DJF seasons with 4 ensemble members.*

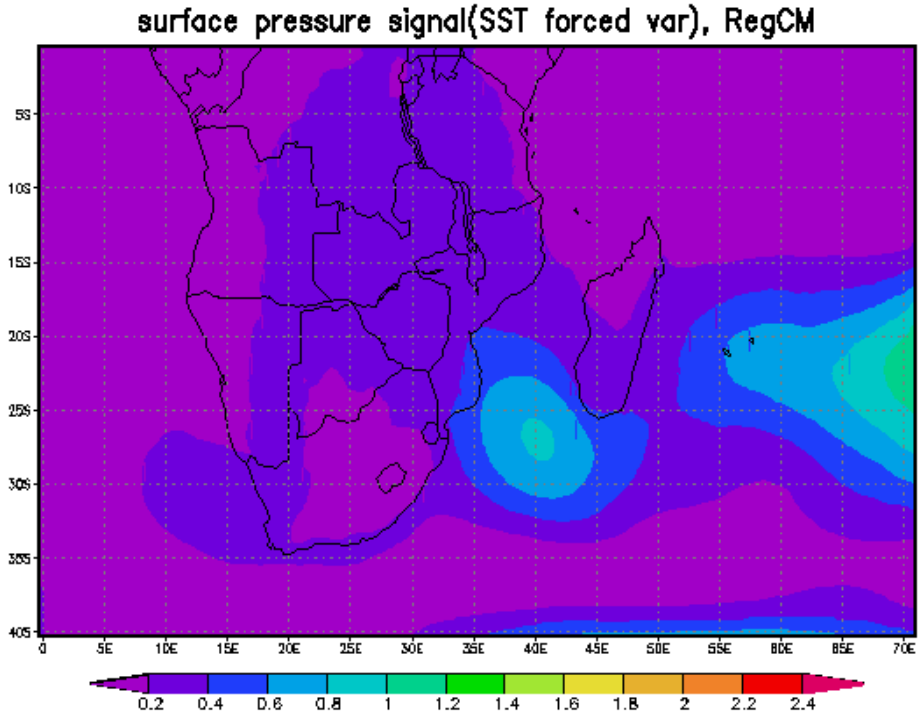

Figure 3.3: *The SST forced surface pressure variance for 10 DJF seasons with 4 ensemble members.*

The SST forced surface pressure variance is the highest over the Indian Ocean east of Madagascar and south-west of Madagascar (Figure 3.3). The variance of between 0.2 and 0.4 joins the latter two regions adjacent to Madagascar and extends towards the tropics over Africa. Seasonal forecasting is based on the fact that the slowly evolving boundary conditions leave some memory in the atmosphere and hence render the atmosphere partly predictable. The most known or rather most understood of the SST-atmosphere relation is ENSO. The simulated SST forced surface pressure variance is the highest over the areas that are affected by ENSO over south-east Africa (Tyson and Preston-Whyte, 2000).

3.2.2. Temperature

The temperature variance is the greatest over land (Figure 3.4). The low variance over the ocean is the desired result because the model is forced with the observed SSTs at the surface. The temperatures over the oceans are therefore the same for the different ensemble members for each year. The small variance is also a result of the slow evolution characteristic of the SSTs. The area with the maximum variance (both the SST forced and the internal dynamics forced variance) is over Botswana. The MAD also shows that the difference between the ensemble members and the ensemble average is high over the area characterised by the maximum variability, but it is not clear why the variability is so high over that region.

3.2.3. Rainfall

As mentioned above the most rainfall variance is associated with the internal dynamics of the model (Figure 3.5). The rainfall variance is high in the Indian Ocean, i.e. north of Madagascar and tropical regions, but smaller over South Africa. RCMs produce spurious rainfall at the boundaries (Walsh and McGregor, 1995) as is found in this study (Figure 3.5 and Figure 3.6). It was found in a study by Walsh and McGregor (1995) that the influence of the lateral boundary spurious rainfall on the internal domain rainfall is small. The spurious rainfall is caused by the inconsistency between the LBCs and the model domain's internal climatology. The influence of the domain boundaries

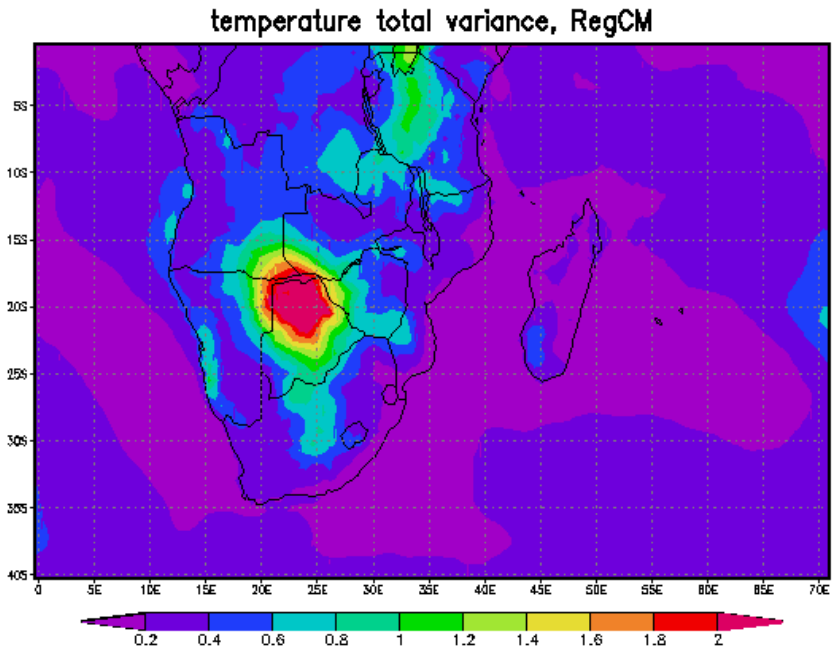

Figure 3.4: *The total air temperature variance for 10 DJF seasons with 4 ensemble members.*

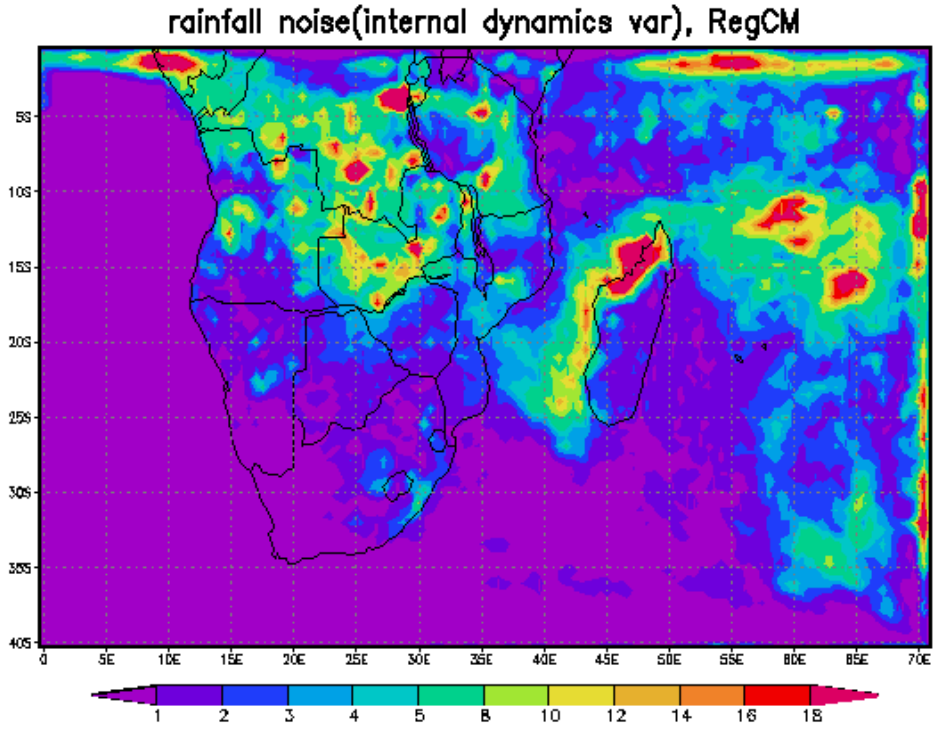

Figure 3.5: *The rainfall internal dynamics variance for 10 DJF seasons with 4 ensemble members.*

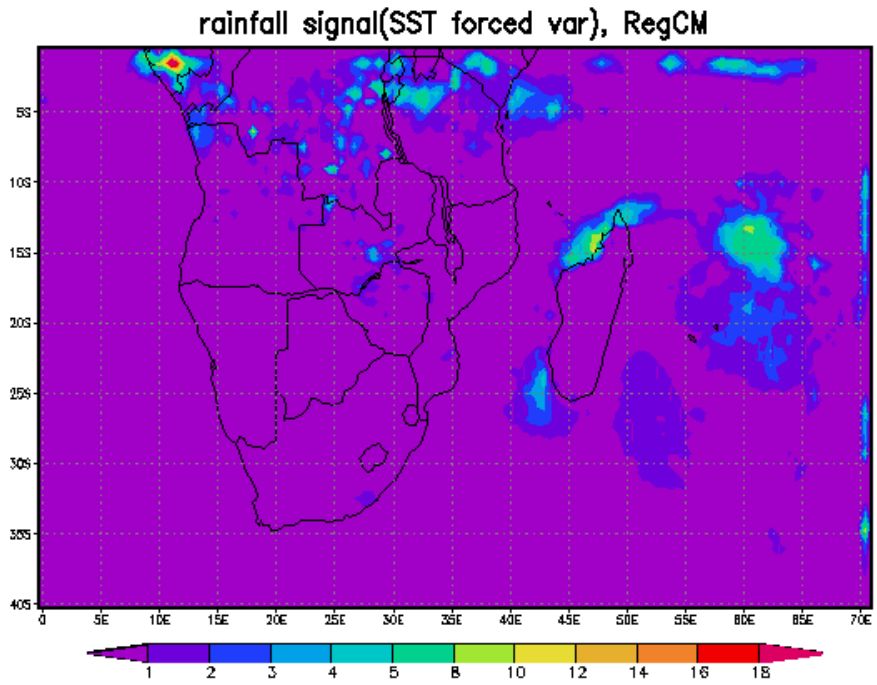

Figure 3.6: *The SST forced rainfall variance for 10 DJF seasons with 4 ensemble members.*

is visible over the eastern and north-eastern boundaries, where high rainfall variance occurs in almost a straight line along the boundaries (Figure 3.5 and Figure 3.6).

The nested system captured the positive west-east rainfall gradient over South Africa. The variance over the eastern part of South Africa which receives the greatest amount of rainfall in summer is higher than over the western side. The SST forced rainfall variance over South Africa is between 0 and 1 while the internal dynamics variance ranges between 0 and 8 (Figure 3.6). The SST forced variance is the minimum over the north-eastern part of South Africa which suggests low predictability over that area. The maximum variance is also associated with the maximum MAD and big differences in the BIAS between the ensemble members which confirms the results from the variance study.

The area of interest in the study is South Africa. The fact that the internal dynamics variance exceeds the SST forced variance suggests that the

variance in a particular season exceeds the variability of the ensemble average over the 10-year period. To further investigate the simulated rainfall variability, analyses are made over South Africa using eight homogeneous regions (Figure 3.7).

3.3. The inter-annual rainfall total over South Africa

South Africa can be divided into homogeneous regions using spatial cluster analysis applied to observed rainfall stations over the whole of South Africa (e.g. Landman and Mason, 1999; Landman and Klopper, 1998; Bartman et al, 2003; Landman and Tennant, 2002). Following the previous studies of dividing South Africa into homogeneous regions, 8 regions were determined using 970 rainfall stations which are evenly distributed over the whole country. Model data of the grid-points within the region are used to construct rainfall time series that can be compared with observed time series. The number of grid points in each region are as follows, region 1: 39, region 2: 43, region 3: 23, region 4: 15, region 5: 42, region 6: 97, region 7: 86, region 8: 97. The total rainfall for each region for the four ensemble members is plotted on a time series together with the ensemble average over the 10-year period. The observed time series is included for the purposes of Chapter 4. The four ensemble members are ensemble member 13, ensemble member 16, ensemble member 18 and ensemble member 20.

3.3.1. Region 1

Region 1 is situated over the western coast and the adjacent interior (Figure 3.7). The region receives most of its rainfall in winter (Figure 1.3). There is a general agreement between the ensemble members (Figure 3.8). Although the ensemble members agree in general and are in phase, the variability amongst them in certain years exceeds the variability of the ensemble average over the 10-year period. The variability characteristic is illustrated by the range of the ensemble average of 27 to 83 mm over the 10-year period and the range of the ensemble members' simulation in 1999/2000 of 40 to

140 mm. The simulated ensemble member rainfall peaks occurred during the 1993/1994, 1995/1996 and 1999/2000 seasons (Figure 3.8). Some ensemble members simulated low rainfall amounts during the three seasons. When the ensemble members are averaged the rainfall amount is reduced significantly due to the high variability of the ensemble members.

3.3.2. Region 2

Region 2 is the southern coast and adjoining interior region (Figure 3.7) which receives its rainfall throughout the year (Figure 1.3). There is a general agreement between the ensemble members in region 2 (Figure 3.9). The maximum simulated rainfall in this region is just above 350 mm (Figure 3.9) while the maximum simulated rainfall in region 1 is 150 mm (Figure 3.8). When comparing the two Figures, the range of the simulated rainfall in region 1 of the y axis is 0 to 160, while in region 2 it is 0 to 400. The change in the simulated rainfall range from region 1 to region 2 is in agreement with the observed range as one moves from west to east.

3.3.3. Region 3 and Region 4

Region 3 and Region 4 are both situated over the eastern coast of South Africa (Figure 3.7). Comparison between regions 1 and 2 (Figure 3.8 and Figure 3.9) and region 3 and 4 (Figure 3.10 and Figure 3.11) further illustrates that the RegCM3 captures the east west rainfall gradient in the country. There is a general agreement amongst the ensemble members (Figure 3.10 and Figure 3.11) , but the agreement is less than that found in region 1 and region 2 (Figure 3.8 and 3.9). The ensemble average corresponds with the majority of the ensemble members as expected, but the range of the ensemble average is still exceeded by the range of the ensemble members in some years.

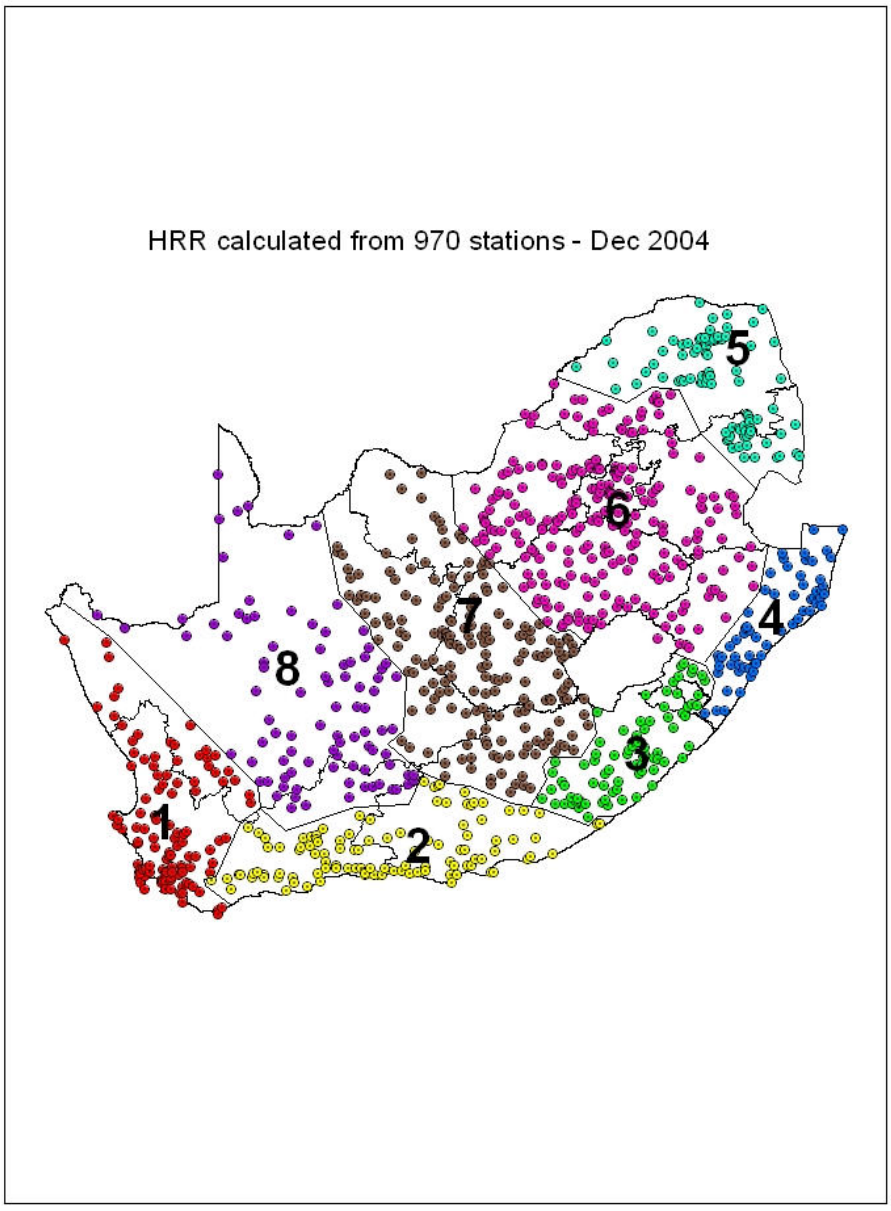

Figure 3.7: *The eight homogeneous regions obtained using spatial cluster analysis and the stations used to determine the regions.*

3.3.4. Region 5

Region 5 is situated on the far north-eastern section of South Africa (Figure 3.7). This area is sometimes influenced by tropical cyclones (Tyson and Preston-Whyte; Taljaard, 1986). The ensemble average variability is very small (Figure 3.12). The minimum simulated ensemble average rainfall is about 300 mm while the maximum is just above 400 mm. The variability between the individual ensemble members in a single year generally exceeds the variability of the ensemble average over the 10-year period.

3.3.5. Region 6

Region 6 is situated in the central north-eastern part of South Africa (Figure 3.7). This region forms part of what is regarded as the most important agricultural region in South Africa. This region covers half of the Northwest Provinces which is regarded as the food basket of the Southern African Developing countries (SADC). Also included in this region is Gauteng Province which is the smallest province in the country but has the highest population density in South Africa. The ensemble members are quite variable amongst themselves and that causes the variability in the ensemble average to be small (Figure 3.13). The two years that the ensemble members are quite variable are 1994/1995 and 1991/1992.

3.3.6. Region 7

Region 7 is the most central part of South Africa. The agreement between the ensemble members is higher in this region as compared to the other seven regions (Figure 3.14). The ensemble members seem to be in phase during

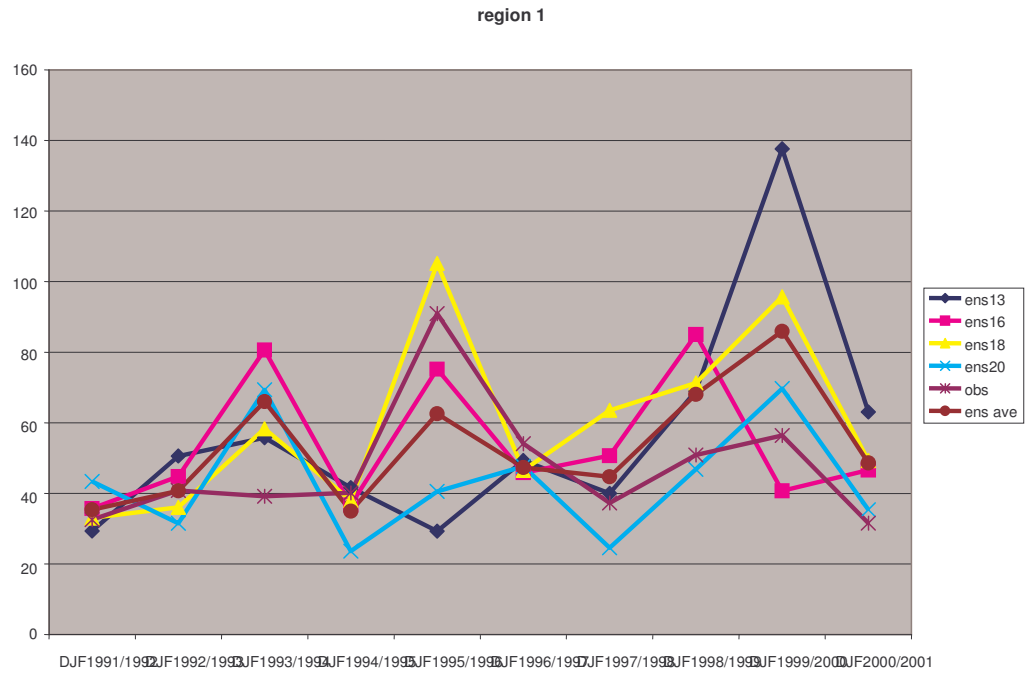

Figure 3.8: *The total 10-year DJF rainfall in mm for region 1 for the four ensemble members, the ensemble average and the observations.*

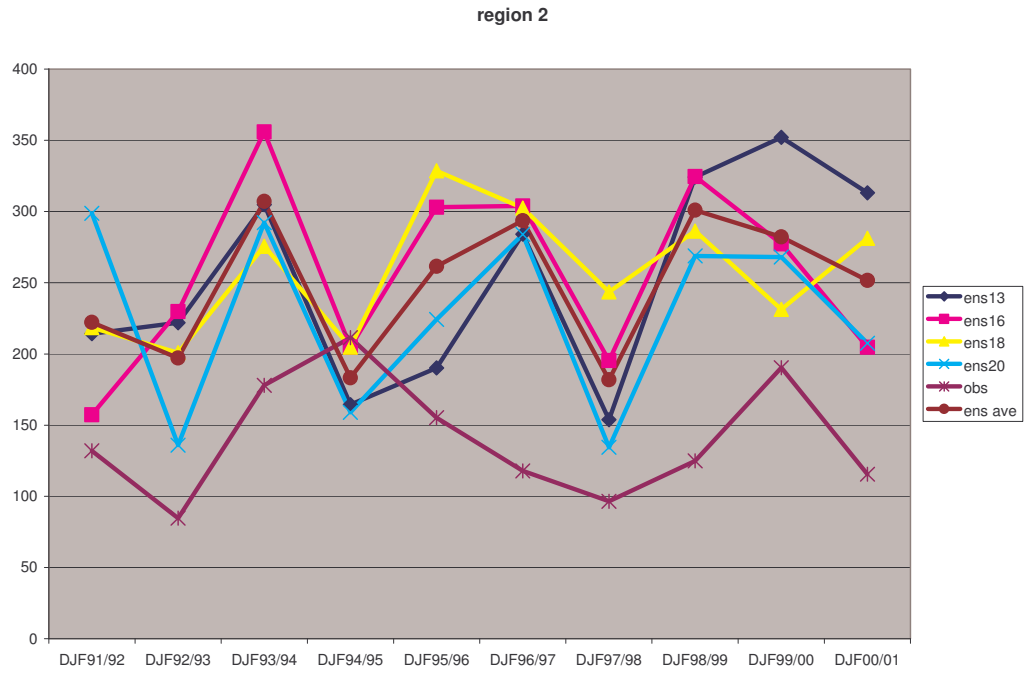

Figure 3.9: *The total 10-year DJF rainfall in mm for region 2 for the four ensemble members, the ensemble average and the observations.*

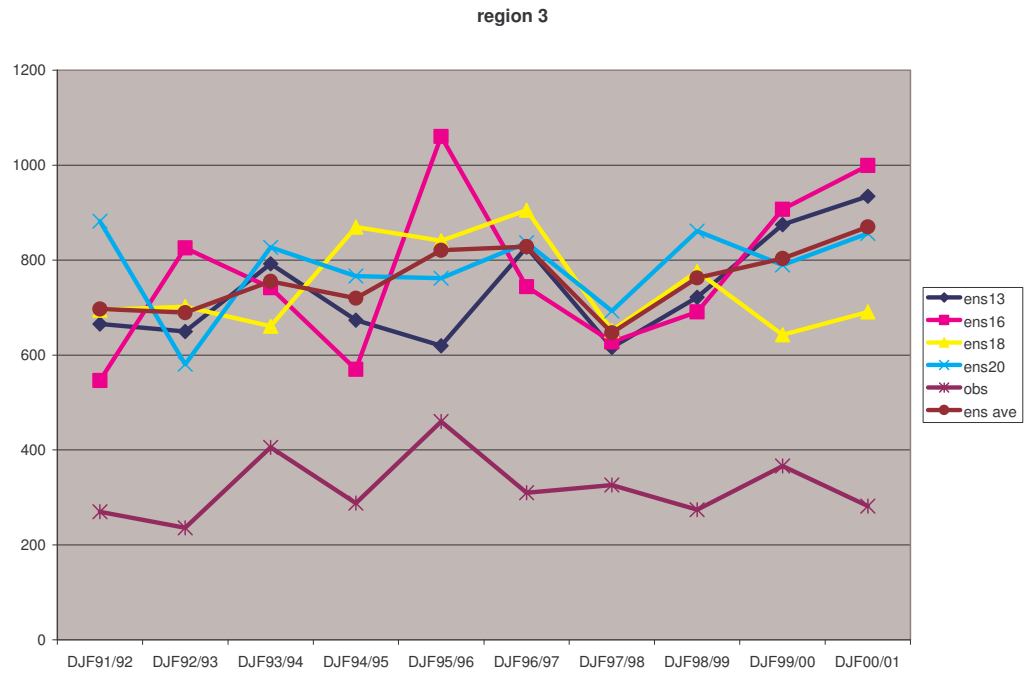

Figure 3.10: *The total 10-year DJF rainfall in mm for region 3 for the four ensemble members, the ensemble average and the observations.*

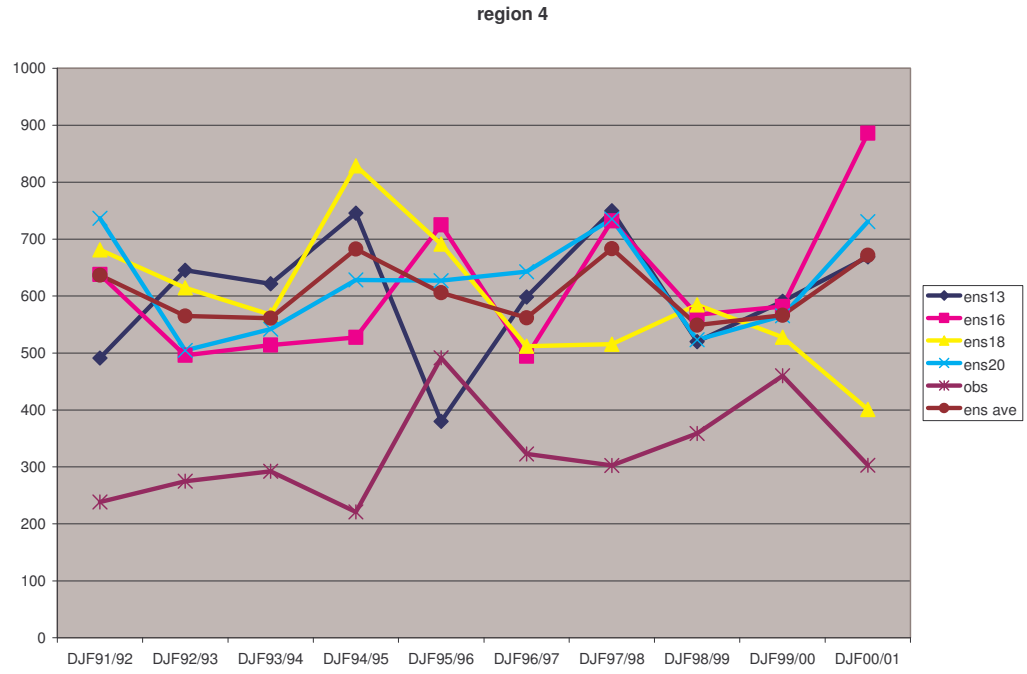

Figure 3.11: *The total 10-year DJF rainfall in mm for region 4 for the four ensemble members, the ensemble average and the observations.*

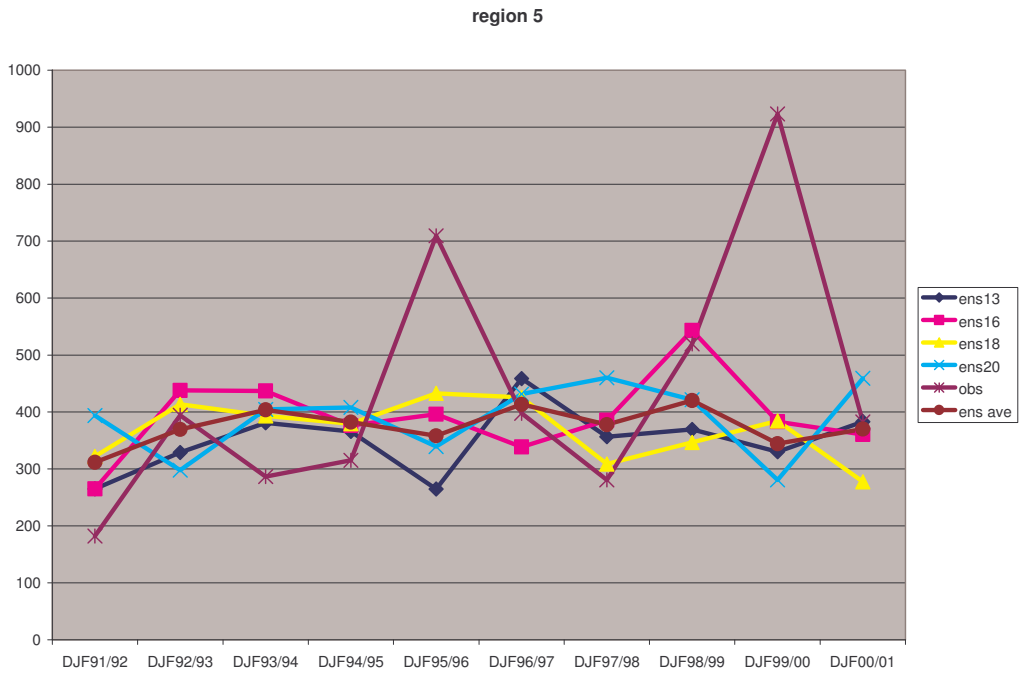

Figure 3.12: *The total 10-year DJF rainfall in mm for region 5 for the four ensemble members, the ensemble average and the observations.*

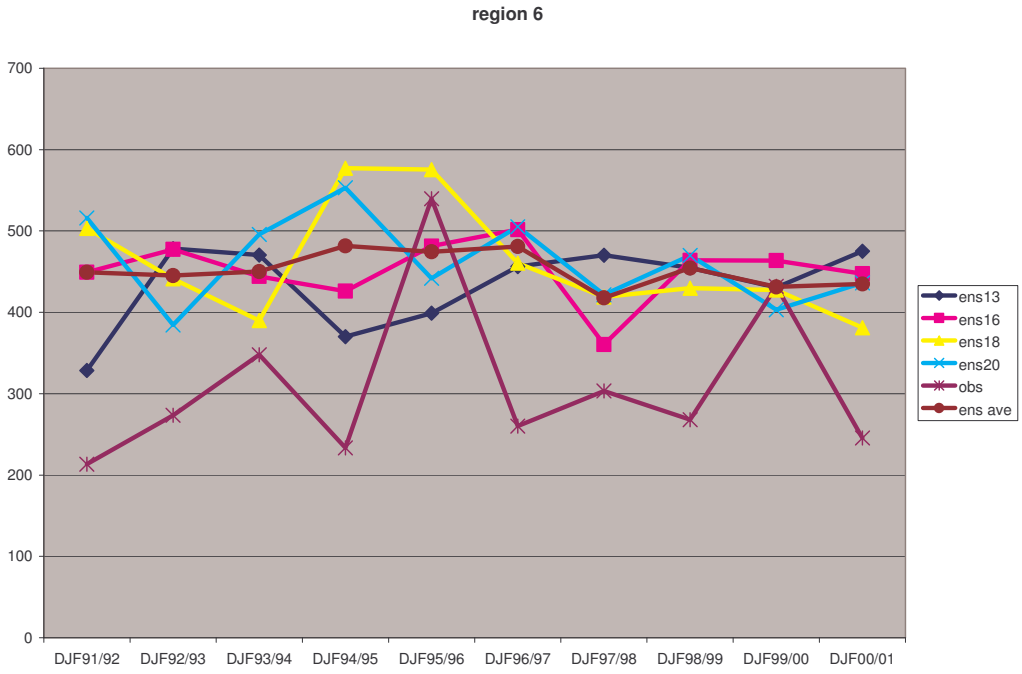

Figure 3.13: *The total 10-year DJF rainfall in mm for region 6 for the four ensemble members, the ensemble average and the observations.*

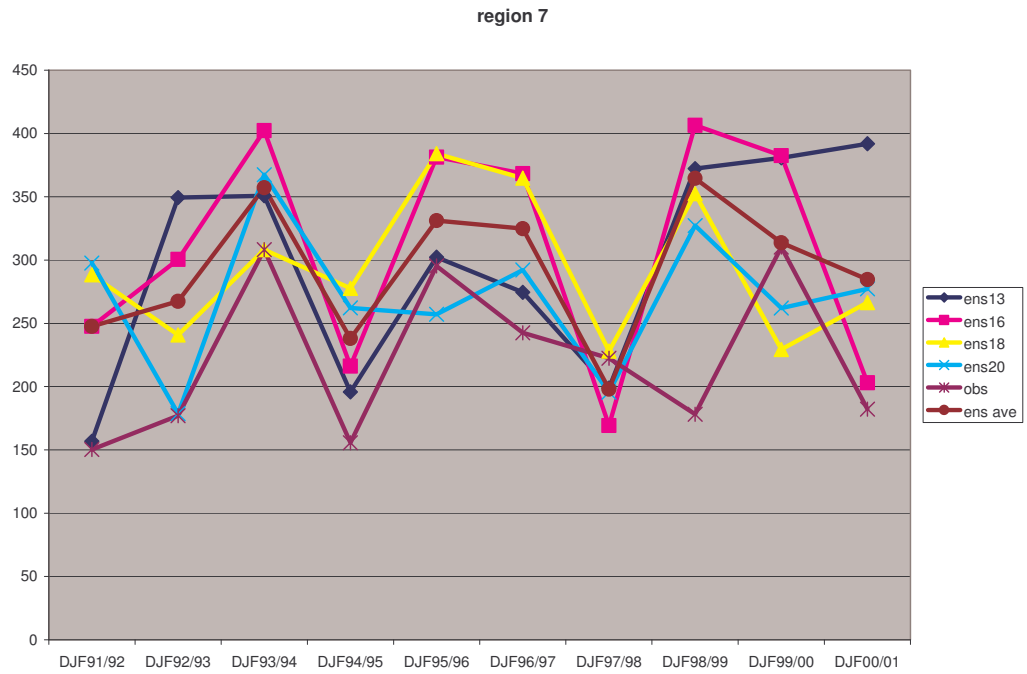

Figure 3.14: *The total 10-year DJF rainfall in mm for region 7 for the four ensemble members, the ensemble average and the observations.*

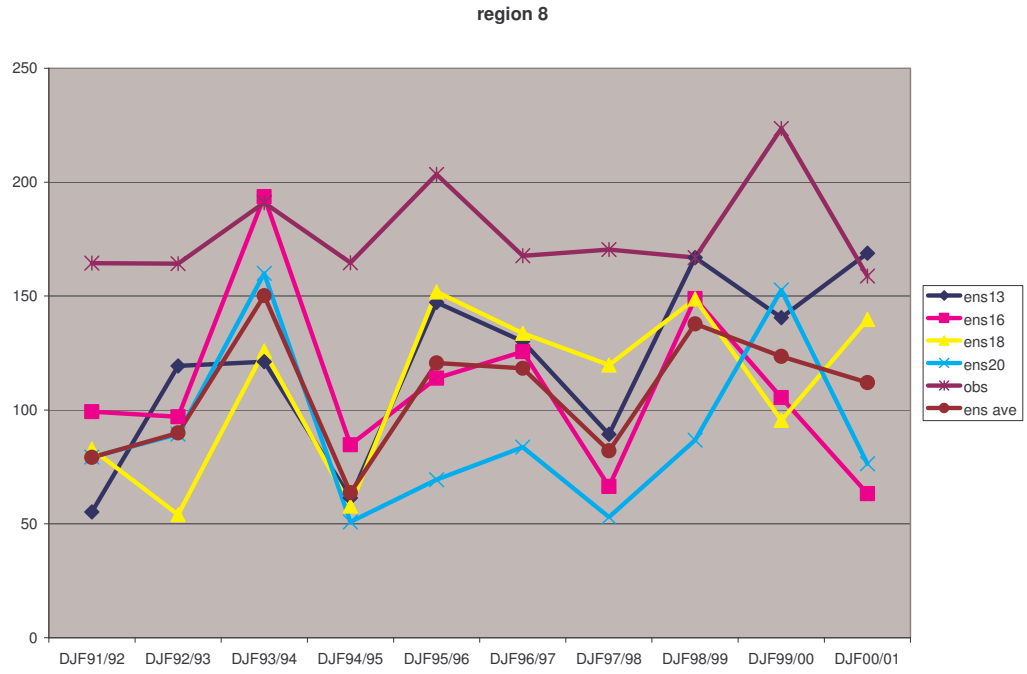

Figure 3.15: *The total 10-year DJF rainfall in mm for region 8 for the four ensemble members, the ensemble average and the observations.*

the most of the 10-years. There are, however, seasons when the variability between the ensemble members is high (e.g. 1998/1999).

3.3.7. Region 8

Region 8 is situated in the central-western part of South Africa. The region forms part of what is regarded as the arid region of South Africa. When comparing Figure 3.14 and Figure 3.15 and looking at the mm range, there is 200 mm difference in the two, with region 8 having the smallest range. There is a general agreement between the ensemble members with a lot of them being in phase over most of the 10-year period (Figure 3.15).

3.4. Summary and Conclusions

The differences between the nested system ECHAM4.5-RegCM3 solutions that are obtained through perturbing the wind fields at initialisation are analysed. The variability associated with the internal dynamics of the models is greater than the variance that is SST forced. The above finding is consistent for all the variables (i.e. surface pressure, temperature and rainfall) that are analysed. These results imply that the variability between the ensemble members for each year exceeds the ensemble average variability over the 10-year period.

The SST forced surface pressure variance is the greatest over the areas which are influenced by ENSO. The temperature total variance over the ocean is small, especially the internal dynamics variance. The values are small because the model is provided with observed SSTs and hence the SSTs for the different ensemble members are similar. The low variability of the SST is also a result of the slow evolution of the SSTs over the DJF period. The SST forced temperature variance over the oceans was expected to exceed the variance associated with the internal variability of the model, because SST anomalies are different from one year to the next.

The internal dynamics forced rainfall variance also exceeds the SST forced variance, but with the rainfall variance the influence of ENSO is not as obvious as it was with surface pressure. The finding about the variability of the ensemble members and the ensemble average variability was further illustrated over South Africa where the range of the ensemble average during the 10-years is more often than not exceeded by the range of ensemble members in a single year. The ensemble average exhibits a small variance because of the high variability of the ensemble members in different seasons. The ensemble members are more in phase over the central parts towards the western coast of the country, with high variability over the regions towards the eastern part of the country.

The aim of this study is not to verify the nested system solutions. However, given that the knowledge of whether or not the model simulates the observed features determines whether or not the system is useful, the solutions are compared with the observations. Comparison of the observed anomaly to the ensemble average anomaly is also necessary and discussed next to determine if the model captures the observed inter-annual rainfall variability.

CHAPTER 4: THE INTERNAL VARIABILITY OF THE ECHAM4.5-RegCM3 SYSTEM

OBSERVATIONS VS. SIMULATIONS

4.1. Introduction

In the previous Chapter a lot of emphasis was put on the variability of the ensemble members, which gives a measure of the internal variability of the ECHAM4.5-RegCM3 system. In this Chapter, surface pressure, temperature and rainfall variances are computed using equation (9) in Chapter 2 using the NCEP reanalyses and CAMS_OPI data. The simulated and observed variances are compared to determine if there is an agreement between the areas of minimum and maximum variance that were observed in the previous Chapter.

4.2. Variances

4.2.1. Surface pressure variances

The variance calculated from the NCEP reanalysis shows that the maximum surface pressure variance is found in the Indian Ocean, south of about 10°S and also south of the continent (Figure 4.1). The observed areas of maximum variance agree with those that were identified in the simulations (Figure 3.1). The results show that the nested system captures the large scale variability as expected.

4.2.2. Temperature variance

The maximum temperature variance from the NCEP reanalysis occurs in Botswana. However, in the simulations it is displaced northwards compared to the reanalysis (Figure 3.4 and Figure 4.2). Although the area of the maximum variance is further north in the simulations, this area extends towards central South Africa. The fact that the models captured the observed variance is

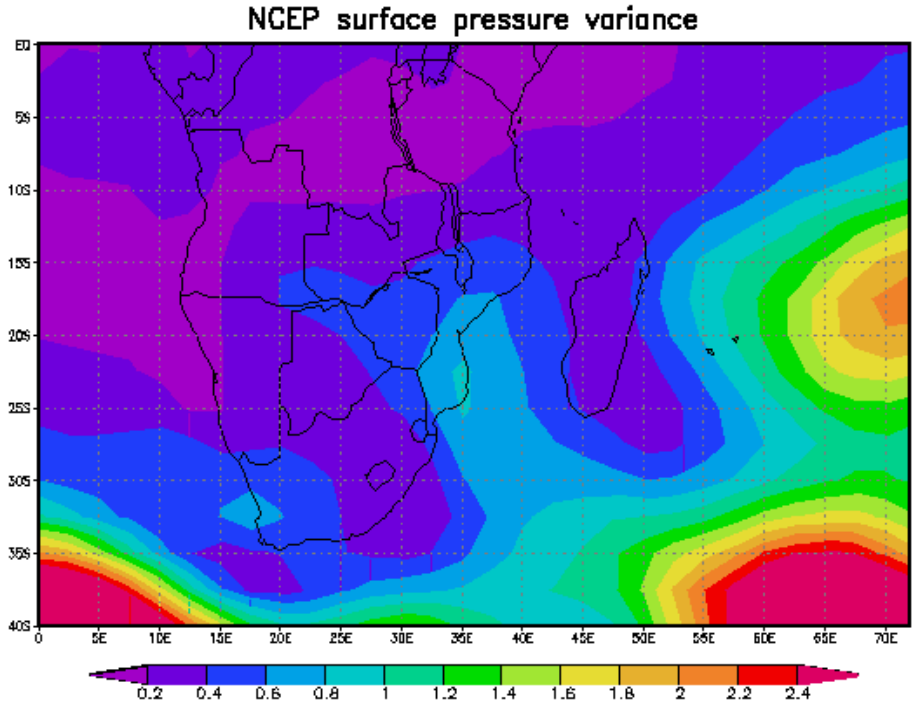

Figure 4.1: *The surface pressure total variance as calculated from the NCEP reanalysis for the DJF season from 1991/1992 to 2000/2001.*

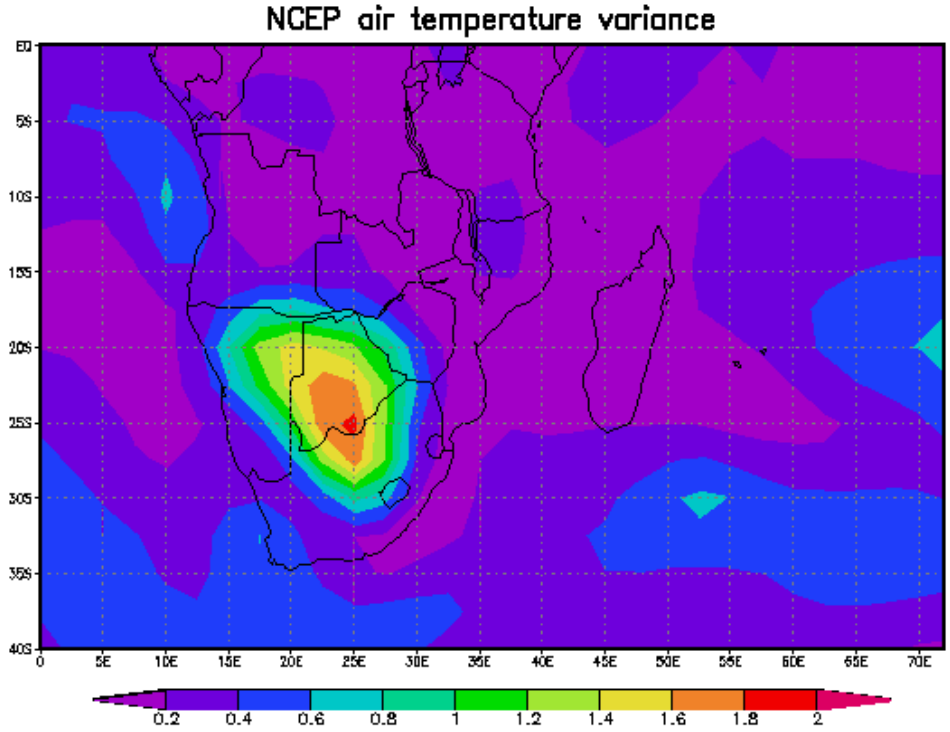

Figure 4.2: *The air temperature total variance as calculated from the NCEP reanalysis for the DJF season from 1991/1992 to 2000/2001.*

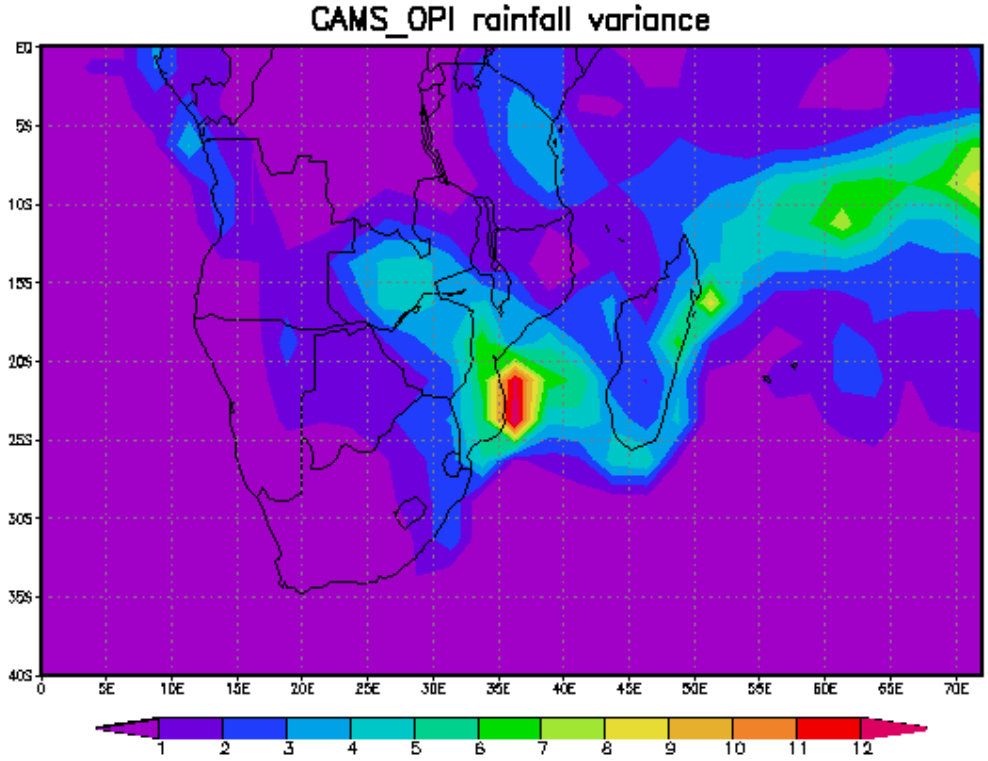

Figure 4.3: *The seasonal rainfall variance as calculated from CAMS_OPI for the DJF season from 1991/1992 to 2000/2001.*

evidence that the ECHAM4.5-RegCM3 system is a skilful tool for climate studies.

4.2.3. Rainfall variance

The RegCM3 was run with a horizontal resolution of 60 km (approximately 0.5°) while CAMS_OPI data has a resolution of 2.5°. Owing to the finer resolution of the RegCM3, the variance patterns are noisier than the patterns associated with the CAMS_OPI data. The NCEP reanalysis are also produced with a resolution of 2.5° but the differences in the resolution is not obvious for the surface pressure and temperature variances, owing to their larger spatial scale pattern. The units used in Figures 3.5 and 3.6 are not similar to those used in Figure 4.3. For Figure 4.3 the variance is calculated using monthly rainfall, while daily averages are used for the two Figures in Chapter 3. There is some agreement between the simulated and the observed variance.

However, the areas of the maximum variance do not correspond. The maximum variance occurs over the coast of Mozambique in the reanalysis while in the simulations it occurs on the western side of Madagascar, north of Madagascar and some areas over tropical Africa. The area in tropical Africa where the modelled variance is high is observed to have very little variance. The low variability of the region may not be a true reflection of the variance in the area because of a lack of observational data. Comparison with the observations is also made over South Africa for rainfall simulations to determine how the nested system performs over the homogeneous regions, in terms of over/under prediction and also capturing the inter-annual rainfall variability.

4.3. The total rainfall over South Africa

The simulated ensemble member's DJF rainfall averaged over the grid-points within each of the regions of Figure 3.7 are compared with the observed regional rainfall. Figures 3.8 to Figure 3.15 in Chapter 3 display time series for the ensemble members, the ensemble average and the observations over the 10-year period. The average difference between the ensemble average time series and the observations gives an idea of whether or not the model is over or under estimating the rainfall. The Figures in Chapter 3 show how the model has been performing over the 10-year period. The mean error (ME) (Figure 4.4) and the mean absolute error (MAE) (Figure 4.5) are calculated to further substantiate the results of Figures 3.8 to 3.15. Comparisons between the observed and the ensemble mean anomaly time series are discussed next. The DJF rainfall anomalies series are plotted (Figure 4.6 to 4.13) to determine if there is a general agreement between the average simulated rainfall and the observed rainfall, with interest in the agreement between the observed and simulated anomaly sign (i.e., if the observed and simulated anomalies are positive or negative).

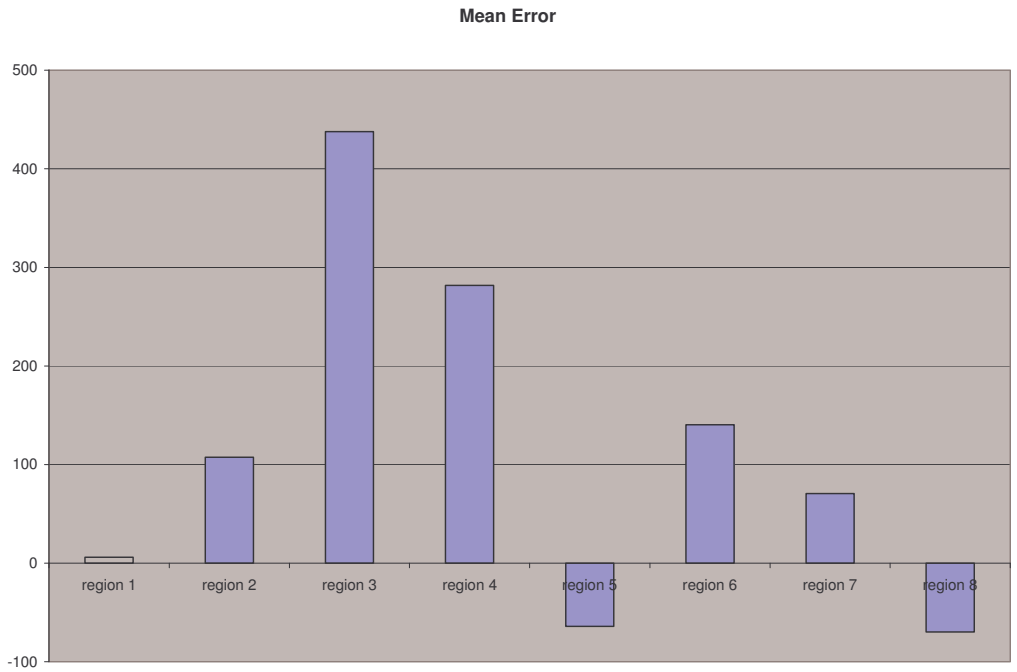

Figure 4.4: *The mean error calculated over the 10 years for DJF based on the ensemble average and observations for the 8 regions.*

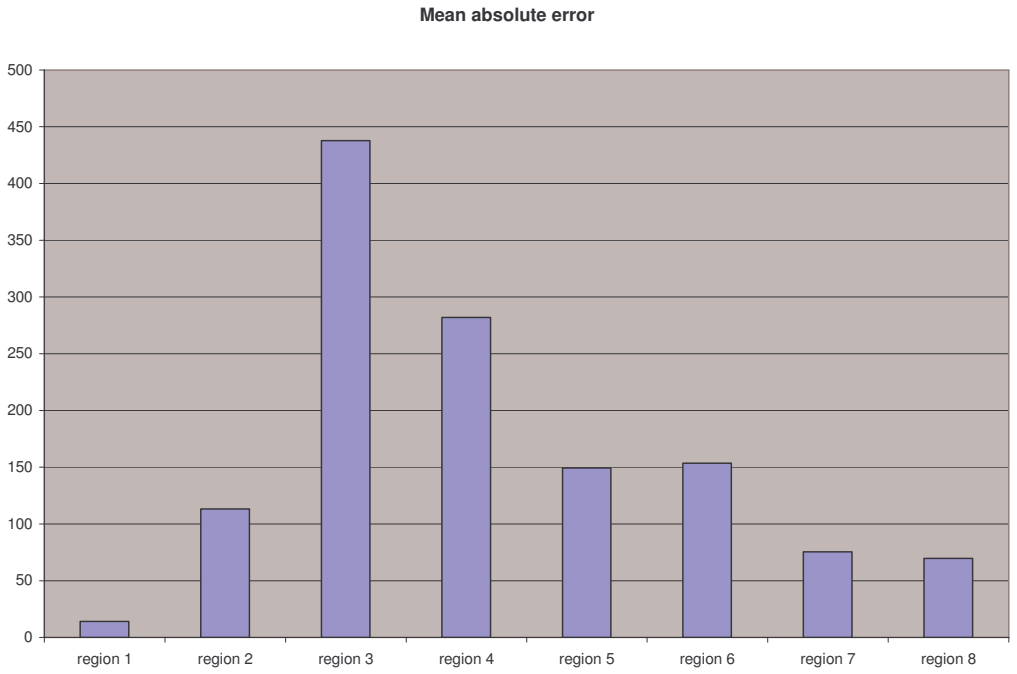

Figure 4.5: *The mean absolute error calculated over the 10 years for DJF based on the ensemble average and observations for the 8 regions.*

4.3.1. Region 1

There is a good agreement between the ensemble average and the observations (Figure 3.8) as reflected by a correlation of 0.4757. The mean error is positive which means that the nested system is over-forecasting rainfall. However, the magnitude of the error is small as compared to the other 7 regions as can be seen on the mean absolute error graph (Figure 4.5). The simulated rainfall anomaly sign agrees in general with the observed anomaly (Figure 4.6). In general the nested system is over-predicting rainfall (Figure 4.4), but there are some seasons when the observed rainfall exceeds the simulated ensemble average. The nested system does not capture the rainfall peak in 1995/1996 according to the ensemble average, but there is one ensemble member that captures the extreme rainfall season. It should however be noted that in the same season there is an ensemble member that gave a big anomaly in the opposite direction. When the latter ensemble member is averaged with the rest it reduces the amplitude of the ensemble average.

4.3.2. Region 2

There is a general rainfall overestimation by the nested system in region 2 (Figure 3.9 and Figure 4.4). The observed total rainfall time series appears below all the ensemble members over the 10-year period except for one season. The observed rainfall ranges from about 80 mm to 220 mm while the simulated rainfall ranges from 180 to 310 mm. The overestimation is further confirmed by the positive mean error value which is higher than in region 1 (Figure 4.4). The agreement between the observations and the simulated rainfall is a lot less in this region as compared to region 1. The correlation between the observations and the ensemble average is 0.1934. During three of the seasons the sign of the average anomaly of the simulated rainfall was opposite to the observed one (Figure 4.7).

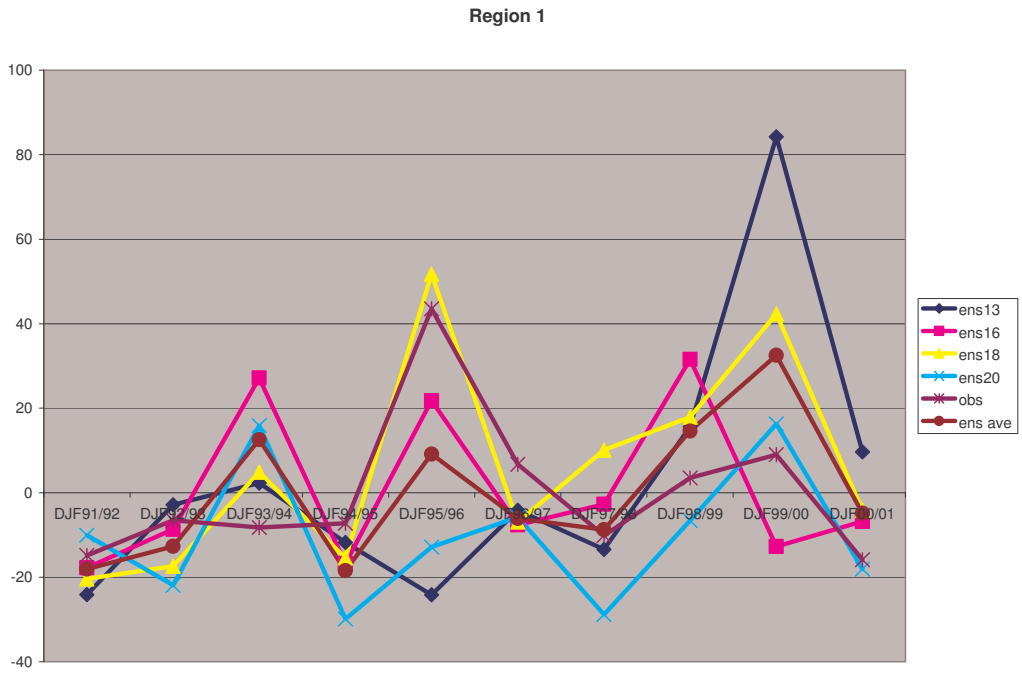

Figure 4.6: *The 10-year ensemble members and the ensemble average simulated and observed rainfall anomaly series in mm in region 1.*

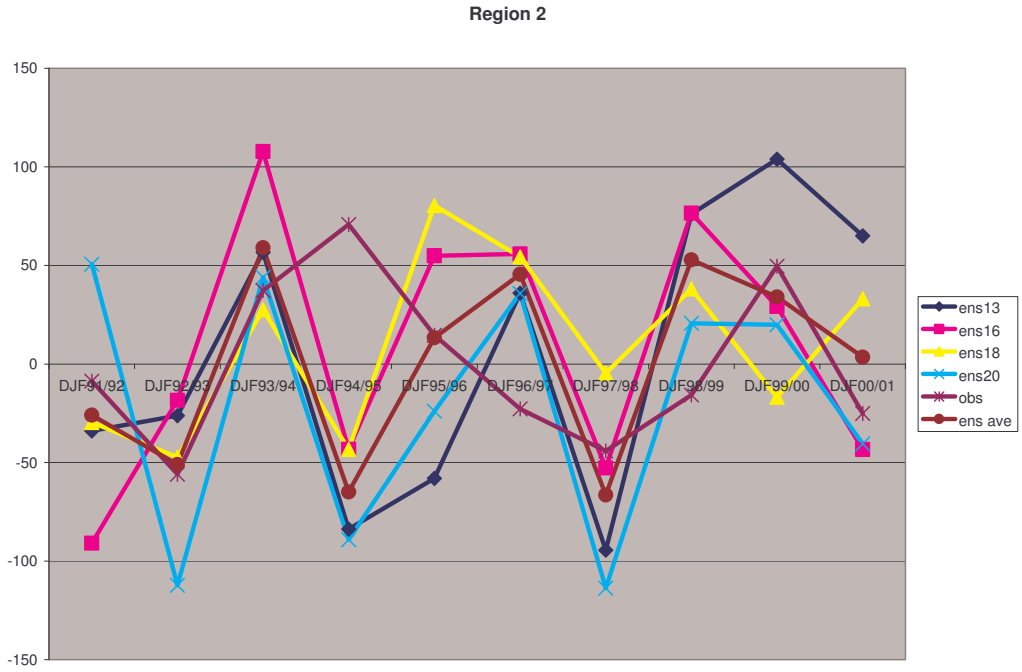

Figure 4.7: *The 10-year ensemble members and the ensemble average simulated and observed rainfall anomaly series in mm in region 2.*

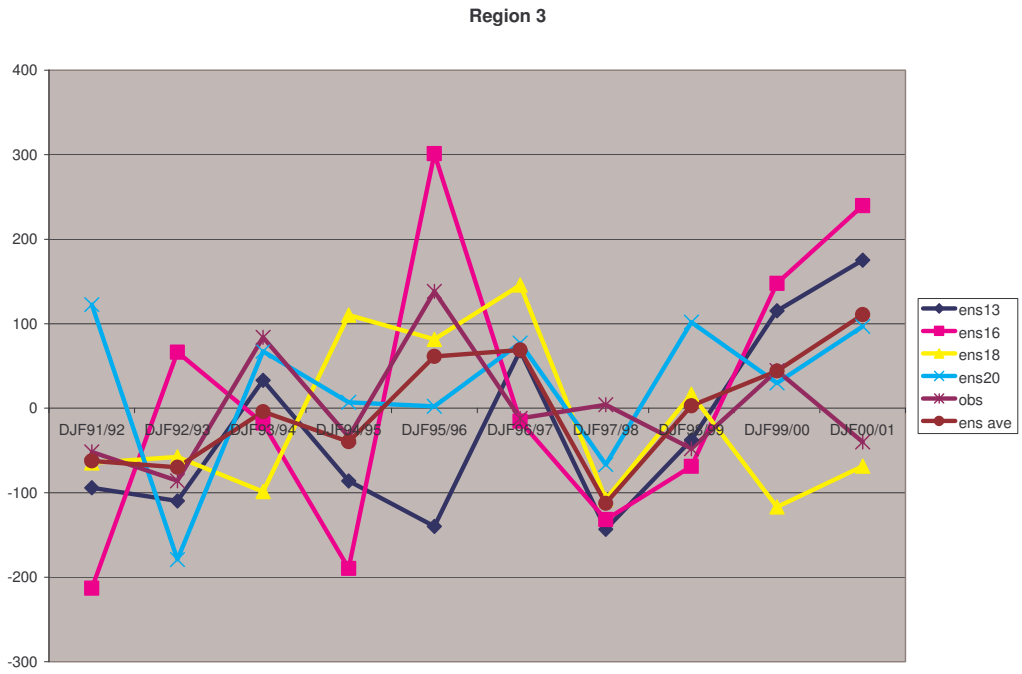

Figure 4.8: *The 10-year ensemble members and the ensemble average simulated and observed rainfall anomaly series in mm in region 4.*

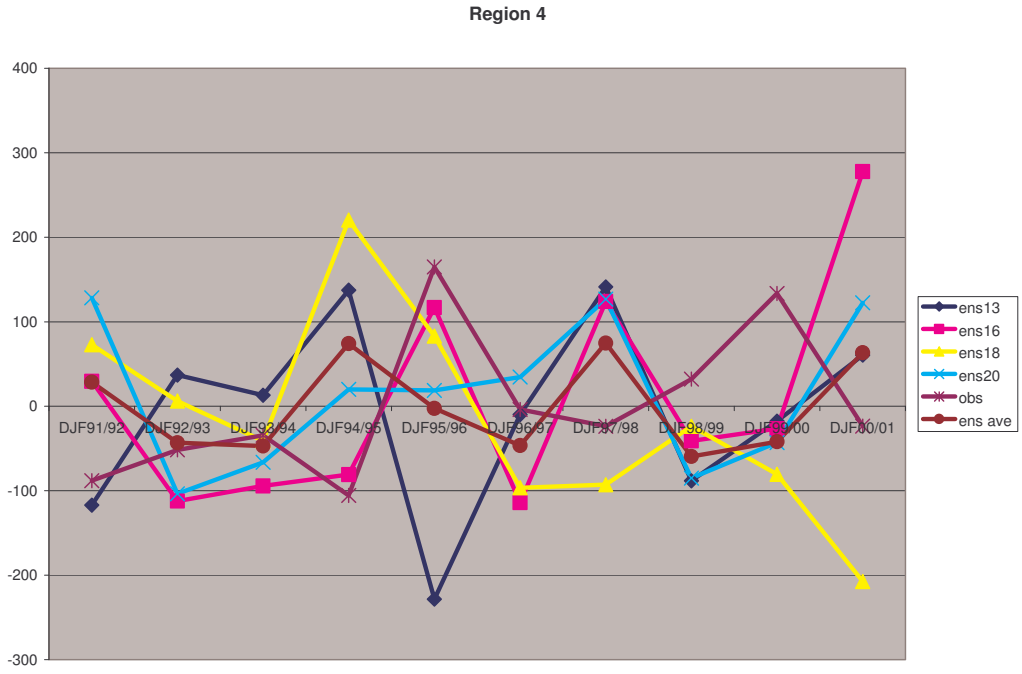

Figure 4.9: *The 10-year ensemble members and the ensemble average simulated and observed rainfall anomaly series in mm in region 4.*

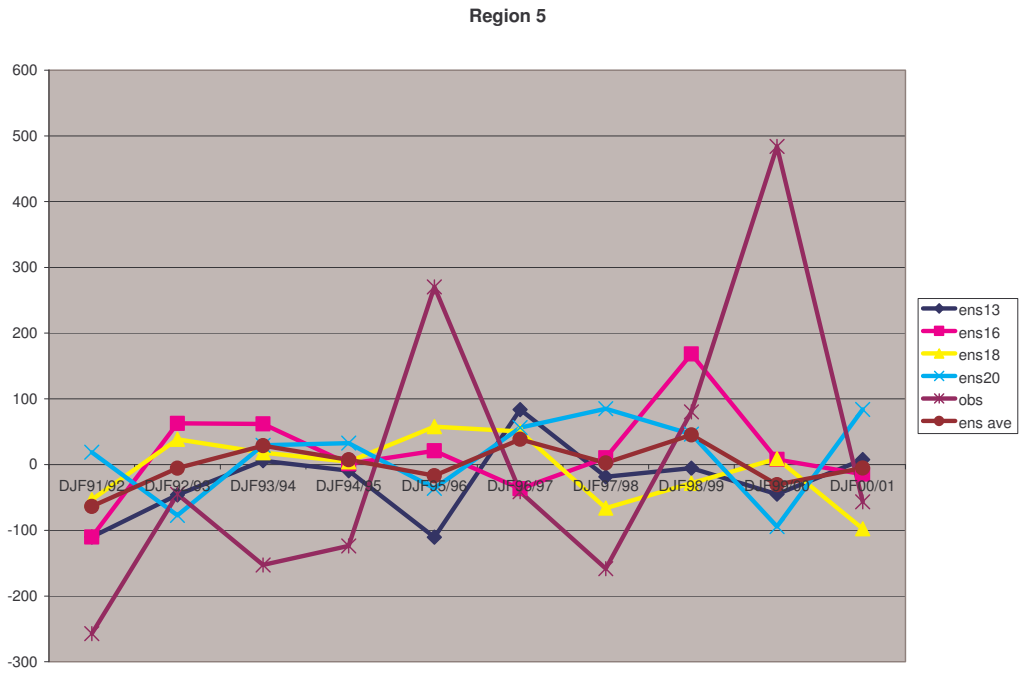

Figure 4.10: *The 10-year ensemble members and the ensemble average simulated and observed rainfall anomaly series in mm in region 5.*

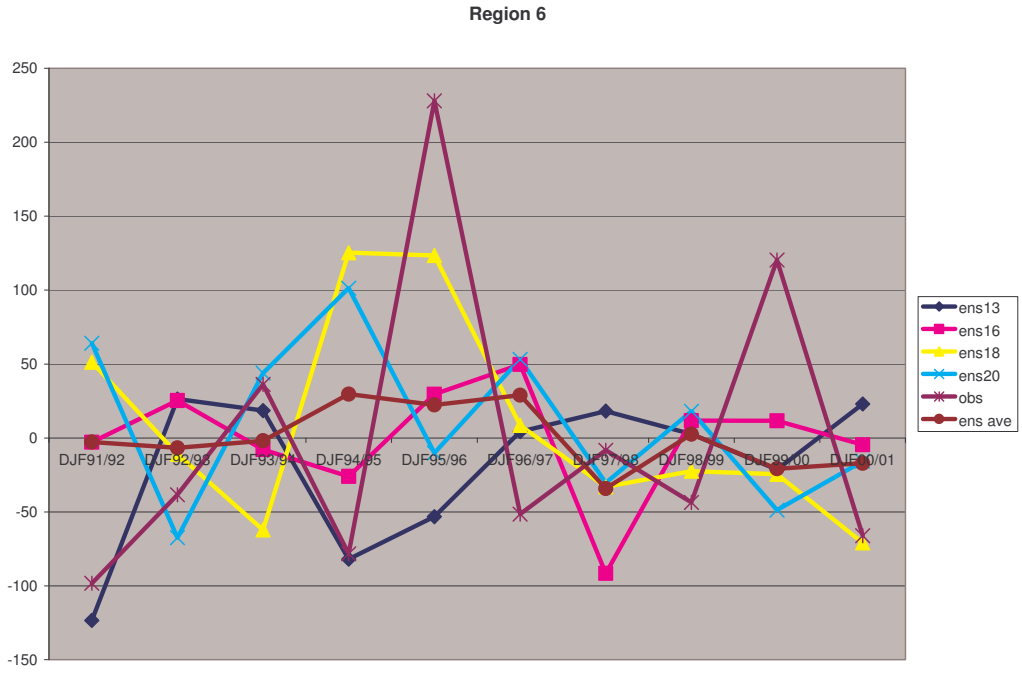

Figure 4.11: *The 10-year ensemble members and the ensemble average simulated and observed rainfall anomaly series in mm in region 6.*

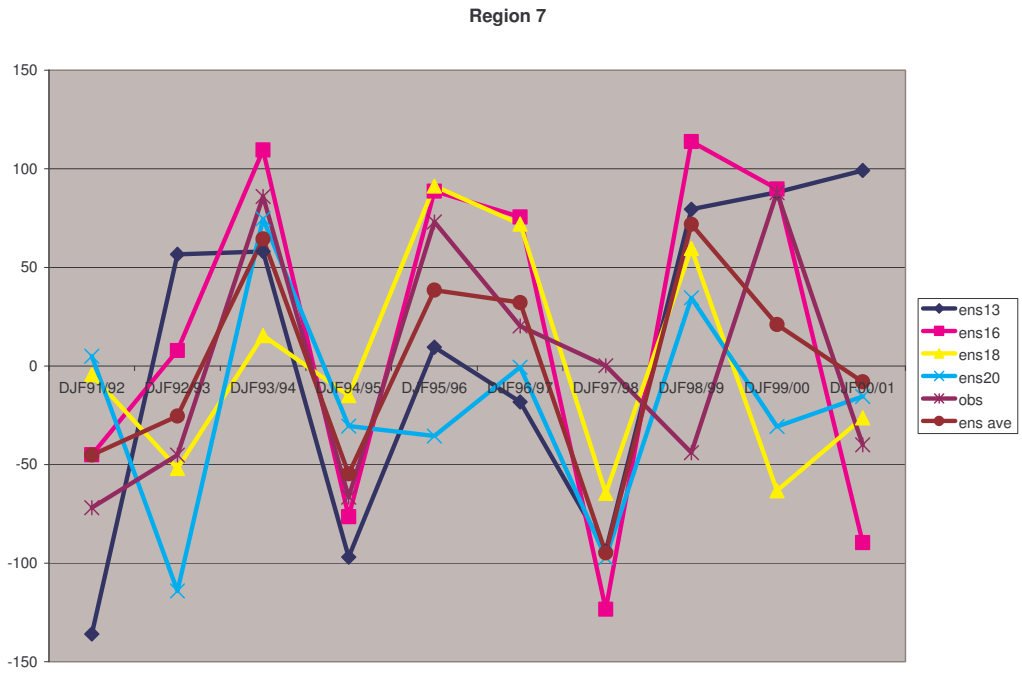

Figure 4.12: *The 10-year ensemble members and the ensemble average simulated and observed rainfall anomaly series in mm in region 7.*

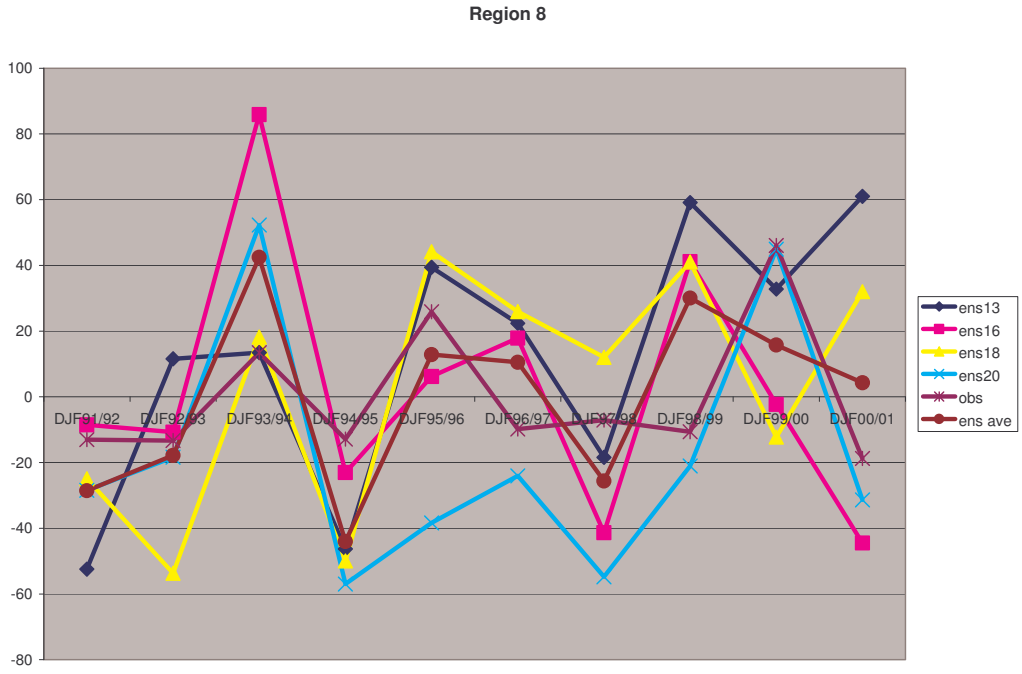

Figure 4.13: *The 10-year ensemble members and the ensemble average simulated and observed rainfall anomaly series in mm in region 8.*

4.3.3. Region 3

In region 3 the nested system overestimates rainfall with about 400 mm. The observed total rainfall time series does not overlap the ensemble average or any of the ensemble members anywhere, with the observed line below the simulated ones (Figure 3.10). The MAE graph (Figure 4.5) shows that the overestimation is the highest in this region. In previous studies the RegCM3 was found to over-predict rainfall in the steepest topographical slopes over West Africa, the Andes and in South Asia (Pal et al, 2005). The RCMs that have been applied over South Africa were also found to over estimate rainfall in region 3 (Engelbrecht et al, 2000; Joubert et al, 1999). In region 3, there are steep coastal margins that are immediately followed by steep topographies as the altitude above sea level increases from low to the highest altitudes over the escarpment (Figure 1.2). There are three seasons when the nested system simulated an opposite ensemble average rainfall anomaly as compared to the observations (Figure 4.8). The correlation between the observations and the ensemble average is 0.3325.

4.3.4. Region 4

Region 4 is also in the eastern coast and as can be seen from Figure 3.11, the nested system overestimates rainfall there as well. Region 4 has the second highest mean absolute error (Figure 4.5). In this region the correlation between the observations and the ensemble average is -0.3992. The nested system does not capture the two peaks in 1995/1996 and 2000/2001, and simulates an opposite sign as compared to the observations (Figure 4.10).

4.3.5. Region 5

In region 5 the nested system generally underestimates rainfall as can be seen from a negative mean error value (Figure 4.4). The underestimation is due to the two extreme seasons of 1995/1996 and 2000/2001 that are not captured by the system (Figure 3.12). The ensemble average anomaly series is close to the zero line, while the observed time series has large amplitudes

(Figure 4.10). The correlation between the observations and the ensemble average is -0.0932.

4.3.6. Region 6

There is a general overestimation of rainfall in region 6 (Figure 3.13). The average ensemble anomaly just oscillates between -50 and 50 (Figure 4.11). The seasonal total rainfall time series further confirms that the nested system for region 6 did not capture the extreme events of 1995/1996 and 1999/2000 (Figure 3.13 and Figure 4.11). The correlation between the observations and the ensemble average is 0.0278.

4.3.7. Region 7

The correlation between the observations and the ensemble average is 0.5138. The correlation value in this region suggests that the nested system performs better in this region than any of the other regions. In general there is an overestimation of rainfall (Figure 4.4) but the magnitude is smaller than in most of the other regions as can be seen from the mean absolute error (Figure 4.5). The time series of simulated rainfall and observed rainfall (Figure 3.14) do not show that the simulated rainfall is overestimated, which explains why the magnitude of the mean absolute error is smaller than in the other regions. The anomaly signs agree in general during the 10 years and there is only one season when the observed and the simulated rainfall have opposite signs (Figure 4.12).

4.3.8. Region 8

In region 8 the system underestimates rainfall (Figure 3.15; Figure 4.4). The mean absolute error is the second lowest, and the correlation is also much higher than over the eastern part of the country with a value of 0.4644. During three seasons the model simulated an opposite anomaly as compared to the observations while during the remaining seven seasons the nested system and the observation have the same sign (Figure 4.13).

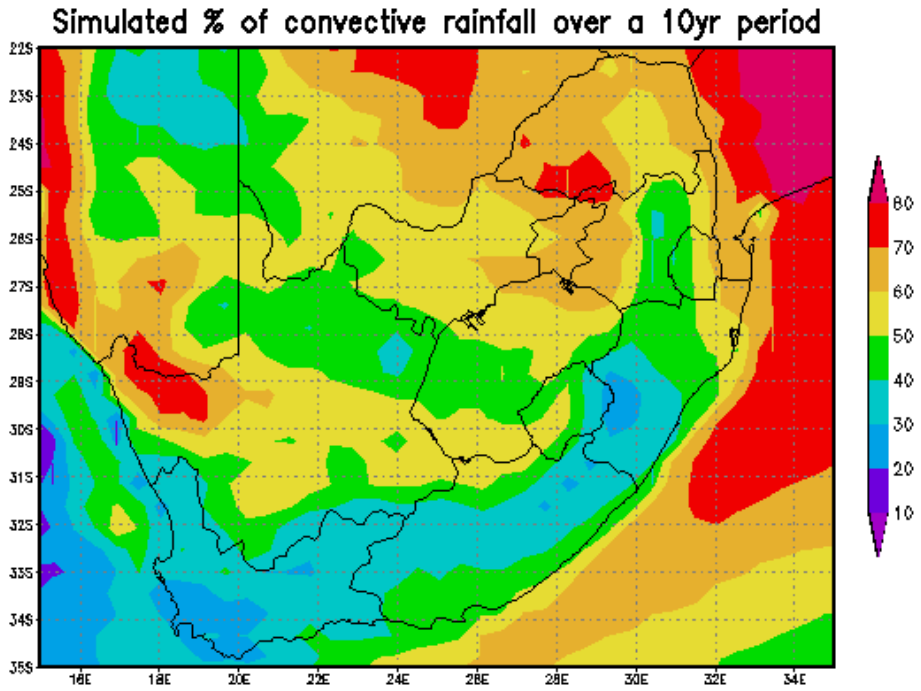

Figure 4.14: *The simulated percentage of convective rainfall relative to the total rainfall over South Africa for DJF 1991/1992-2000/2001.*

4.4. Summary and Conclusions

The areas of maximum variability for surface pressure and air temperature from the NCEP reanalysis correspond with that of the simulations. The CAMS_OPI rainfall variability also corresponds to some extent with the simulated rainfall variability. The simulated rainfall variability is noisy while the observed variability is smooth owing to the difference in the resolution of the two data sets. Over the tropical regions the observed variability is small while in the simulations it is large. The observed variability may not be a true representation of what happens in the area due to the lack of observations in the region.

The nested system solutions correspond with the observations mostly over the central part of South Africa with the least correspondence over the east where the model overestimates the rainfall. The rainfall overestimation is a

feature that may be attributable to the steep topographic gradients in the area as was found in previous studies. When the anomalies are analysed the model still performs better in the central and western parts than in the eastern part of South Africa. The skill of statistical downscaling models was also found to be higher in the central interior of South Africa (Landman and Tennant, 2002). The area where the models seem to be performing the best has the highest correlation with the SSTs in the Equatorial Pacific Ocean (Kruger, 1998).

The highest correlations between the observed DJF rainfall and the simulated ensemble average are over the western parts of the country. However, correlation does not take into account the underestimation found in region 8 (Figure 3.15). The percentage of convective rainfall relative to the total rainfall was plotted to determine how much of the rainfall is of convective origin and what percentage is of large scale origin (Figure 4.14). The model is able to capture that over the central parts (region 7) rainfall is mainly of large scale origin where very little underestimation is found, as opposed to region 8 where the rainfall is mainly of convective origin. Moreover, the model is also able to capture that most of the rainfall that occurs over the coasts and the adjacent interior is of large scale origin.

In Chapter 3 simulations from the RegCM3 obtained through nesting the RegCM3 inside the GCM solutions generated by perturbing the wind fields at initialisation were analysed. The ensemble members were found to be highly variable, providing evidence that the simulations from different initial conditions diverge as a result of the internal variability of the models. Although the ensemble members are different the ensemble average anomaly sign over South Africa is generally the same as the observed anomaly sign.

The above simulations were different from each other due to the internal variability of both the GCM and the RCM. In seasonal prediction it has already been established that multiple realisations should be made in sensitivity studies as well as in the operational forecasting to quantify the uncertainty associated with non-linearities in the GCMs. It has, however, not been established yet, whether or not multiple realisations should be made to

quantify the uncertainty associated with the RCM's internal variability. It is important that the question is answered before the RCMs is used operationally.

CHAPTER 5: THE INTERNAL VARIABILITY OF THE RegCM3 (SEASONAL)

5.1. Introduction

In the previous chapters it was established that the nested system solutions capture the inter-annual rainfall variability in general. The ensemble members diverged from one another due to the internal variability of both the GCM and the RCM. In this Chapter the contribution of non-linearities in the RCMs to the total variability of the solutions described in the previous two chapters is investigated. In this part of the study only two years that were highly anomalous are analysed. DJF 1991/1992 was associated with dry conditions (Figure 2.1) while DJF 1995/1996 (Figure 2.2) was associated with wet conditions. The two seasons were defined as ENSO seasons by Trenberth (1997); the dry season was associated with the low phase of the oscillation while the wet season was associated with the high phase of the oscillation.

The section on the internal variability of the GCM and the RCM discusses the variability of the ensemble members that are generated to quantify the non-linearities in both the GCM and the RCM. In the previous chapters the area averages in the homogeneous regions were considered but in this section the rainfall totals are displayed over the whole of South Africa. The section on the internal variability of the RCM discusses the ensemble members generated in order to quantify the uncertainty associated with non-linearities in the RCMs alone.

The simulated seasonal total rainfall anomalies over South Africa for each ensemble member as well as the ensemble average for the two seasons are compared with each other and with the observations. The observed anomalies for the two seasons, 1991/1992 and 1995/1996, are calculated using the average of the 10-year period from 1991/1992 to 2000/2001. The simulated ensemble members and ensemble average anomalies for the two years are obtained through subtracting the ensemble average calculated over the 10-years. The ensemble average is calculated like before using the four

ensemble members described in the previous chapters over the 10-year period.

5.2. 1991/1992

5.2.1. The internal variability of the GCM and the RCM

The ensemble average anomaly obtained through perturbing the wind fields at initialisation for the GCM is generally negative (Figure 5.1). The negative anomalies over the eastern part of the country are not as big as they are in the observations. There are areas towards the eastern coast where the ensemble average gives positive anomalies.

The solutions obtained from the ensemble members are quite distinct. Ensemble member 13 gives a negative anomaly over the whole country (Figure 5.2), and ensemble member 16 gives a negative pattern over most of the country, but with some positive anomaly areas towards the north-eastern parts (Figure 5.3). Ensemble member 18 also has some positive anomalies towards the north-eastern parts (Figure 5.4) while ensemble member 20 is dominated by the positive anomalies over the eastern half of South Africa (Figure 5.5).

The results show that the nested system solution is sensitive to the SST forcing fields, because the ensemble average captures the negative anomalies over the larger part of South Africa for DJF 1991/1992 (Figure 5.1). If ensemble member 13 were the only one to be used then the model solution would have been closer to the observations as opposed to when the ensemble average is used. It is, however, interesting that although the ensemble members are different the majority of the ensemble members captured the sign of the observed anomaly over the larger part of the country. The positive anomalies in three of the ensemble members towards the eastern coast resulted in the ensemble average anomaly being positive over

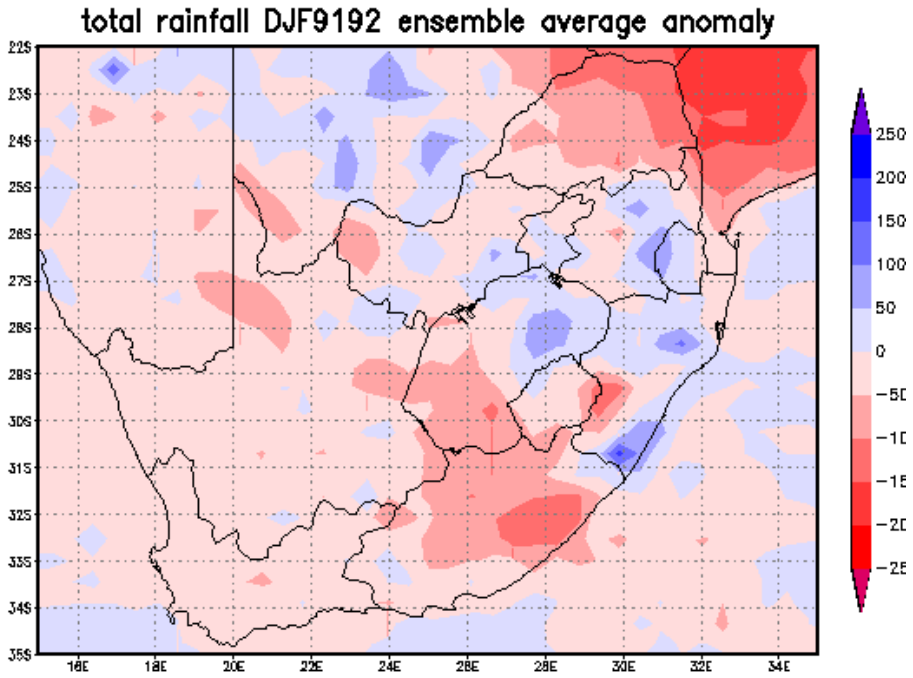

Figure 5.1: *The DJF 1991/1992 GCM internal variability induced ensemble average RCM total rainfall anomaly in mm.*

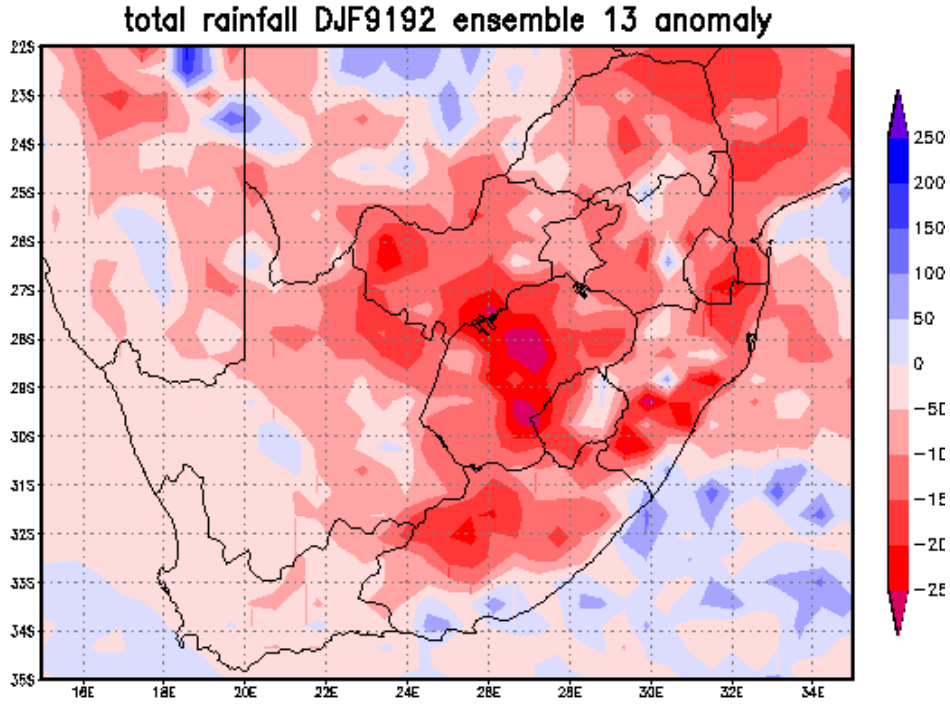

Figure 5.2: *The DJF 1991/1992 Ensemble member 13 total rainfall anomaly in mm.*

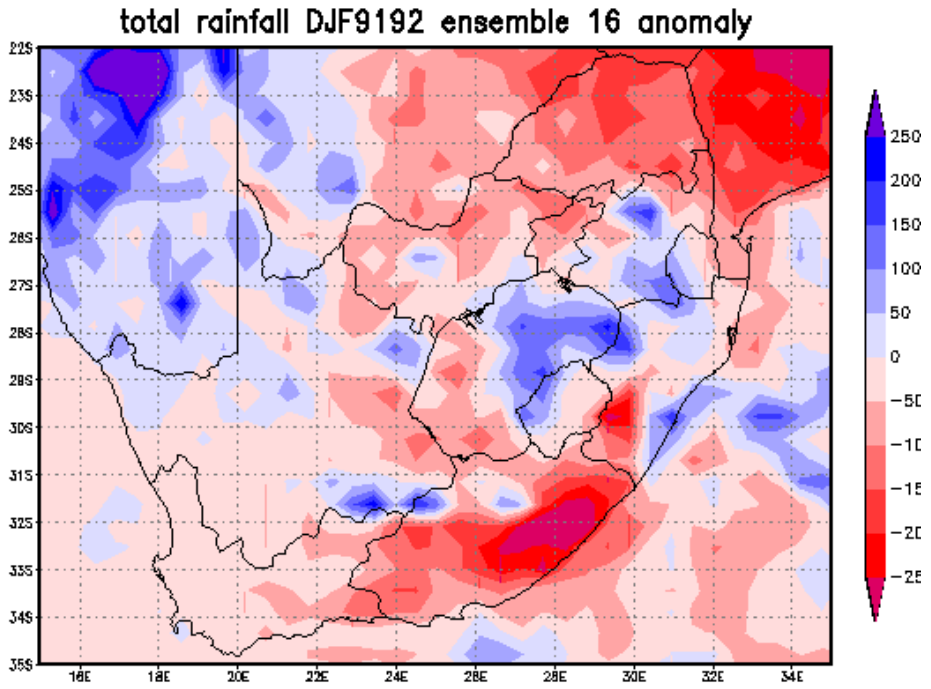

Figure 5.3: *The DJF 1991/1992 Ensemble member 16 total rainfall anomaly in mm.*

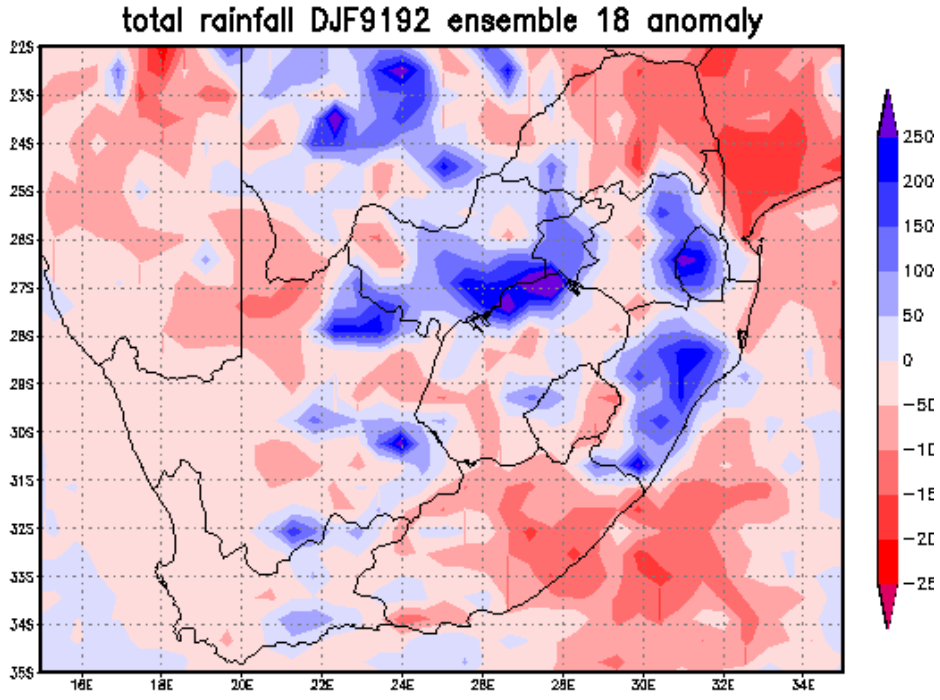

Figure 5.4: *The DJF 1991/1992 Ensemble member 18 total rainfall anomaly in mm.*

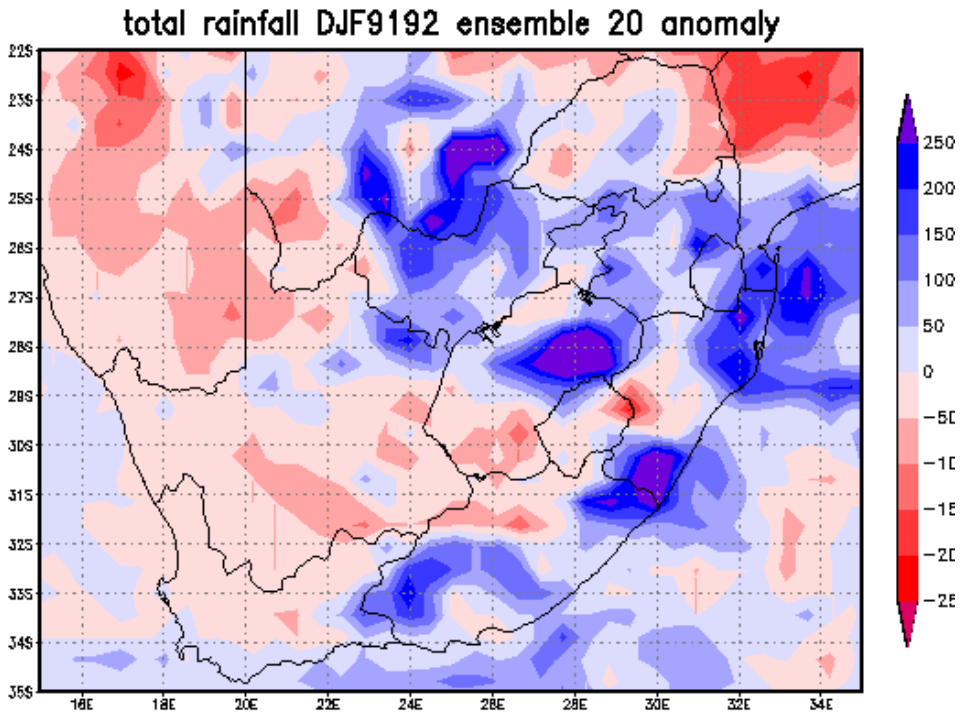

Figure 5.5: *The DJF 1991/1992 Ensemble member 20 total rainfall anomaly in mm.*

that area. However, the area is smaller in the ensemble average. While there is an ensemble member that got the direction of the anomalies far better than the rest there is one that simulated an opposite anomaly sign to the observed. If ensemble member 20 were the only one considered then the model solution would have seemed less useful. Given that the ensemble members are different only due to the internal variability of the models there is no way of predetermining which ensemble member will be the most useful. The results confirm that the use of ensemble averages improves skill over a single realisation.

5.2.2. Internal variability of the RegCM3

Four ensemble members are generated using only ensemble member 13 of the GCM to force the RegCM3. The ensemble members that are generated differ from each other by one model day obtained from using the LAF technique. The resulting anomalies obtained from each ensemble member

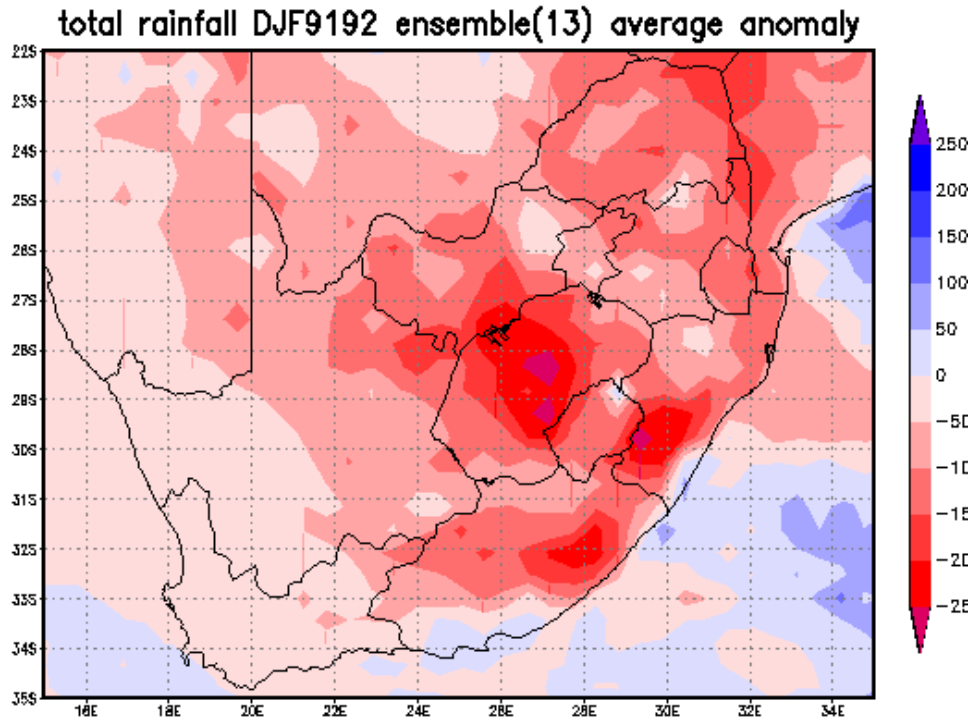

Figure 5.6: *The DJF 1991/1992 Ensemble member 13 ensemble average total rainfall anomaly in mm.*

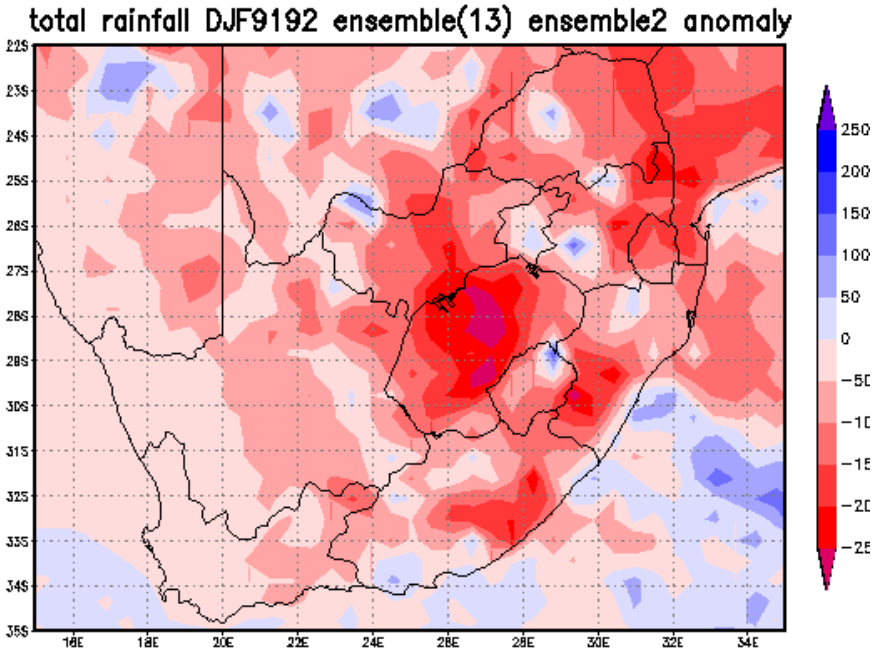

Figure 5.7: *The DJF 1991/1992 Ensemble member 13 ensemble member 2 total rainfall anomaly in mm.*

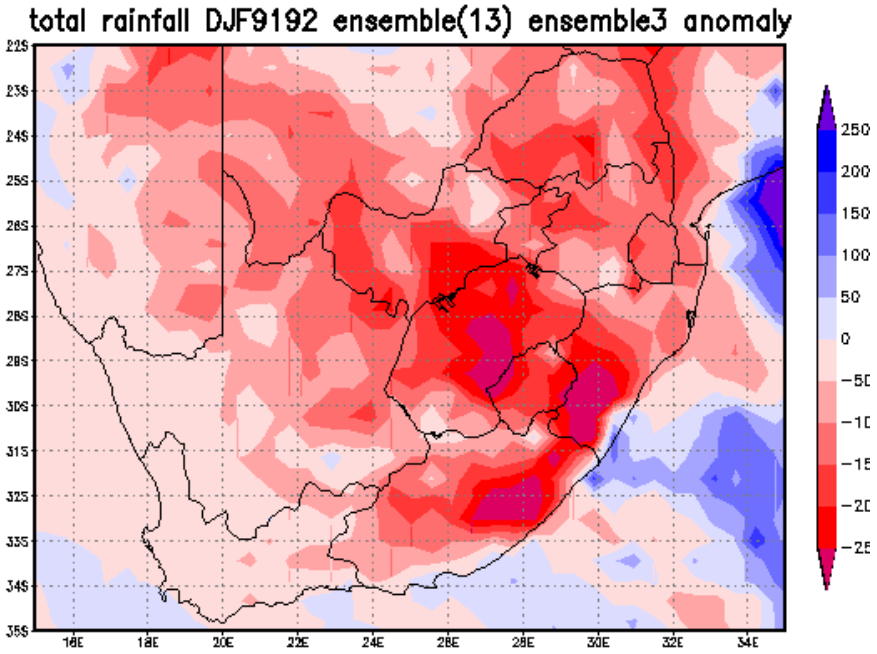

Figure 5.8: *The DJF 1991/1992 Ensemble member 13 ensemble member 3 total rainfall anomaly in mm.*

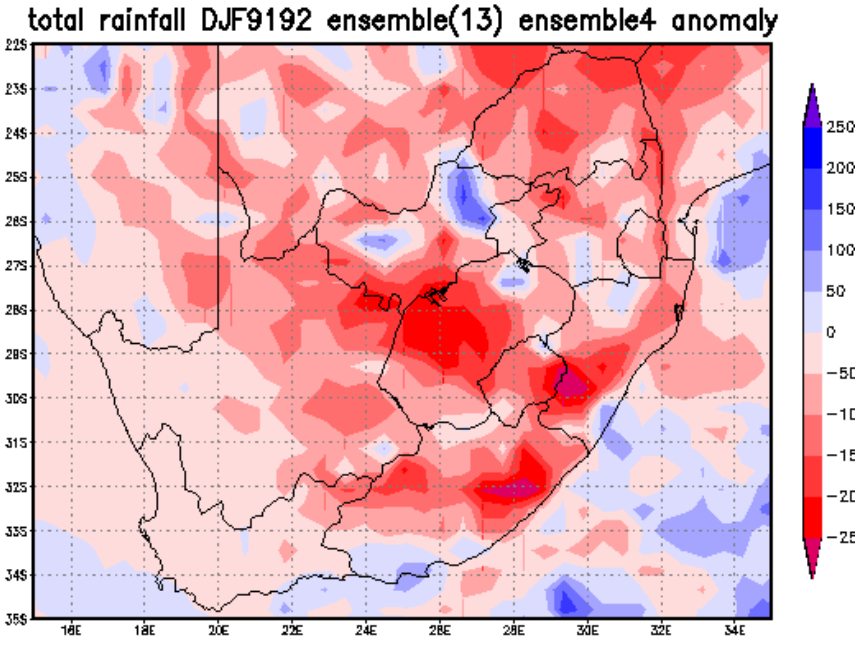

Figure 5.9: *The DJF 1991/1992 Ensemble member 13 ensemble member 4 total rainfall anomaly in mm.*

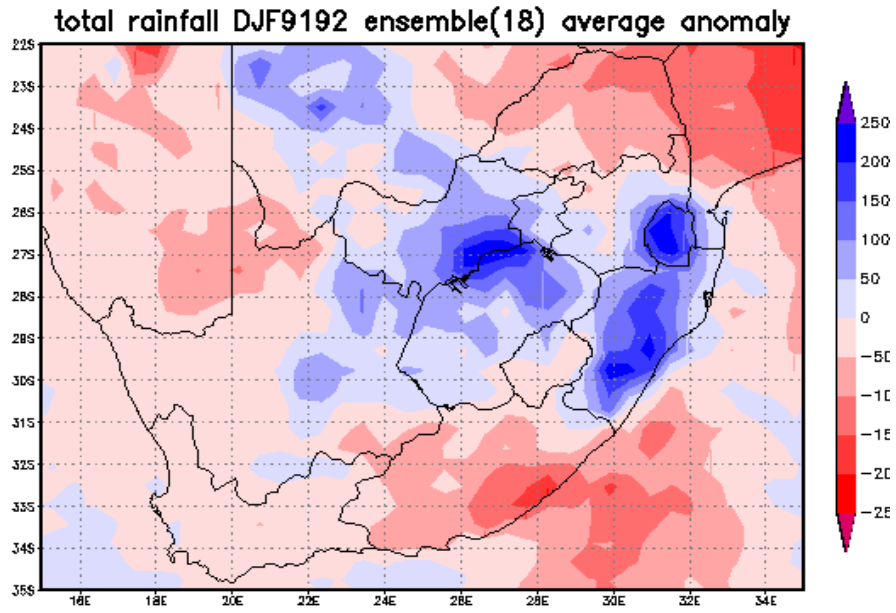

***Figure 5.10**: The DJF 1991/1992 Ensemble member 18 ensemble average total rainfall anomaly in mm.*

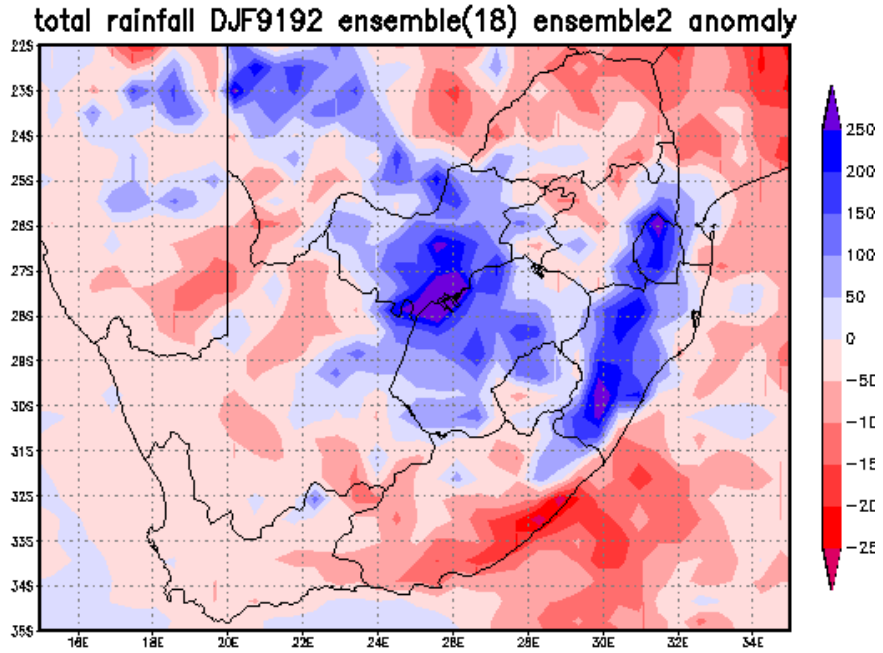

***Figure 5.11:** The DJF 1991/1992 Ensemble member 18 ensemble member 2 total rainfall anomaly in mm.*

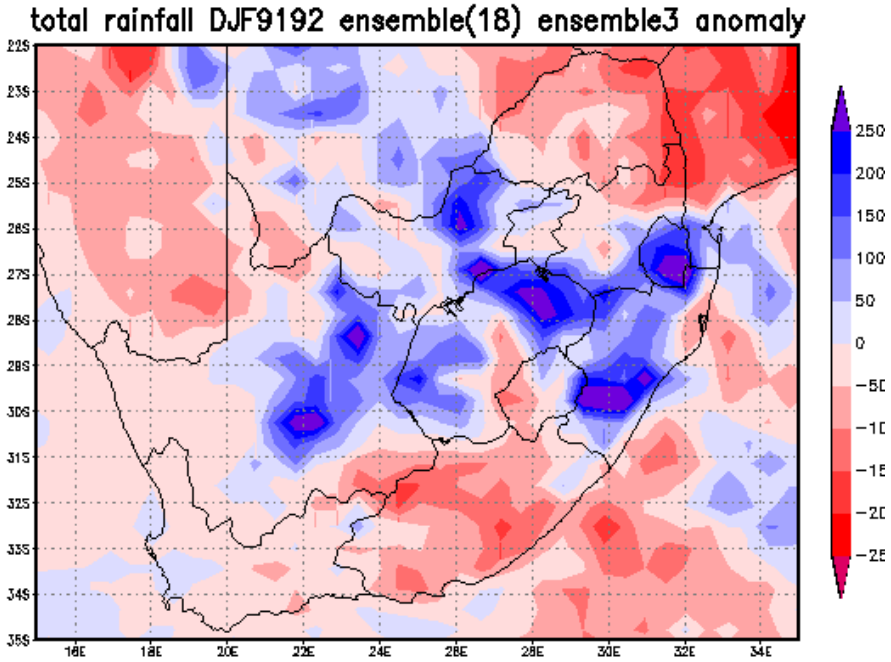

Figure 5.12: *The DJF 1991/1992 Ensemble member 18 ensemble member 3 total rainfall anomaly in mm.*

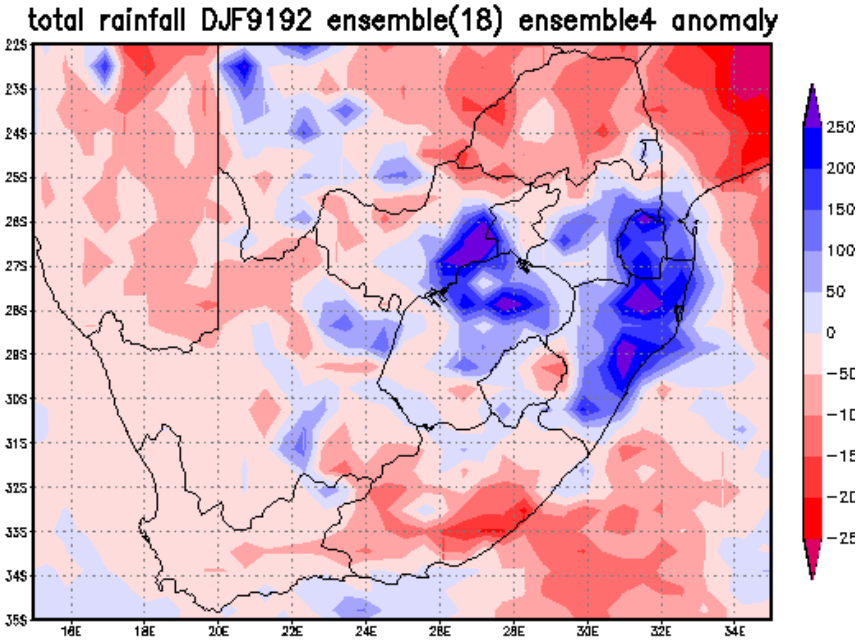

Figure 5.13: *The DJF 1991/1992 Ensemble member 18 ensemble member 4 total rainfall anomaly in mm.*

are found to be generally similar. The differences in the anomaly of each ensemble member (Figure 5.2; Figure 5.7; Figure 5.8 and Figure 5.9) and the anomaly of the ensemble average (Figure 5.6) are small. The same procedure is followed using ensemble member 18 and the ensemble members are also found to be generally the same (Figure 5.4; Figure 5.11; Figure 5.12; Figure 5.13). Ensemble member 18 simulated some positive anomalies and as a result all the ensemble members and the ensemble average (Figure 5.10) that are generated from ensemble member 18 also have positive anomalies which were not observed (Figure 2.1). The results suggest that the internal variability of the RCM does not contribute much to the variability of the simulations. Therefore, the variability of the ensemble members generated from a nested system is mainly a result of the non-linearities in the forcing GCM.

5.3. 1995/1996

5.3.1. The internal variability of the GCM and the RCM

A similar procedure is followed as above, but for the wet season of 1995/1996 (Figure 2.4). The ensemble average from the GCM got the general direction of the wet anomalies over a larger part of the country (Figure 5.14). The simulated anomalies of the ensemble average are again small over the eastern part of the country as compared to the observed anomaly with some parts of the north-eastern part having an opposite sign to the observed. This season was very wet and the observed positive anomalies are quite high over the north-eastern part of South Africa, but the model did not capture these extreme anomalies. This season is one of the seasons that led to the mean error graph of region 5 (Figure 4.4) in Chapter 4 to be negative.

The ensemble members obtained from perturbing the wind fields of the GCM at initialisation and then nesting the RegCM3 in the different solutions are different from one another (Figure 5.15; Figure 5.16; Figure 5.17 and Figure 5.18) similar to what was also found for 1991/1992. Ensemble member 13

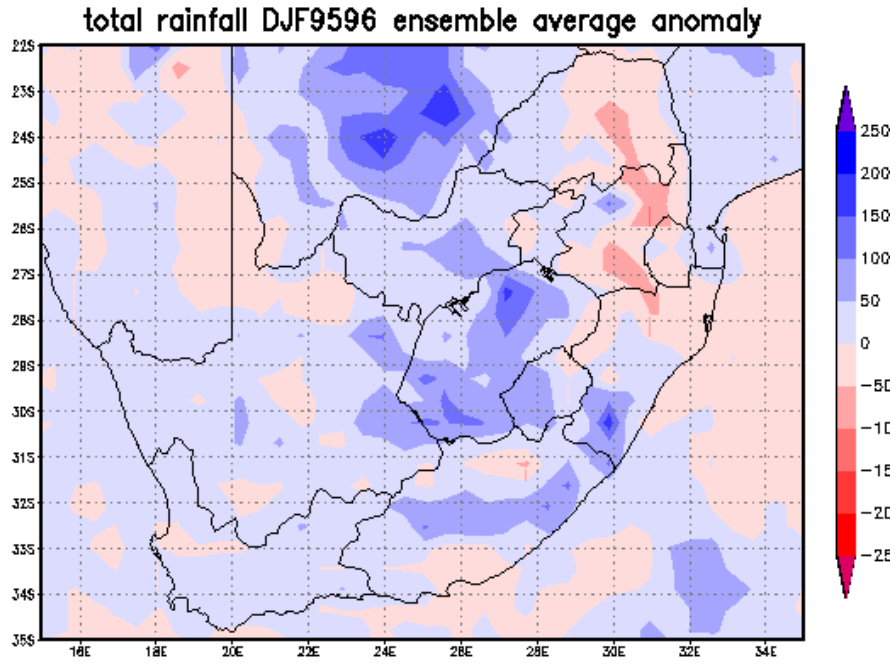

Figure 5.14: *The DJF 1995/1996 GCM internal variability induced ensemble average RCM total rainfall anomaly in mm.*

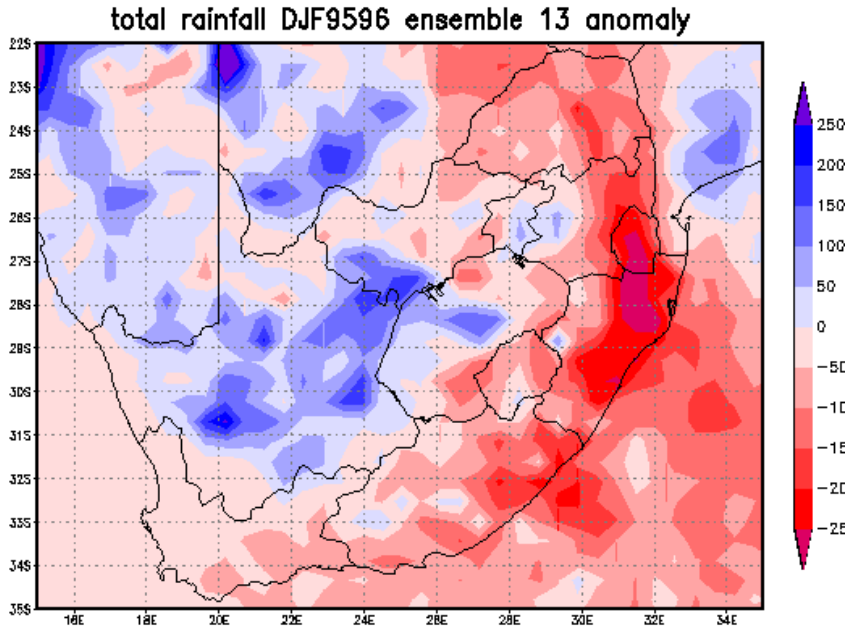

Figure 5.15: *The DJF 1995/1996 Ensemble member 13 total rainfall anomaly in mm.*

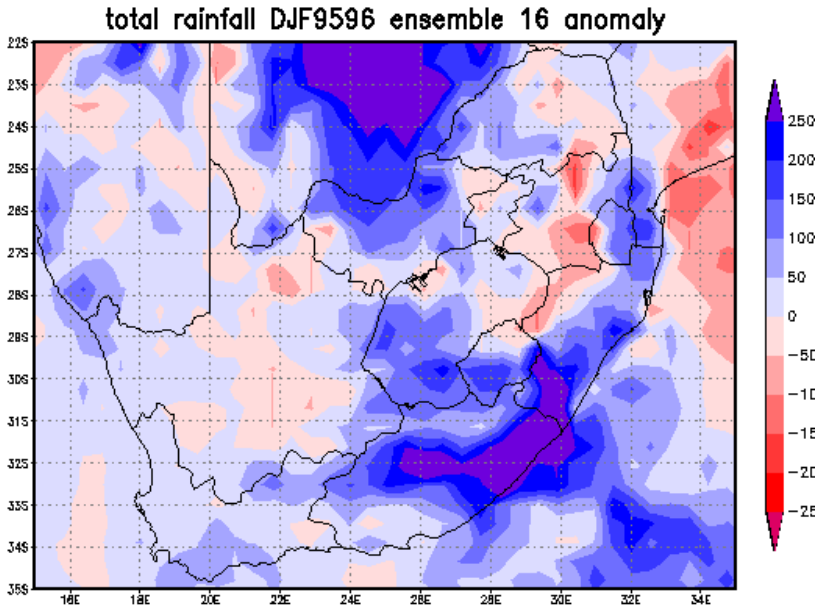

Figure 5.16: *The DJF 1995/1996 Ensemble member 16 total rainfall anomaly in mm.*

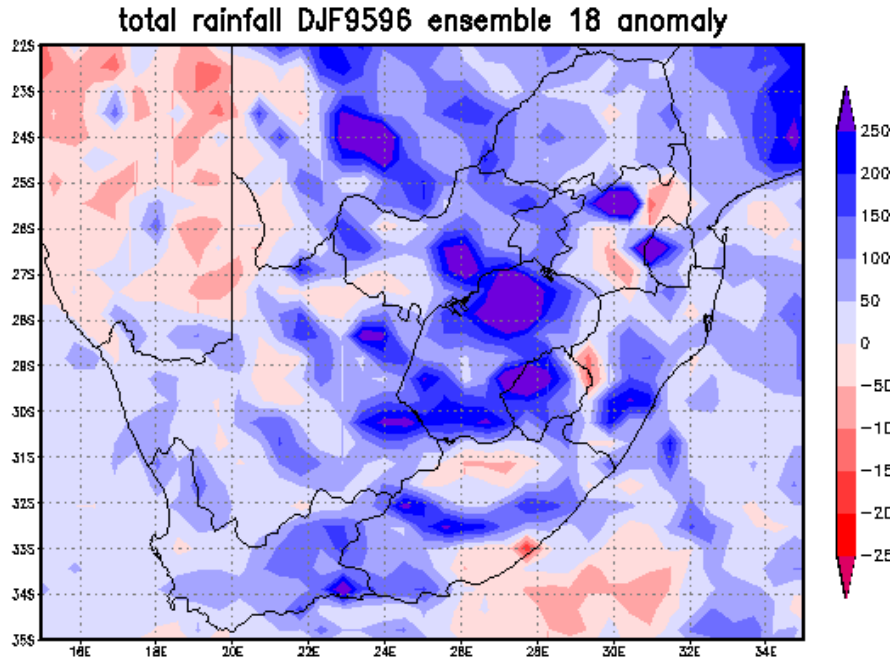

Figure 5.17: *The DJF 1995/1996 Ensemble member 18 total rainfall anomaly in mm.*

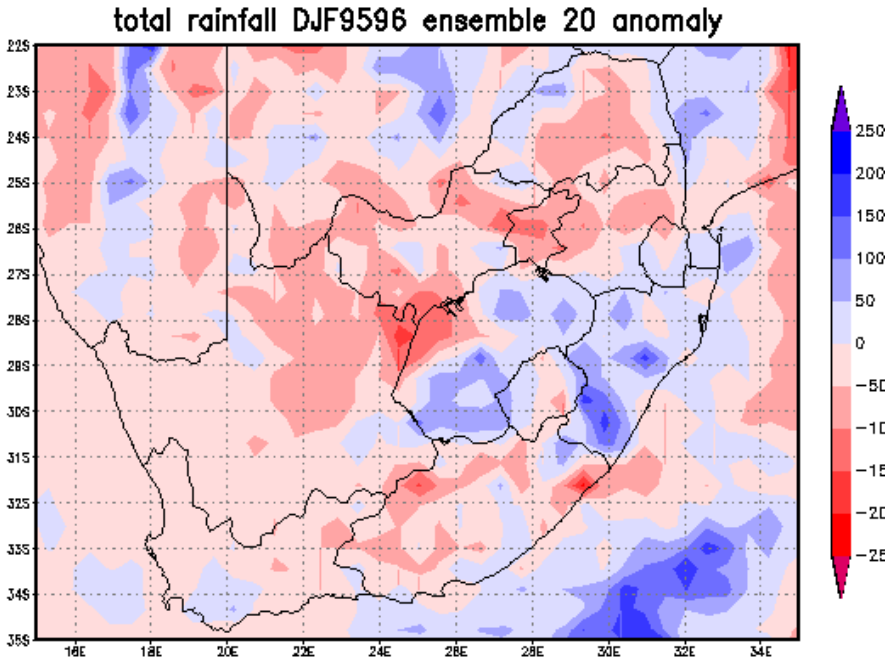

Figure 5.18: *The DJF 1995/1996 Ensemble member 20 total rainfall anomaly in mm.*

gives negative anomalies over the larger part of the country except over the north-western parts (Figure 5.15), Ensemble member 16 shows positive anomalies over a larger part of SA except for a small region over the north-eastern parts (Figure 5.16). Ensemble member 18 gives positive anomalies over almost the whole of SA (Figure 5.17) while ensemble member 20 gives a general negative anomaly pattern except over the eastern coast (Figure 5.18). For 1995/1996 ensemble member 13 is quite different from the observations while ensemble member 18 is closer to the observations. In 1991/1992 ensemble member 13 performed better than all the other ensemble members and in this season it is performing the worst. This shows there is not a single ensemble member out of the four which can be singled out to be performing the best over the 10-year test period.

5.3.2. The internal variability of the RegCM3

Four RegCM3 ensemble members are nested in GCM ensemble members 13 and 18 as was done before for 1991/1992 season. The RegCM3 ensemble

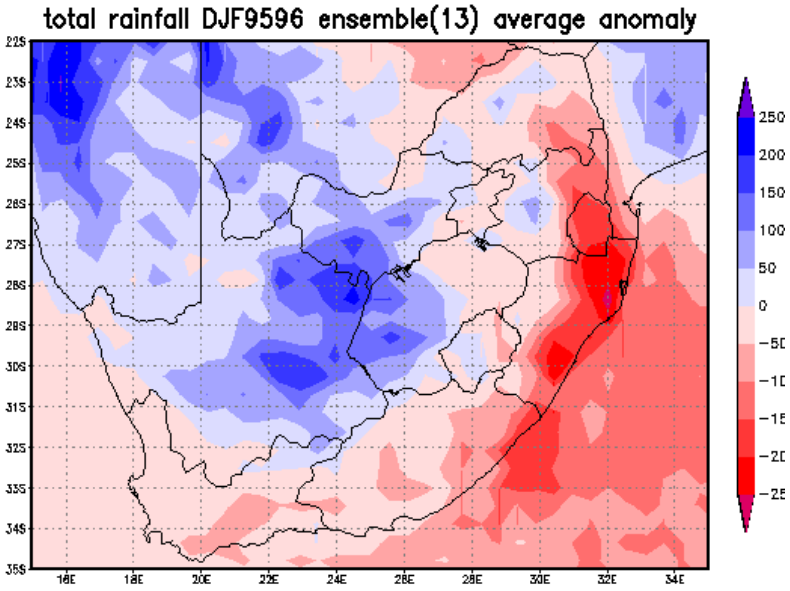

Figure 5.19: *The DJF 1995/1996 Ensemble member 13 ensemble average total rainfall anomaly in mm.*

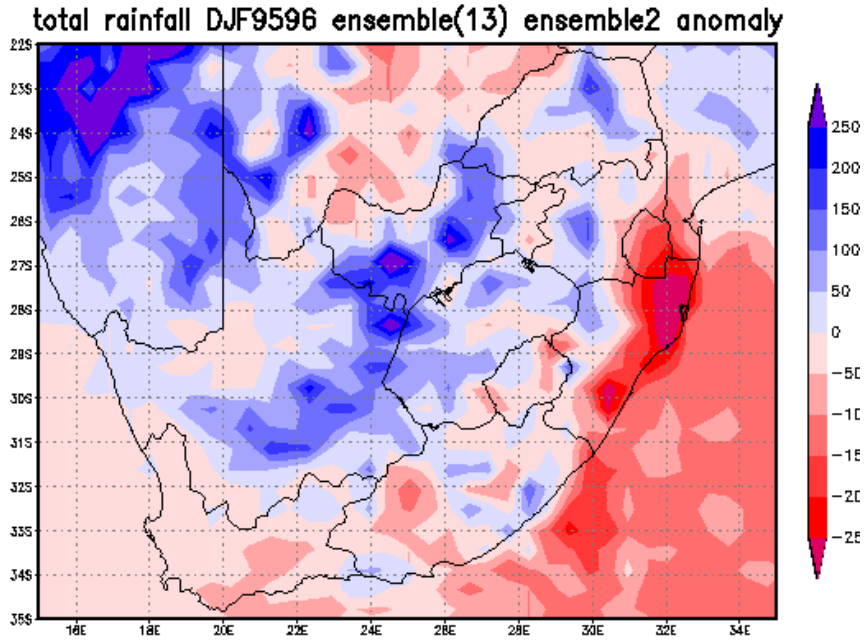

Figure 5.20: *The DJF 1995/1996 Ensemble member 13 ensemble member 2 total rainfall anomaly in mm.*

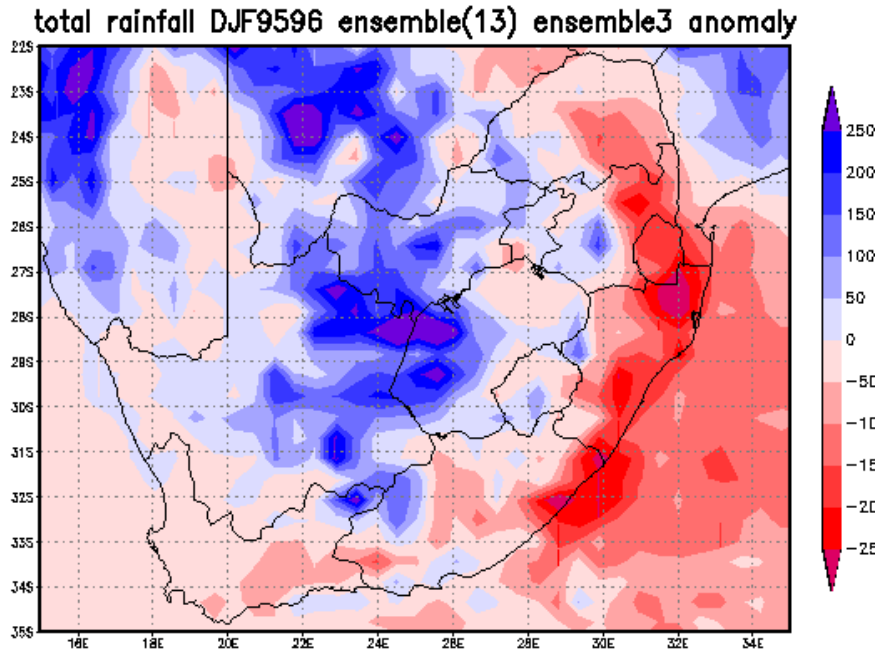

Figure 5.21: *The DJF 1995/1996 Ensemble member 13 ensemble member 3 total rainfall anomaly in mm.*

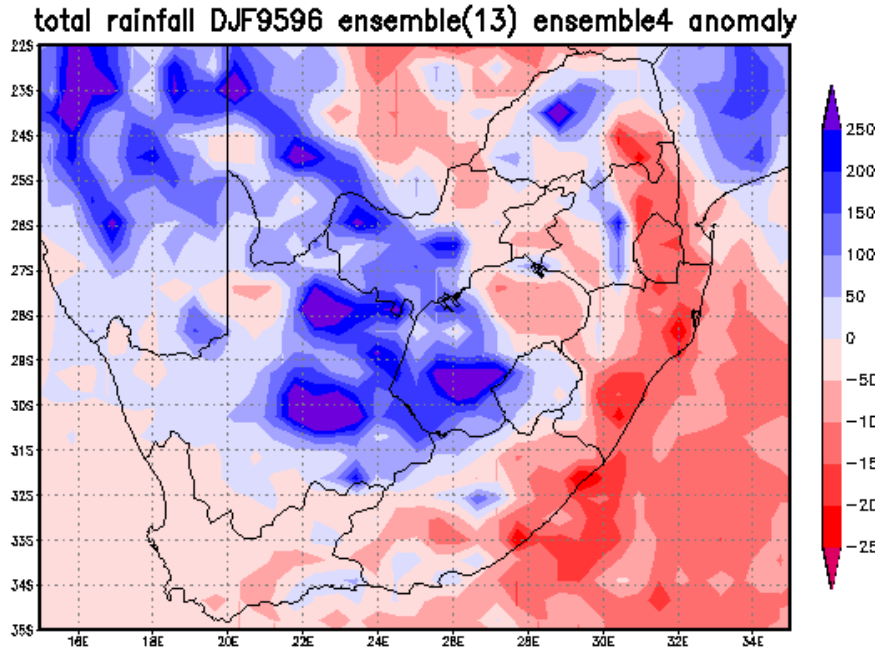

Figure 5.22: *The DJF 1995/1996 Ensemble member 13 ensemble member 4 total rainfall anomaly in mm.*

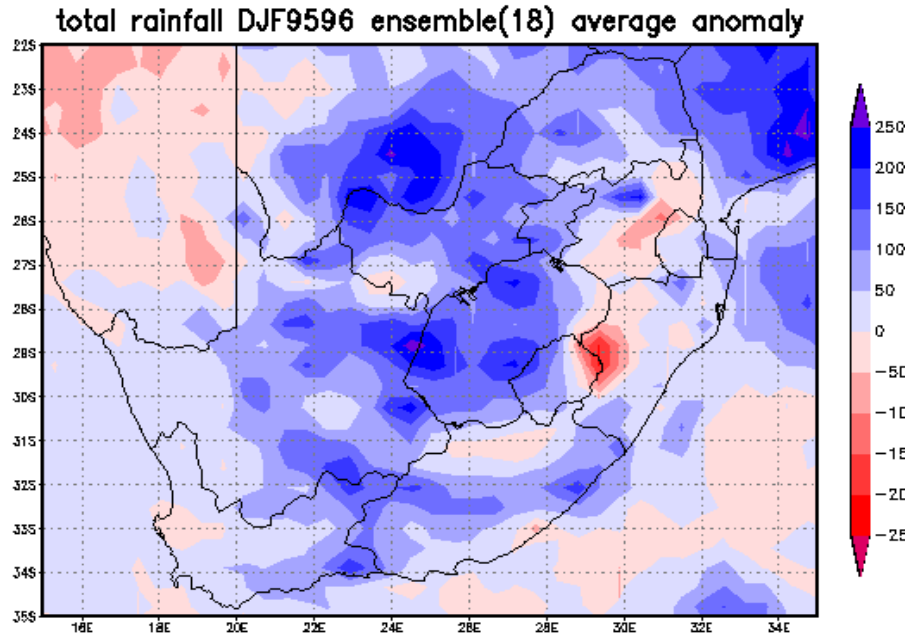

Figure 5.23: *The DJF 1995/1996 Ensemble member 18 ensemble average total rainfall anomaly in mm.*

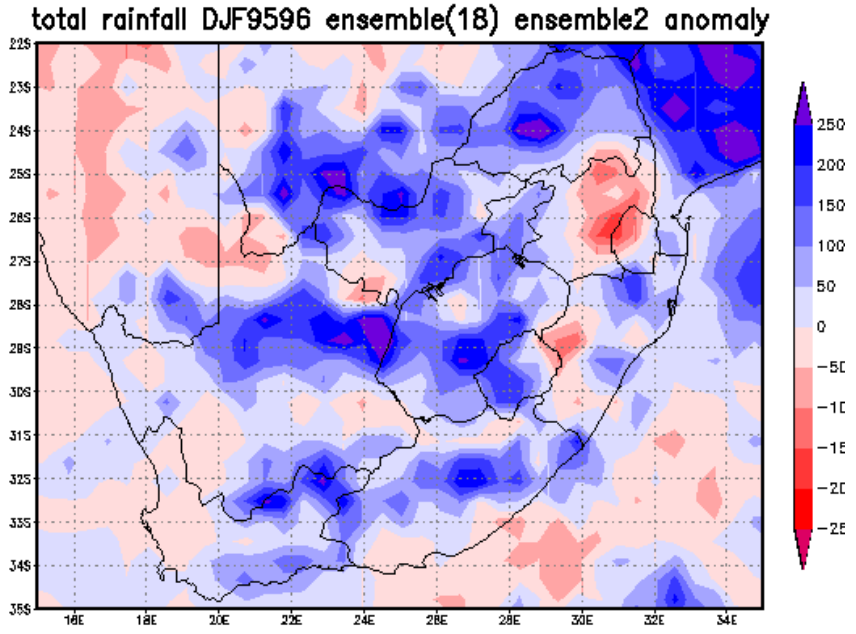

Figure 5.24: *The DJF 1995/1996 Ensemble member 18 ensemble member 2 total rainfall anomaly in mm.*

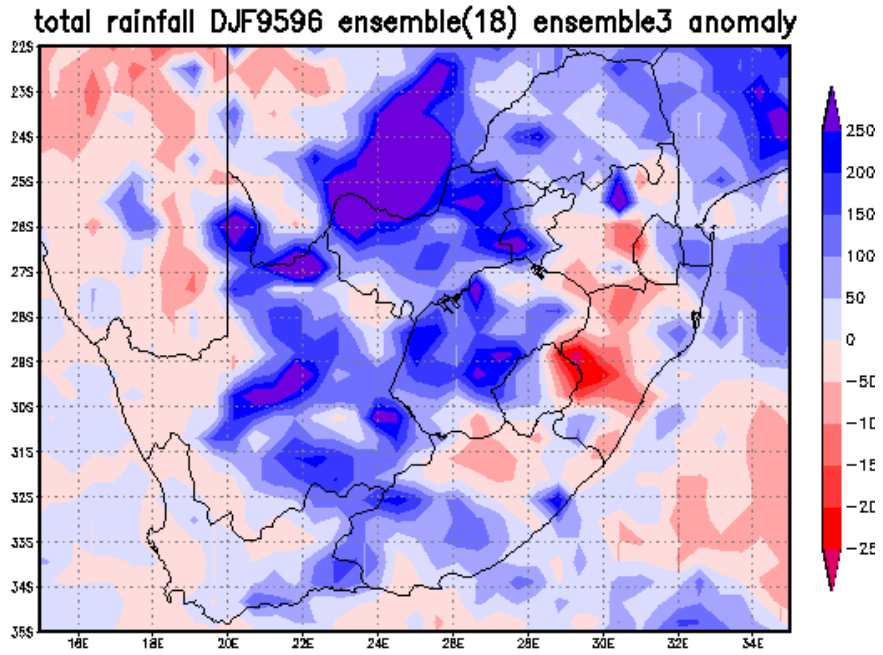

Figure 5.25: *The DJF 1995/1996 Ensemble member 18 ensemble member 3 total rainfall anomaly in mm.*

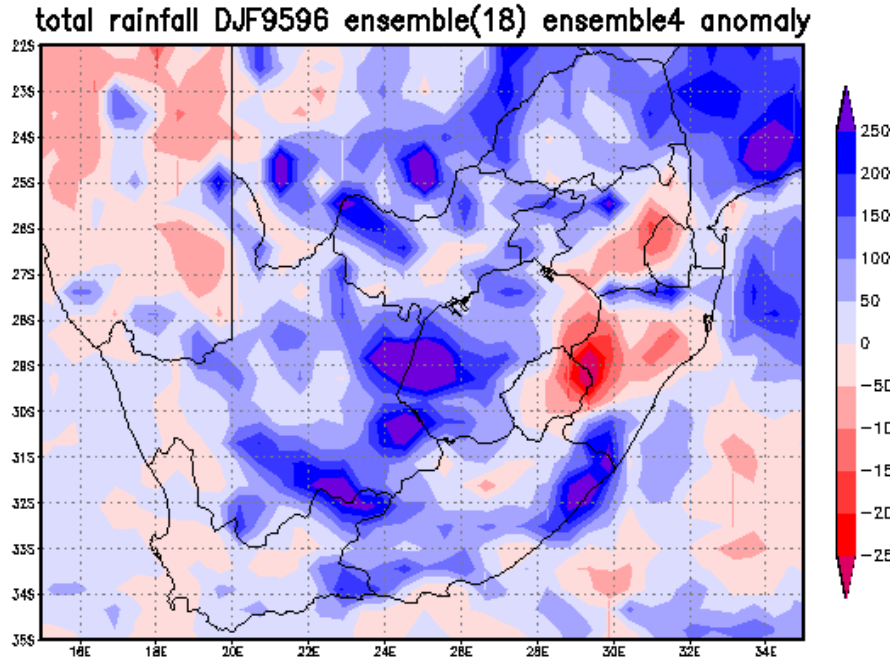

Figure 5.26: *The DJF 1995/1996 Ensemble member 18 ensemble member 4 total rainfall anomaly in mm.*

members that are related to ensemble member 13 are all generally similar to one another (Figure 5.15; Figure 5.20, Figure 5.21; Figure 5.22) as well as to the ensemble average (Figure 5.19). Ensemble member 13 did not perform well during the 1991/1992 season especially over the coastal areas. All the RegCM3 ensemble members that are generated from ensemble member 13 performed in the same way. The differences in the simulations are very small. Ensemble member 18 performed well in this season as can be seen from the ensemble average (Figure 5.23). All four of the RegCM3 runs nested in GCM ensemble member 18 performed in the same way giving mainly positive anomalies over a larger part of the country with small differences amongst the ensemble members (Figure 5.17; Figure 5.24; Figure 5.25; Figure 5.26).

5.4. Summary and Conclusions

In this Chapter two highly anomalous rainfall seasons were analysed and the models' internal variability based on the two seasons was discussed. The four ensemble members obtained through perturbing the wind fields of the ECHAM4.5 at initialisation and nesting the RegcM3 within the different solutions and four ensemble members through initialising the RegCM on different days but using a single GCM realisation were analysed. The former gives the measure of the internal variability of both the GCM and the RCM while the latter gives the internal variability of the RCM. The model solutions obtained through perturbing the wind fields of the GCM at initialisation are quite different from one another while those obtained through initialising the RegCM3 on different days are generally similar. These results suggest that the variability that is found amongst the ensemble members that were generated through perturbing the wind fields of the GCM at initialisation is mostly a result of the non-linearities in the GCM.

The model captured the general direction of the rainfall anomalies in the two seasons. The anomalies associated with the ensemble averages are quite small when compared to the observations and also when compared to the individuals ensemble member anomalies. These small anomalies in the

ensemble average are due to the high variability of the ensemble members. Ensemble member 13 performed the best for the 1991/1992 season and in 1995/1996 the situation was reversed. Ensemble member 20 performed the worst in the 1991/1992 season. In both seasons the ensemble average captured the general direction of the observed anomaly even though some ensemble members were misleading. The results confirm that the use of ensembles improves skill over a single realisation.

The results in this Chapter suggest that most of the variability that is found in the ensemble members obtained from a nested system is mainly due to non-linearities in a GCM. The RCM solutions' variability seem to be influenced more by lateral boundary forcing than it is by the model's internal dynamics and physics. It is of interest to determine how the internal variability of the models influences the daily simulations because daily simulations are aggregated when seasonal totals are considered. In the next Chapter the same datasets that were analysed in this Chapter are analysed again but for intra-seasonal variability considerations.

CHAPTER 6: THE INTERNAL VARIABILITY OF THE RegCM3 (INTRA-SEASONAL)

6.1. Introduction

The statistics of a season cannot change without a corresponding change in the statistics of the daily events within a season. Dynamical models used here offer an opportunity to investigate the simulated intra-seasonal variability because the models give output occurs every 6 hours. Giorgi and Bi (2000) analysed sensitivity experiments in which random perturbations were applied to the ICs and LBCs of a set of seasonal RCM simulations in order to investigate the internal variability of the RCM. The response was found not to affect significantly the domain-wide average climatology, but it substantially influenced the day-to-day model solution, especially precipitation, and aspects of the model climate such as the frequency of occurrence of heavy precipitation events.

In the previous chapter it was established that the variability of the ensemble members seasonal total rainfall obtained from a nested system is more due to the non-linearities in the GCM than those in the RCM. The RCM's internal variability did not influence much the seasonal total rainfall. This chapter aims to investigate the daily rainfall total to determine the extent to which the internal variability of the RCM influences the variability of the daily rainfall events in a season. The analyses in this chapter are based on the spatial averaged observed and simulated daily rainfall in the 8 homogeneous regions (Figure 3.7).

6.2. The internal variability of the GCM and the RegCM3

The MAD (equation 10) as defined in Chapter 2 is used to determine the magnitude of the differences between the ensemble members and the ensemble average for the 88 days (i.e. 01 December to 26 February) during

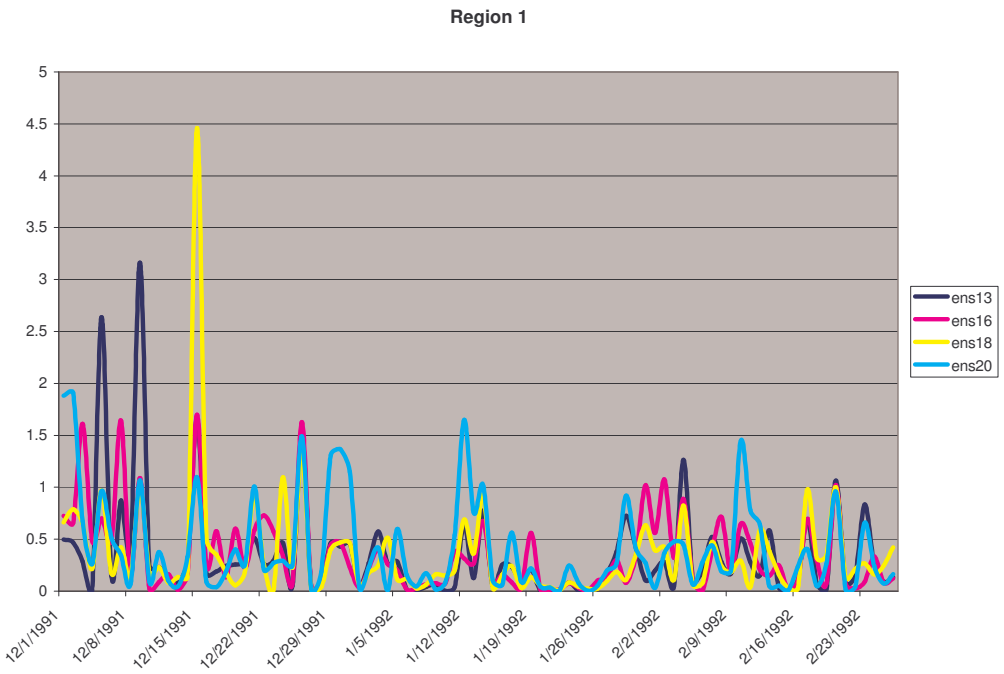

***Figure 6.1**: The daily MAD for DJF 1991/1992 for the different ensemble member over region 1 for the ensemble members in mm.*

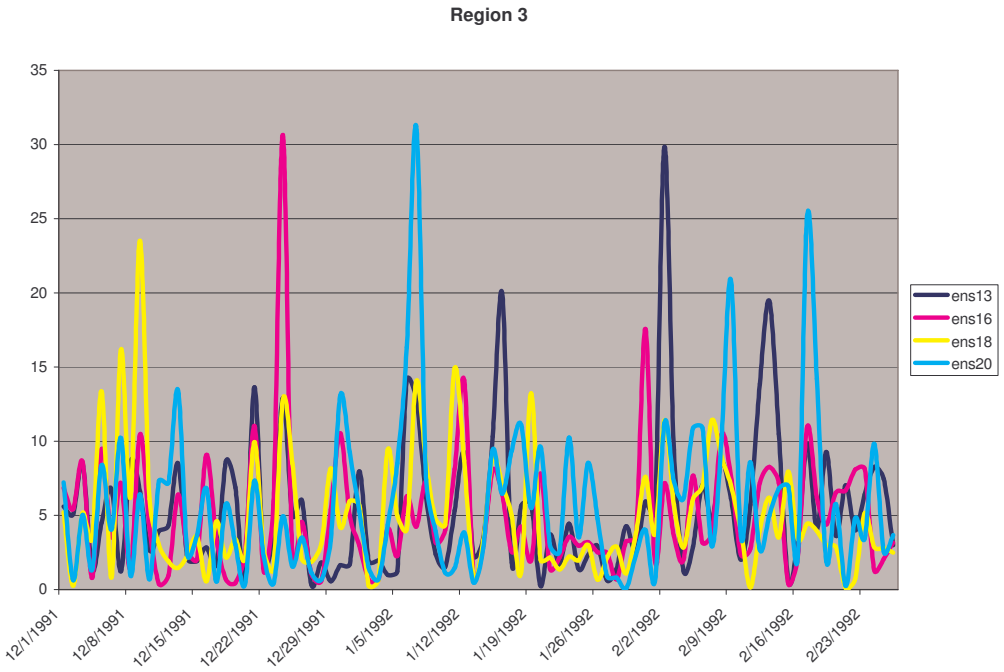

***Figure 6.2**: The daily MAD for DJF 1991/1992 for the different ensemble member over region 3 for the ensemble members in mm.*

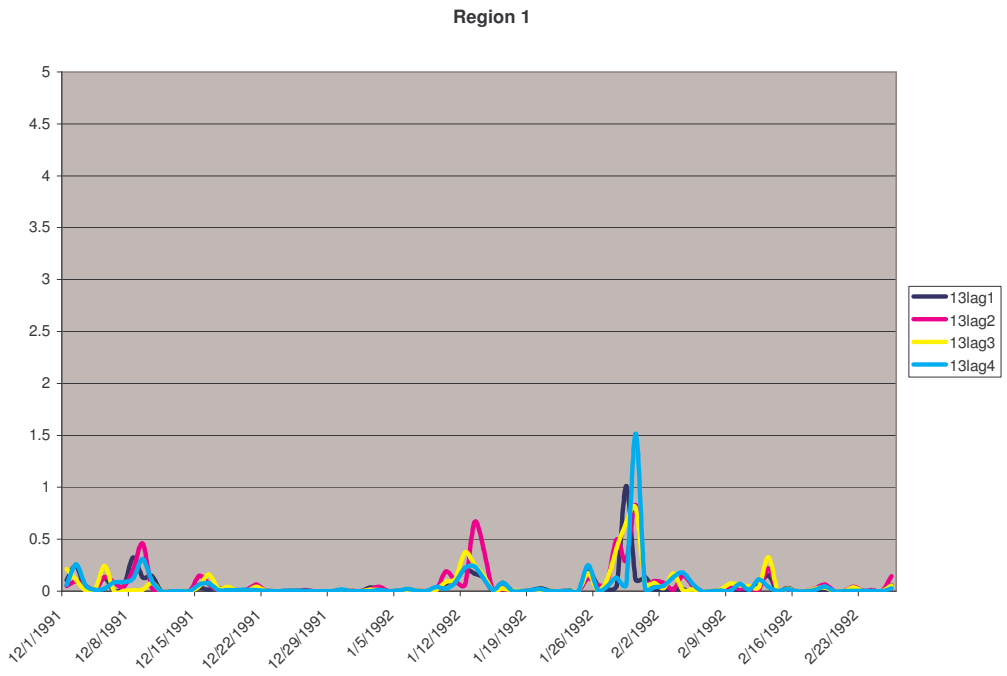

***Figure 6.3**: The daily MAD for DJF 1991/1992 for the different ensemble member over region 1 for the ensemble members of ensemble member 13 in mm.*

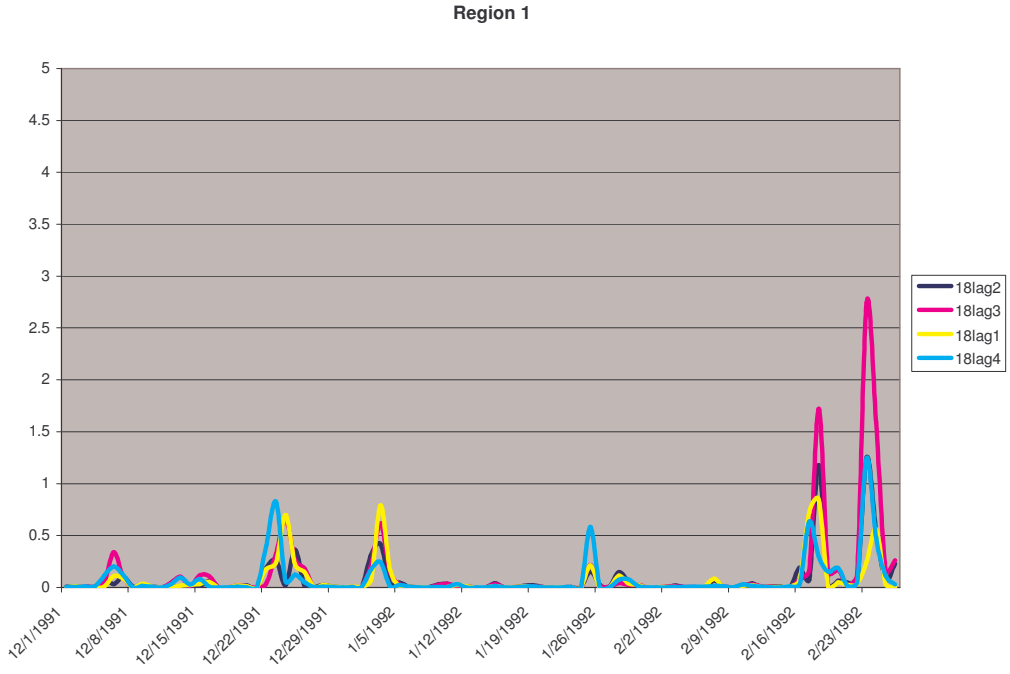

***Figure 6.4**: The daily MAD for DJF 1991/1992 for the different ensemble member over region 1 for the ensemble members of ensemble member 18 in mm.*

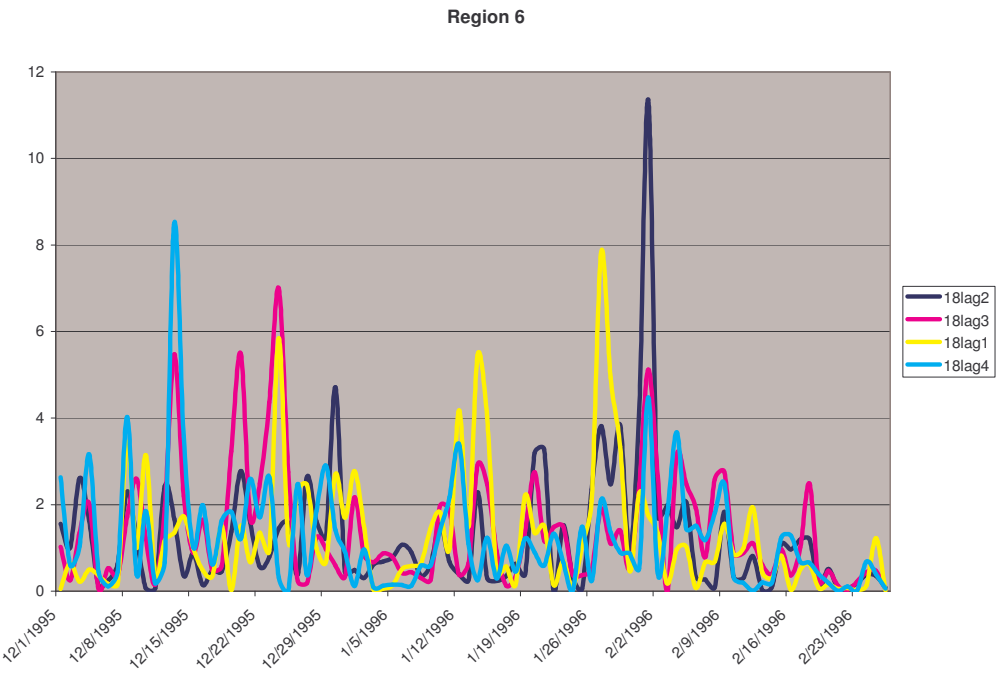

***Figure 6.5**: The daily MAD for DJF 1995/1996 for the different ensemble member over region 6 for the ensemble members of ensemble member 18 in mm.*

the two DJF seasons of 1991/1992 and 1995/1996. The procedure that is followed to produce the simulations is the same as in Chapter 5. The magnitude of the difference between the daily ensemble average rainfall and the individual ensemble members increases as one moves from the west towards the eastern parts of South Africa (Figure 6.1 and Figure 6.2). The finding is consistent with Giorgi and Bi (2000) findings where they found the BIAS to be higher for seasons with higher rainfall amounts as compared to low rainfall seasons. Figure 6.1 to Figure 6.5 have different scales in the y-axis. The MAD time series associated with the internal variability of the GCM and the RCM (Figure 6.1) is higher than that of the RCM alone (Figure 6.3).

The variability associated with the non-linearities in the RCM is not small enough to be ignored over the eastern part (e.g region 6) (Figure 6.5). The internal variability of the RCM influences the timing of the events (Figure 6.5). The ensemble average used in the calculation of the MAD in Figure 6.5 is obtained through using the RegCM3 ensemble members of ensemble

member 18. The time series shows that there is some variability of the daily events when different ICs are used with the same LBCs. The difference between the ensemble member solutions and the ensemble average goes up to 11 mm/day. The next section discusses the influence of the non-linearities in the models to the number of rainfall events in three equi-probable categories of below-normal; normal and above-normal.

6.3. Percentiles

The total number of days for each ensemble member in a season is 88, and only two seasons are analysed and therefore each ensemble member has 176 days. There are four ensemble members and therefore the total number N in equation (14) is 704 days. The position of the percentiles (P) is calculated as P*705/100. For the observations we only have 2 seasons with 88 days and therefore the position of the percentiles is calculated as P*177/100. The procedure that is followed to calculate the rainfall values associated with the percentiles is explained in Chapter 2.

The position of the 33.33 percentile is 234.97 and the position of the 66.67 percentile is 469.95 and the associated values for the 8 homogeneous regions are in Table 6.1. The rainfall values that are between 0 and the 33.33 percentile fall into the below-normal category, those that are between the 33.33 and the 66.67 percentiles are in the normal category while those that are above the 66.67 percentile are in the above-normal category. The same procedure is followed to determine the number of events in the different categories for the observed daily rainfall. The values of the 33.33 and the 66.67 percentiles associated with the observations are also in Table 6.1.

***Table 6.1**: The 33.33 and 66.67 percentiles for the RegCM3 determined from the 2 seasons as well as observations.*

	33.33 percentile	**66.67 percentile**	**33.33 (obs) percentiles**	**66.67(obs) percentiles**
Region 1	0.054881	0.359759	0	0.09
Region 2	0.552048	2.510094	0.2	1.079878
Region 3	3.400439	10.09129	1.639939	4.37
Region 4	2.470063	7.729837	0.73	3.91878
Region 5	1.625738	4.274322	1.259878	4.14817
Region 6	3.269787	5.869811	1.729878	4.248658
Region 7	0.89652	3.209939	0.729878	2.26939
Region 8	0.117554	0.651762	0.02	0.539268

6.3.1. Observations

***Table 6.2**: The observed number of events in the three categories in DJF 1991/1992.*

Cat	Reg 1	Reg 2	Reg 3	Reg 4	Reg 5	Reg 6	Reg 7	Reg 8
Below	33	39	41	35	38	39	41	47
Normal	33	30	32	38	38	24	26	23
Above	25	22	18	18	15	28	24	21

***Table 6.3**: The observed number of events in the three categories in DJF 1995/1996.*

Cat	Reg 1	Reg 2	Reg 3	Reg 4	Reg 5	Reg 6	Reg 7	Reg 8
Below	32	23	19	26	22	21	19	24
Normal	25	29	30	22	23	37	35	27
Above	34	39	42	43	46	33	37	40

The summer season of 1991/1992 was dry. Table 6.2 shows that most of the observed daily rainfall events that occurred in this season were in the below-normal category. In all the regions expect region 6, the above-normal category has the least number of events. Region 6 has the least number of

events in the normal category but it follows the same trend as the other regions of having a high number of events in the below-normal category. In 1995/1996 wet conditions were experienced over the whole of South Africa. The highest number of the observed daily rainfall events in this season (Table 6.3) are in the above-normal category for all regions except region 6. In region 6 the highest number of events is in the normal category and the next highest is above-normal.

6.3.2. The internal variability of the GCM and the RCM

6.3.2.1. Ensemble member 13

***Table 6.4**: Ensemble member 13 1991/1992 daily rainfall categories distribution.*

Cat	Reg 1	Reg 2	Reg 3	Reg 4	Reg 5	Reg 6	Reg 7	Reg 8
Below	41	35	34	40	35	52	43	39
Normal	24	23	29	24	33	17	32	29
Above	23	30	25	24	20	19	13	20

***Table 6.5**: Ensemble member 13 1995/1996 daily rainfall categories distribution.*

Cat	Reg 1	Reg 2	Reg 3	Reg 4	Reg 5	Reg 6	Reg 7	Reg 8
Below	32	36	30	41	40	31	31	25
Normal	31	28	34	32	24	36	25	23
Above	25	24	24	15	24	21	32	40

In Chapter 5 it was found that when seasonal totals were considered the ensemble member 13 was closest to the 1991/1992 observations. Most of the daily rainfall events are simulated to be in the below-normal category as in the observations (Table 6.4). In 1995/1996 ensemble member 13 was one of the worst performing ensemble members especially along the coastal regions. The season was very wet but the nested system simulated the season to be dry over the most part of the country. The nested system overestimated the

number of daily rainfall events in the below-normal category and underestimated those in the above-normal category (Table 6.5).

6.3.2.2. Ensemble member 16

***Table 6.6**: Ensemble member 16 1991/1992 daily rainfall categories distribution.*

Cat	Reg 1	Reg 2	Reg 3	Reg 4	Reg 5	Reg 6	Reg 7	Reg 8
Below	34	46	44	33	42	33	42	36
Normal	28	25	22	24	23	24	24	26
Above	26	17	22	31	23	31	22	26

***Table 6.7**: Ensemble member 16 1995/1996 daily rainfall categories distribution.*

Cat	Reg 1	Reg 2	Reg 3	Reg 4	Reg 5	Reg 6	Reg 7	Reg 8
Below	24	17	14	20	12	16	17	17
Normal	25	33	30	35	35	41	29	29
Above	39	38	44	33	41	31	42	42

Ensemble member 16 performed reasonably well in both the seasons. Most of the events in the 1991/1992 season which was dry are in the below-normal category (Table 6.6.), while in 1995/1996 they are in the near-normal and the above-normal category (Table 6.7), which means that the simulations are consistent with the observations.

6.3.2.3. Ensemble member 18

***Table 6.8**: Ensemble member 18 1991/1992 daily rainfall categories distribution.*

Cat	Reg 1	Reg 2	Reg 3	Reg 4	Reg 5	Reg 6	Reg 7	Reg 8
Below	31	32	35	30	31	27	32	38
Normal	33	27	29	23	29	29	28	29
Above	24	29	24	35	28	32	28	21

***Table 6.9**: Ensemble member 18 1995/1996 daily rainfall categories distribution.*

Cat	Reg 1	Reg 2	Reg 3	Reg 4	Reg 5	Reg 6	Reg 7	Reg 8
Below	21	20	26	21	17	19	15	18
Normal	30	33	32	34	33	31	31	27
Above	37	35	30	33	38	38	42	43

The performance of ensemble member 18 was reasonably well in 1991/1992 because it gave negative anomalies over the most part of South Africa. However there are areas in the north-eastern parts that are simulated to have positive anomalies that are not found in the observations. Most of the rainfall events in 1991/1992 are in the below-normal category (Table 6.8). Ensemble member 18 performed best in 1995/1996 giving positive anomalies almost over the whole of South Africa. These positive anomalies are also indicated by the high number of events in the above-normal category (Table 6.9).

6.3.2.4. Ensemble member 20

***Table 6.10**: Ensemble member 20 1991/1992 daily rainfall categories distribution.*

Cat	Reg 1	Reg 2	Reg 3	Reg 4	Reg 5	Reg 6	Reg 7	Reg 8
Below	2 5	22	21	23	29	24	24	28
Normal	32	35	34	33	26	31	35	39
Above	31	31	33	32	33	33	29	21

***Table 6.11**: Ensemble member 20 1995/1996 daily rainfall categories distribution.*

Cat	Reg 1	Reg 2	Reg 3	Reg 4	Reg 5	Reg 6	Reg 7	Reg 8
Below	26	26	30	26	28	32	30	33
Normal	32	31	25	30	32	26	31	33
Above	30	31	33	32	28	30	27	22

Ensemble member 20 performed the worst of all the members in 1991/1992 because it gave positive anomalies over a larger part of the north-eastern

section of South Africa. The highest number of daily events in areas where the model over estimated rainfall is split between the near-normal and the above-normal categories (Table 6.10). In 1995/1996 the rainfall simulations divided the country into equal areas of above-normal and below-normal simulated rainfall figures, manifested in the more or less equal number of events for each category (Table 6.11).

6.3.2.5. The Ensemble average

***Table 6.12**: Ensemble average 1991/1992 daily rainfall categories distribution.*

Cat	Reg 1	Reg 2	Reg 3	Reg 4	Reg 5	Reg 6	Reg 7	Reg 8
Below	6	10	9	7	15	18	8	10
Normal	48	49	53	44	49	41	49	42
Above	34	29	26	37	24	29	31	36

***Table 6.13**: Ensemble average 1995/1996 daily rainfall categories distribution.*

Cat	Reg 1	Reg 2	Reg 3	Reg 4	Reg 5	Reg 6	Reg 7	Reg 8
Below	2	3	6	9	8	19	4	0
Normal	34	42	43	47	43	34	40	28
Above	51	43	39	32	37	35	44	60

The simulated daily rainfall amounts from the four solutions obtained through nesting the RegCM3 within the four GCM ensemble members are averaged. The number of events in the three categories were determined using these ensemble average for 88 days of the two seasons. In 1991/1992 most of the daily rainfall events are found to be in the normal category (Table 6.12). This is consistent with the finding from the previous chapter where the magnitude of the anomaly sign of the ensemble average was found to be small. When the ensemble average is considered it no longer becomes obvious that most of the events, from the different ensemble members fell in the below-normal category. In 1995/1996 the highest number of anomalies occurs both in the near-normal and the above-normal category (Table 6.13). The number of events in the normal category explains why the magnitude of the anomalies is

small for the ensemble average as compared to the individual ensemble member anomalies as well as the observations.

6.3.3. The internal variability of the RCM

6.3.3.1. Ensembles of ensemble member 13 in 1991/1992

***Table 6.4**: Ensemble member 13 1991/1992 daily rainfall categories distribution.*

Cat	Reg 1	Reg 2	Reg 3	Reg 4	Reg 5	Reg 6	Reg 7	Reg 8
Below	41	35	34	40	35	52	43	39
Normal	24	23	29	24	33	17	32	29
Above	23	30	25	24	20	19	13	20

***Table 6.14**: Ensemble member 13 lag 2 1991/1992 daily rainfall categories distribution.*

Cat	Reg 1	Reg 2	Reg 3	Reg 4	Reg 5	Reg 6	Reg 7	Reg 8
Below	39	38	36	39	41	51	42	41
Normal	23	23	29	25	23	19	22	26
Above	26	27	23	24	24	18	24	21

***Table 6.15**: Ensemble member 13 lag 3 1991/1992 daily rainfall categories distribution.*

Cat	Reg 1	Reg 2	Reg 3	Reg 4	Reg 5	Reg 6	Reg 7	Reg 8
Below	40	37	44	35	41	53	49	44
Normal	30	25	27	34	27	17	20	27
Above	18	26	17	19	20	18	19	17

***Table 6.16**: ensemble member 13 lag 4 1991/1992 daily rainfall categories distribution.*

Cat	Reg 1	Reg 2	Reg 3	Reg 4	Reg 5	Reg 6	Reg 7	Reg 8
Below	36	39	37	39	36	43	40	39
Normal	29	19	28	24	31	24	30	31
Above	23	30	23	25	21	21	18	18

Table 6.4 is repeated here for comparison purposes. The highest number of the daily events of RegCM3 ensemble members generated from the GCM ensemble member 13 fall into the below-normal category (Table 6.4; Table 6.14; Table 6.15; Table 6.16). This finding explains why the seasonal total rainfall of all the RegCM3 ensemble members is almost similar.

6.3.3.2. Ensembles of ensemble member 13 in 1995/1996

***Table 6.5**: Ensemble member 13 1995/1996 daily rainfall categories distribution.*

Cat	Reg 1	Reg 2	Reg 3	Reg 4	Reg 5	Reg 6	Reg 7	Reg 8
Below	32	36	30	41	40	31	31	25
Normal	31	28	34	32	24	36	25	23
Above	25	24	24	15	24	21	32	40

***Table 6.17**: Ensemble member 13 lag 2 1995/1996 daily rainfall categories distribution.*

Cat	Reg 1	Reg 2	Reg 3	Reg 4	Reg 5	Reg 6	Reg 7	Reg 8
Below	26	29	24	35	19	20	17	16
Normal	28	29	40	41	42	38	32	26
Above	34	30	24	12	27	30	39	46

***Table 6.18**: Ensemble member 13 lag 3 1995/1996 daily rainfall categories distribution.*

Cat	Reg 1	Reg 2	Reg 3	Reg 4	Reg 5	Reg 6	Reg 7	Reg 8
Below	32	29	25	34	25	22	14	20
Normal	27	31	42	40	42	41	32	31
Above	29	28	21	14	21	25	42	37

***Table 6.19**: Ensemble member 13 lag 4 1995/1996 daily rainfall categories distribution.*

Cat	Reg 1	Reg 2	Reg 3	Reg 4	Reg 5	Reg 6	Reg 7	Reg 8
Below	24	24	20	30	26	17	19	17
Normal	33	35	45	38	34	40	25	24
Above	31	29	23	20	28	31	44	47

Table 6.5 is also repeated here for comparison purposes. In 1991/1992 ensemble member 13 performed the worst especially over the coastal regions. The season was very wet and the observations reflect that through a high number of daily events in the above-normal category (Table 6.3). All the ensemble members that were generated from ensemble member 13 give the least number of the rainfall events in the above-normal category except over the western interior (Table 6.5; Table 6.17; Table 6.18; Table 6.19).

6.3.3.3. Ensembles of ensemble member 18 in 1991/1992

***Table 6.8**: Ensemble member 18 1991/1992 daily rainfall categories distribution.*

Cat	Reg 1	Reg 2	Reg 3	Reg 4	Reg 5	Reg 6	Reg 7	Reg 8
Below	31	32	35	30	31	27	32	38
Normal	33	27	29	23	29	29	28	29
Above	24	29	24	35	28	32	28	21

***Table 6.20**: Ensemble member 18 lag 2 1991/1992 daily rainfall categories distribution.*

Cat	Reg 1	Reg 2	Reg 3	Reg 4	Reg 5	Reg 6	Reg 7	Reg 8
Below	27	30	35	27	28	25	30	39
Normal	38	30	26	30	37	29	29	27
Above	23	28	27	31	23	34	29	22

***Table 6.21**: Ensemble member 18 lag 3 1991/1992 daily rainfall categories distribution.*

Cat	Reg 1	Reg 2	Reg 3	Reg 4	Reg 5	Reg 6	Reg 7	Reg 8
Below	27	31	37	29	33	23	32	35
Normal	38	30	23	25	31	31	24	31
Above	23	27	28	34	24	34	32	22

***Table 6.22**: Ensemble member 18 lag 4 1991/1992 daily rainfall categories distribution.*

Cat	Reg 1	Reg 2	Reg 3	Reg 4	Reg 5	Reg 6	Reg 7	Reg 8
Below	28	31	38	26	31	29	35	37
Normal	35	31	21	26	34	27	24	28
Above	25	26	29	36	23	32	29	23

Ensemble member 18 performed reasonably well, in 1991/1992 but there were areas over the north-eastern part of the country where the model simulated positive anomalies that were not observed. The positive anomaly regions are represented by the high number of events in region 6 and region 4 in the above-normal category for all ensemble members generated from ensemble member 18. In the other regions the highest number of events is in the below-normal or normal category. The distribution of the number of events in the different categories is almost similar for the different RegCM3 ensemble members (Table 6.8; Table 6.20; Table 6.21; Table 6.22).

6.3.3.4. Ensembles of ensemble member 18 in 1995/1996

***Table 6.9**: Ensemble member 18 1995/1996 daily rainfall categories distribution.*

Cat	Reg 1	Reg 2	Reg 3	Reg 4	Reg 5	Reg 6	Reg 7	Reg 8
Below	21	20	26	21	17	19	15	18
Normal	30	33	32	34	33	31	31	27
Above	37	35	30	33	38	38	42	43

***Table 6.23**: Ensemble member 18 lag 2 1995/1996 daily rainfall categories distribution.*

Cat	Reg 1	Reg 2	Reg 3	Reg 4	Reg 5	Reg 6	Reg 7	Reg 8
Below	20	20	32	20	17	27	17	20
Normal	34	31	21	38	32	27	30	31
Above	34	37	35	30	39	34	41	37

***Table 6.24**: Ensemble member 18 lag 3 1995/1996 daily rainfall categories distribution.*

Cat	Reg 1	Reg 2	Reg 3	Reg 4	Reg 5	Reg 6	Reg 7	Reg 8
Below	25	20	28	24	20	28	20	19
Normal	23	26	32	37	26	22	27	29
Above	40	42	28	27	42	38	41	40

***Table 6.25**: Ensemble member 18 lag 4 1995/1996 daily rainfall categories distribution.*

Cat	Reg 1	Reg 2	Reg 3	Reg 4	Reg 5	Reg 6	Reg 7	Reg 8
Below	26	18	24	26	19	33	22	22
Normal	28	32	32	36	22	21	21	23
Above	34	38	32	26	47	34	45	43

Ensemble member 18 performed very well in the 1995/1996 season. The highest number of the daily rainfall events was simulated to be in the above-normal category for all the RegCM3 ensemble members generated from the ECHAM4.5 ensemble member 18 (Table 6.9; Table 6.23; Table 6.24; Table 6.25).

6.4. Summary and Conclusions

The Mean Absolute Difference (MAD) was calculated for the 8 homogeneous regions using the 4 ensemble members obtained through perturbing the wind fields of the GCM at initialisation and then nesting the RegCM3 within the different solutions. The MAD was also calculated for the ensemble members

obtained through initialising the RCM on different days to differ the initial conditions but keeping the LBCs the same. The MAD values associated with the internal variability of the nested system exceeds the values associated with non-linearities in the RCM alone. The MAD values increases as one moves towards the eastern part of the country. The MAD values associated with the RCM's internal variability are not small enough to be ignored in the eastern part of the country. The values show that the RCM's internal variability influences the timing of the daily rainfall events.

The three categories (i.e. below-normal, normal and above-normal) were identified using the 33.33 and the 66.67 percentiles as the cut-off for the normal category. The solutions that showed positive seasonal rainfall anomalies are characterised by a high number of daily events in the above-normal category while those that give negative anomalies are associated with a high number of daily events in the below-normal category. The internal variability of the RegCM3 does not affect the number of events in the different categories much.

The ensemble average obtained from the four ensemble members of the GCM has the least number of rainfall events in the below-normal category. For 1991/1992 most of the events are in the near-normal category while in 1995/1996 the events are spread between near-normal and above-normal categories. The findings explain why the magnitude of the anomalies associated with the ensemble average is small for the two seasons as compared to the anomalies in the individual ensemble members and observations.

CHAPTER 7: SUMMARY AND CONCLUSIONS

South Africa is located in the subtropics and as a result is affected by circulation systems prevailing in the tropics, subtropics and the mid-latitudes. These circulations control the rainfall over South Africa. The subtropical control is exerted through the continental high, the AOH and IOH. The mid-latitude control is effected through the cold fronts that usually migrate into the country in austral winter. The tropical atmosphere is exerted through the cloud bands that are associated with the ITCZ. These circulations make the rainfall of South Africa to be highly seasonal, with most of the rainfall experienced in austral summer. In the summer season defined as DJF here, the tropical circulation dominates over South Africa and therefore most of the rainfall that is received during this part of the summer season is due to tropical cloud bands. Most of the agriculture in South Africa is dependent on rainfall and it has also been found that the GDP correlates highly with the summer rainfall. It is for that reason that accurate seasonal or intra-seasonal forecasts which are produced at least one season in advance will help in the financial and environmental management in the country.

The atmosphere is a chaotic system and hence this chaos limits its predictability. It has, however, been found that the tropical atmosphere does not conform to the definition of chaos. The tropical atmosphere is almost entirely determined by the surface boundary conditions of the SSTs. It is therefore expected that accurate predictions of the SSTs would allow prediction of the tropical rainfall. The predictability of seasonal mean circulation in areas outside the tropics is enhanced by the high predictability of the tropical rainfall for a given SST. This study concentrates on DJF because it is in this season that the tropical circulation dominates over South Africa. Statistical and numerical models have been developed to model the response of the atmosphere to SSTs. Numerical models that are generally used to model the atmosphere are called the general circulation models. The general circulation models used for climate studies are called global climate models (GCMs).

The GCMs are generally run at a resolution of roughly 300 km. However, this resolution has been found to be too course for small scale features such as precipitation. Precipitation events are highly localised in time and space. As a result it is desirable that the models simulate the atmospheric processes at a higher resolution. The cost of running GCMs at a high resolution is high and as a result downscaling has been introduced as a way of producing high resolution simulations at a lesser cost. Downscaling is possible through dynamical and statistical methods. The former method utilises a high resolution RCM to derive regional climate information over an area of interest. An RCM is nested within a GCM or reanalyses which provides the required large scale conditions (ICs and LBCs).

The GCMs represent the atmospheric processes that are chaotic by nature. The atmospheric models are therefore nonlinear and as a result they are sensitive to small perturbations. Two GCM solutions that are started with slightly different initial conditions will diverge substantially after a few days of simulation. The sensitivity of the GCMs to small perturbations led to the birth of ensembles. In seasonal forecasting multiple GCM realisations are produced to quantify the uncertainty associated with the non-linearities or with the internal variability of the GCM.

In regional climate modelling, an RCM is nested within a GCM or within reanalyses which provide the ICs and the time dependent LBCs. The lateral boundary forcing limits the degrees of freedom of RCMs, so that the RCM climatology will not strongly diverge from the forcing fields. The RCMs are in fact expected to reproduce the large scale features that are being fed to them at the boundaries. The RCMs are nonlinear models and as a result, although they are restricted at the boundaries, they are expected to exhibit a certain level of the internal variability. It is therefore expected that in a nested system where a GCM is used to provide LBCs, the nested system solutions will be functions of the internal variability of both the GCM and the RCM. In forecasting, multiple realisations are already made to quantify the uncertainty associated with the GCM's non-linearities. This study is aimed to investigate whether or not in regional climate modelling multiple realisations need to be made to quantify the uncertainty associated with the non-linearities in the

RCM. To do that the contribution of the RCM's non-linearities towards the variability of ensemble members is analysed.

In this study four ensemble members are produced from the ECHAM4.5 through perturbing the wind fields at initialisation. The four solutions from the ECHAM4.5 are then used to nest the RegCM3. The simulations are generated over a 10-year period from 1991/1992 to 2000/01. The rainfall variability of the ensemble members is analysed to determine the amount variability associated with both models. The SST forced variance and the model's internal dynamics variance are calculated. The former variance measures the variability of the ensemble average over the 10-year period while the latter variance measures the variability of the ensemble members in a single year. The results show that in general the internal dynamics variance is higher than the SST forced variability. The results are further confirmed through analysing rainfall data for the 8 homogeneous regions over South Africa. The variability of the ensemble members within the different regions is found to be generally higher than the variability of the ensemble average over the 10-year period.

It is expected that when dry conditions are experienced most ensemble members will lean towards below-normal rainfall and during wet seasons most ensemble members will lean towards above-normal rainfall. The simulations are compared with the observations to determine how the model is performing in general and also to determine if the spread of the ensemble members will lean towards the expected categories. The sign of the majority of the ensemble member's anomalies agree with the observed anomalies. The magnitude of the simulated anomalies of the ensemble average is smaller than the observed anomalies or the anomalies of the individual ensemble members because of the high variability in the ensemble members. The models are found to perform best over South Africa, in the central region where the rainfall is mainly large scale and where the correlation with the SSTs in the equatorial Pacific Ocean is highest. The model overestimates rainfall in areas of steep topographic gradients as was found with most other RCMs.

The variability of the ensemble members described above is due to the internal variability of the GCM and the RCM. To analyse the influence that the RCM has towards the total variability of the ensemble members, RCM solutions are made using one ECHAM4.5 realisation. Four RCM realisations are made through starting the RCM integrations on four consecutive model days. The procedure ensures that the LBCs stay the same and hence the solutions will vary as a result of the internal variability of the RCM. The simulations are made for two seasons that were highly anomalous: one was dry (1991/1992) and associated with El Niño conditions while the other was wet (1995/1996) and associated with La Niña conditions.

High variability is found with the ensemble members that are obtained through nesting the RegCM3 within the ECHAM4.5 ensemble members. However, it is found that the simulations of the ensemble members obtained through initialising the RegCM3 on different days are almost similar to one another. This suggests that the variability that is observed on the original four ensemble members is mainly due to the internal variability of the GCM as opposed to the RCM. The RCM's internal variability therefore makes a very small contribution towards the variability of the ensemble members, suggesting that the LBCs play a more important role than does the ICs.

The intra-seasonal variability is also analysed. The rainfall events are divided into three equi-probable categories (below-normal, normal, and above-normal). During the wet season (1995/1996) most of the rainfall events fall in the above-normal category, while during the dry season (1991/1992) most of the events fall in the below-normal category. The characteristic of the simulated daily events is the same as observed with many above-normal events in the wet season, and many below-normal events in the dry season. When the daily events of the ensemble average are considered, most of the events fall within the normal category. This happens because the ensemble mean is close to zero when the vastly different ensemble members are averaged. When the ensemble members associated with the non-linearites of the RCM are considered, the timing of the daily events is found to be different, but the number of events in a particular category is almost similar.

The RegCM3 has been proven to be a useful downscaling tool. The internal variability of the RCM does not influence the variability of the nested system solutions to a great extent. The major contributor towards the characteristic of the ensemble members is the LBCs, because it is found that when LBC are kept the same, the solutions are generally similar. The results suggest that when forecasts are made both for seasonal and intra-seasonal time scales there is no need to produce multiple realisations to try and take into consideration the internal variability of the RCMs.

REFERENCES

Allan R.J., J.A. Lindesay and C.J.C. Reason, 1994: Multidecadal Variability in the Climate System over the Indian Ocean Region during the Austral Summer. *Journal of Climate*, **8**, 1853-1872.

AMS statement, 2000: Seasonal to Inter-annual climate prediction. *Bulletin of American Meteorological Society,* **82,** 701-703.

Anderson J., H. van den Dool, A. Barnston, W. Chen, W. Stern, and J. PLoshay, 1999: Present day Capabilities of Numerical and Statistical Models for Atmospheric Extra-tropical Seasonal Simulation and Prediction. *Bulletin of the American Meteorological Society*, **80**, 1349-1361.

Anderson J.L. and J.J. Ploshay, 1999: Impact of initial conditions on seasonal simulations with an atmospheric general circulation model. *Quarterly Journal of Meteorology*. **126,** 2241-2264.

Anthes R.A., 1990: Recent Applications of the Penn State/NCAR Mesoscale to Synoptic, Mesoscale and Climate Studies. *American Meteorological Society*, **71**, 1610-1629.

Bartman A.G., W.A. Landman and C.J. DE W. Rautenbatch, 2003: Recalibration of general circulation model output to austral summer rainfall over southern Africa. *International Journal of Climatology*, **23**, 1407-1419.

Chervin R.M., W. L. Gates and S.H. Schneider, 1974: The effect of time averaging and the noise level of climatological statistical generated by atmospheric general circulation models. *Journal of the atmospheric sciences*, **31**, 2216-2219.

Cook C., C.J.C. Reason and B.C. Hewitson, 2004: Wet and dry spells within particularly wet and dry summers in the South African summer rainfall region. *Climate Research*. **26**, 17-31.

Crimp S.J. and S.J. Mason, 1998: The extreme precipitation event of 11 to 16 February 1996 over South Africa. *Meteorological Atmospheric Physics,* **70,** 29-42.

D'Abreton, P.C. and J.A. Lindesay, 1992: Water vapour transport over southern Africa during wet and dry early and late summer months. *International Journal of Climatology*, **13**, 151-170.

DeWitt D.G., 2006:223 Monell Building,IRI - International Research Institute for Climate Prediction (IRI) Lamont-Doherty Earth Observatory Columbia University 61 Route 9W Palisades, NY 10964-8000 United States, Phone: (845) 680-4415, Fax: (845) 680-4865, daved@iri.columbia.edu.

Druyan L.M., M. Fulakeza and P. Lonergan, 2002: Dynamical Downscaling of Seasonal Climate Predictions over Brazil. *American Meteorological Society,* **15,** 3411-3426.

Druyan L.M., M. Fulakeza, P. Lonergan and M. Saloum, 2000: A regional model study of synoptic features over West Africa. *Monthly weather review*. **129**, 1564-1577.

Engelbrecht F.A., C.J. de W. Rautenbach, J.L. Mcgregor and J.J. Katzfey, 2002: January and July climate simulations over the SADC region using the limited area model DARLAM. *Water SA,* **28,** 361-373.

Fennessy, M.J. and J. Shukla, 1999: Seasonal Prediction over North America with a Regional Model Nested in a Global Model. *Journal of Climate,* **13**, 2605–2627.

Frederiksen CS, H. Zhang, R.C. Balgovind, N. Nicholls, W. Drosdowsky and L. Chambers, 2000: Dynamical Seasonal Forecasts during the 191997/1998 ENSO Using Persisted SST Anomalies. *Journal of climate,* **14**, 2675-2695.

Gallee H., W. Moufouma-Okia, P. Benchtold, O. Brasseur, I. Dupays, P. Marbaix, C. Messager, R. Ramel, and T. Lebel, 2004: A high-resolution

simulation of a West African rainy season using a regional climate model. *Journal of Geophysical Research*, **109**, D05108.

Gershunov A., T.P. Barnett, D.R. Cayan, T. Tubbs and L. Goddard, 2000: Predicting and Downscaling ENSO Impacts on Intraseasonal Precipitation Statistics in California: The 1997/1998 Event. *Journal of Hydrometeorology*, **1**,201-210.

Giorgi F. and L.O. Mearns, 1999: Introduction to special section: regional climate modelling revisited. *Journal of Geophysical research*, **104**, 6335-6351.

Giorgi, F., M. R. Marinucci, G.T. Bates, 1993a: Development of a Second-Generation Regional Climate Model (RegCM2). Part I: Boundary-Layer and Radiative Transfer Processes. *Monthly Weather Review*, **121**, 2794–2813.

Giorgi, F., M. R. Marinucci, G.T. Bates, G. De Canio, 1993b: Development of a Second-Generation Regional Climate Model (RegCM2). Part II: Convective Processes and Assimilation of Lateral Boundary Conditions. *Monthly Weather Review,* **121**, 2814–2832.

Giorgi, F.and M.R. Marinucci, 1996: An Investigation of the Sensitivity of Simulated Precipitation to Model Resolution and Its Implications for Climate Studies. *Monthly Weather Review,* **124**,148–166.

Giorgi, F., 1990: Simulation of Regional Climate Using a Limited Area Model Nested in a General Circulation Model. *Journal of Climate,* **3**, 941–964.

Giorgi F. and X. Bi, 2000: A study of the internal variability of a regional climate model. *Journal of Geophysics research*, **105**, 503-29,521.

Goddard L., S.J. Mason, SE Zebiak, CF Ropelewski, R Basher and MA Cane, 2000: Current approaches to seasonal-to-inter-annual climate predictions. *International Journal of Climate*. **21**, 1111-1152.

Gong X., A.G Barnston and M N. Ward, 2003: Notes and Correspondence, The Effect of spatial aggregation on the skill of seasonal precipitation forecasts. *Journal of Climate*,**16**, 3059-3071.

Grell, G. A., Dudhia, J. and Stauffer, D. R. (1994a): A description of the fifth-generation penn state/ncar mesoscale model (MM5), *National Center for Atmospheric Research Technical Report. TN-398+STR*,121pp.

Grell, G. (1993). Prognostic evaluation of assumptions used by cumulus parameterization. *Monthly Weather Review*, **121**, 764-787.

Hack, J., B. Bolville ,B. Briegleb, J. Kiehl, P. Rasch and D. Williamson: (1993). Description of the ncar community climate model (ccm2), *National Centre for Atmospheric Research Technical report.*

Harrison, M.S.J., 1984a: The annual rainfall cycle over the central interior of South Africa. *South African Geographical Journal,* **66**,47-64.

Harrison, M.S.J., 1984b: A generalized classification of South African summer rain-bearing synoptic systems. *Journal of Climatology*.,**4**,547-560.

Hoffman R.N. and E. Kalnay, 1982: Lagged average forecasting, an alternative to Monte Carlo forecasting. *Tellus*, **35 A**, 100-118.

Janowiak, J. E. and P. Xie*,* 1999: *CAMS_OPI*: a global satellite-raingauge merged product for real-time precipitation monitoring applications. *Journal of Climate*, **12**, 3335-3342.

Ji, Y., and A. D. Vernekar, 1996: Simulation of the Asian Summer Monsoons of 1987 and 1988 with a Regional Model Nested in a Global GCM. *Journal of Climate,* **10**, 1965–1979.

Joubert A. M., J.J. Katzfey, J.L. Mcgregor and K.C. Ngunyen, 1999: Simulating midsummer climate over southern Africa using a nested regional climate model. *Journal of Geophysical research,* **104**, 19015-19025.

Jury M.R., H.M. Mulenga and S.J. Mason, 1998: Exploratory Long-range Models to Estimate Summer Climate Variability over southern Africa. *Journal of Climate,* **12,**1892-1899.

Jury M. J., 2001: Economic Impacts of Climate Variability in South Africa and Development of Resource Prediction Models. *Journal of applied meteorology*, **41**, 46-55.

Kalnay, E., and Coauthors, 1996: The NCEP/NCAR 40-Year Re-analysis Project. *Bulletin of American Meteorological Society*., **77**, 437-471.

Kiehl, J.,Hack, J., Bonan, G., Boville, B., Breigleb, B., Williamson, D. and Rasch, P. (1996). Description of the ncar community climate model (CCM3), National Centre for Atmospheric Research Technical Report, TN-420 + STR. 152 pp.

Kim J., N. L. Miller, J. D. Farrara, and S. Hong, 2000: A seasonal precipitation and stream flow hindcast and prediction study in the western United States during the 1997/1998 winter season using a Dynamic Downscaling System. *Journal of Hydrometeorology,* **1,** 311-329.

Klopper E. and W.A. Landman, 2003: A simple approach for combining seasonal forecasts for southern Africa. *Meteorological Applications*, **10**, 319-327.

Kruger, AC, 1998: The influence of the decadal-scale variability of summer rainfall on the impact of El Niño and La Niña Events in South Africa. *International Journal of Climatology*. **19,** 59-68.

Kunkel K. E., K. Andsager, X. Liang, R. W Arritt, E.S. Tackle, W.J. Gutowski Jr and Z.Pan, 2002: Observations and Regional Climate Model Simulations of Heavy Precipitation Events and Seasonal Anomalies: A comparison. *Journal of Hydrometeorology*, **3**, 322-334.

Landman W.A. and L. Goddard, 2002: Statistical Recalibration of GCM Forecasts over Southern Africa Using Model Output Statistics. *Journal of Climate*,**15**, 2038-2055.

Landman W.A., S.J. Mason, P.D. Tyson and W.J. Tennant, 2001: Statistical downscaling of GCM simulations to Streamflow. *Journal of Hydrology*, **252**, 221-236.

Landman W.A., and W.J Tennant, 2000: Statistical Downscaling of Monthly forecasts. *International Journal of Climatology*, **20**, 1521-1532.

Landman W.A., S.J. Mason, P.D. Tyson and W. J. Tennant, 2000: Retro-active skill of multi-tiered forecasts of summer rainfall over southern Africa. *International Journal of Climatology*, **21**, 1-19.

Landman W.A. and S.J. Mason, 2001: Forecasts of Near-Global Sea Surface Temperatures Using Canonical Correlation Analysis. *Journal of Climate*, **14**, 3819-3833.

Landman W.A. and L. Goddard, 2005: Predicting southern African summer rainfall using a combination of MOS and perfect prognosis. *Geophysical Research Letter*, **33**, L158098.

Landman W.A. and L. Goddard, 2003: Model Output Statistics Applied to Multi-Model Ensemble Forecasts for Southern Africa, in 7th International Conference on Southern Hemisphere Meteorology and Oceanography. *American Meteorological Society* .249-250.

Landman W. A. and S.J. Mason (b), 1999: Change in the association between Indian Ocean sea-surface temperatures and summer rainfall over South Africa and Namibia. *International Journal of Climatology*. **19**, 1477-1492.

Landman W.A. and S.J. Mason (a), 1999: Operational Long-lead prediction of South African rainfall using canonical correlation analysis. *International Journal of climate*, **19**, 1073-1090.

Landman W.A., A. Seth and S.J. Camargo, 2005: The effect of regional climate model domain choice on the simulation of tropical cyclone-like vortices in the south-western Indian Ocean. *Journal of Climate*, **10**, 1263-1274.

Lau, N, -C. 1992: Climate variability simulated in GCMs. Climate system modelling (Ed Trenberth K.E). Cambridge University Press, 617-642.

Leung L. R. and S. J. Ghan, 1998: Pacific Northwest Climate Sensitivity simulated by a regional climate model Driven by a GCM. Part I: Control Simulations. *Journal of Climate*, **12,** 2010-2030.

Leung L. R., L.O. Mearns, F. Giorgi and R. L. Wilby, 2003: Regional climate research, needs and opportunities. *American meteorological society,***84***,* 89-95.

Makarau A. and M. Jury, 1997: Seasonal cycle of convective spells over southern Africa during austral summer. *International Journal of Climatology*, **17**, 1317-1332.

Mason, S.J., 1995: Sea-surface temperature-South African Rainfall associations, 1910-1989. *International Journal of Climatology*, **15**, 119-135.

Mcgregor JL, K.J. Walsh and J. J. Katzfey, 1993: Nested Modelling for Regional climate studies. *John Wiley and sons,* 367-385.

Miron, O. and J.A. Lindesay, 1983: A note on changes in air flow patterns between wet and dry spells over South Africa, 1963-1979. *South African Geographical Journal*, **65**, 141-147.

Miron, O. and P.D. Tyson, 1984: Wet and dry conditions and pressure anomaly fields over Southern Africa and adjacent Ocean 1963-79. Monthly Weather Review, **112**, 2127-2132.

Pal, J., Small, E. and Eltahir, E. (2000). Simulation of regional-scale water and energy budgets: Representation of sub grid cloud and precipitation processes

within RegCM, *Journal of Geophysical Research-Atmospheres*, **105**, 29579-29594.

Pal J.S., F. Giorgi, X. BI, N. Elguindi, F. Solmon, X, Gao, R. Francisco, A. Zakey, J. Winter, M. Ashfaq, F.S. Syed, J.L. Bell, N.S. Diffenbaugh, J. Karmacharya, A. Konare, D. Martinez, R.P. da Rocha, L.C. Sloan and A. Steiner, 2005: The ICTP RegCM3 and RegCNET: Regional Climate Modelling for the Developing World. *Submitted to the Bulletin of the American Meteorological Society*,39 pp.

Pan Z., E. Tackle, W. Gutowski and R. Turner, 1998: Long simulation of Regional Simulation of Regional Climate as a Sequence of Short Segments. *Monthly Weather Review*. **127**, 308-321.

Philander S. G., 1990: El Niño, La Niña, and the Southern Oscillation. *Academic press Inc. Harcourt Brace Jovanovich*. 293pp.

Qian J., A. Seth and S. Zebiak, 2003: Reinitialised versus Continuous Simulations for Regional Climate Downscaling. *Monthly Weather Review*, **131**, 2857-2873.

Rautenbach CJdeW., 1998: The unusual rainfall and sea-surface temperature characteristics in the South African region during the 1991/1992 summer season. *Water SA*, **24**, 165-172.

Reason CJC and JRE Lutjeharms, 1998: Variability of the South Indian Ocean and implications for the southern African rainfall. South African *Journal of Science*. **94**, 115-123.

Reason CJC, 2000: Evidence for the Influence of the Agulhas Current on the Regional Atmospheric Circulation Patterns. *Journal of Climate*, **14,** 2769-2778.

Reason CJC, and H Mulenga, 1999: Relationships between South African rainfall and SST anomalies in the southwest Indian Ocean. *International Journal of Climatology*, **19**, 1651-1673.

Reason CJC, 2001: Sensitivity of the southern African circulation dipole sea-surface temperature patterns in the South Indian Ocean. *International Journal of Climatology*, **22**, 377-393.

Renwick JA, J.J. Katzfey, J.L. McGregor and K.C. Nguyen, 1999: On regional Model Simulations of Climate Change over New Zeeland. *Weather and Climate,* **19,** 3-14.

Reynolds, R.W., and T. M. Smith, 1994: Improved global *sea surface temperature analyses using optimum interpolation. Journal* of Climate, **7**, 929-948.

Robertson A.W., U. Lali, S. E. Zebaik and L. Goddard, 2004: Improved Combination of Multiple Atmospheric GCM Ensembles for Seasonal Prediction. *Monthly Weather review*, **132**, 2732-2744.

Roeckner, E., and Coauthors (1996): The atmospheric general circulation model ECHAM4: Model description and simulation of present day climate. Report 218, Max Planck Institute for Meteorology, Hamburg, Germany, P90.

Rojas M. and A. Seth, 2003: Simulation and Sensitivity in a Nested Modelling System for South America. Part II: GCM Boundary Forcing. *Journal of climate*.**16**,2454-2471.

Ropelewski, C. F. and Halpert, M. S. 1987. 'Global and regional scale precipitation patterns associated with the El Niño/Southern Oscillation', Monthly Weather Review, **115**, 1606-1626.

Ropelewski, C. F. and Halpert, M. S. 1989. 'Precipitation patterns associated with the high index of the Southern Oscillation', *Journal of Climatology*., **2**, 268-284.

Seth A., and F Giorgi, 1998: The effects of Domain choice on Summer precipitation simulation and sensitivity in a regional climate model. *Journal of climate*, **11,** 2698-2712.

Seth A. and M. Rojas, 2003: Simulation and Sensitivity in a nested Modelling System for South America. Part I: Reanalyses Boundary Forcing. *Journal of Climate*, **16**, 2437-2453.

Shukla J., J. Anderson, D. Baumhefner, D. Baumhefner, C. Brankovic, Y. Chang, E. Kalnay, L.Marx, T. Palmer, P. Paolino, J. PLoshay, S. Schubert, D. Straus, M. Suarez, and J. Tribbia, 2000: Dynamical Seasonal Prediction. *Bulletin of the American Meteorological Society*.**81**: 2593-2606.

Shukla, J., 1998: Predictability in the midst of chaos: A scientific basis for climate forecasting. *Science,* **282,** 728–731.

South African Weather Service, 2006: Seasonal Forecast for Southern Africa: http://www.weathersa.co.za/FcastProducts/LongRange/DOC/SeasonalForecast.doc.

Steyn AGW, Smit CF, Du Toit SHC, and Strasheim C, 1974: Modern Statistics in Practice. *JL Van Sckaike*. 559 pp.

Taljaard, J.J., 1986: Change of rainfall distribution and circulation patterns over South Africa in summer. *Journal of Climatology*, **6**, 579-592.

Taljaard, J.J., 1989: Climate and circulation anomalies in the South African region during the dry summer of 1982/3. *Weather Bureau Technical Paper No, 21*, 45pp.

Taljaard, J.J. and P.C.L. Steyn, 1991: Relationships between atmospheric circulation and rainfall in the South African region. *Weather Bureau Technical Paper No. 24*, 62pp.

Taljaard, J.J., 1994: Atmospheric circulation systems, synoptic climatology and weather phenomenon of South Africa. Part1: Controls of the Weather and Climate of South Africa. *Weather Bureau Technical Paper No. 27*, 65 pp.

Taljaard, J.J., 1995a: Atmospheric circulation systems, synoptic climatology and weather phenomena of South Africa. Part2: Atmospheric circulation systems in the South African region. *Weather Bureau Technical Paper No. 28,* 65pp.

Taljaard, J.J., 1995b: Atmospheric circulation systems, synoptic climatology and weather phenomena of South Africa. Part3: The synoptic climatology of South African in January and July. *Weather Bureau Technical Paper No. 29,* 64pp.

Taljaard, J.J., 1995c: Atmospheric circulation systems, synoptic climatology and weather phenomena of South Africa. Part4: Surface pressure and wind phenomena in South Africa. *Weather Bureau Technical Paper No.30*, 42pp.

Tennant W.J. and B.C. Hewitson, 2002: Intra-seasonal rainfall characteristics and their importance to the seasonal prediction problem. *International journal of climatology*, **22**, 1033-1048.

Tennant W., 2003: An Assessment of Intra-seasonal Variability from 13 Yr GCM simulations. *Monthly Weather Review*, **131**, 1975-1991.

Tiedtke, M., 1989: A comprehensive mass flux scheme for cumulus parameterisation in large-scale models. *Monthly Weather Review*, **117**, 1779-1800.

Trenberth K.E., 1997: The definition of El Niño. *Bulletin of the American Society*,**78**, 2771-2777.

Tyson PD and Preston-Whyte RA, 2000: The Weather and Climate of Southern Africa second edition. *Oxford University Press.* 396pp.

Van Heerden J. and JJ Taljaard,1998: Africa and Surrounding Waters. Chapter 3D. *Meteorological Monographs*, **27**,141-168.

Walsh K. and J. Mcgregor, 1997: An assessment of simulations of climate variability over Australia with a limited area model. *International Journal of Climatology,***17***,* 201-223.

Walsh K. and J. McGregor, 1995: January and July Climate simulations over the Australian Region Using a Limited-Area Model: Journal of Climate. **8**,2387-2403.

Wilby RL and TML Wigley, 2000: Precipitation predictors for downscaling: Observed and General Circulation Model Relationships. *International Journal of Climatology*. **20**, 641-661.

Wilks DS, 2001: Realizations of Daily Weather in Forecast Seasonal Climate. *Journal of Hydrometeorology*, **3**, 195-207.